2003-04-28

Monitoring Vapor Phase Concentration in Supersonic Flows

Paolo Paci
Worcester Polytechnic Institute

MONITORING VAPOR PHASE CONCENTRATION

IN SUPERSONIC FLOWS

by

Paolo Paci

A Thesis

Submitted to the Faculty

of the

WORCESTER POLYTECHNIC INSTITUTE

in partial fulfillment of the requirements for the

Degree of Master of Science

in

Chemical Engineering

by

April 29, 2003

APPROVED:

Dr. Barbara E. Wyslouzil, Advisor

Dr. Ravindra Datta, Head of Department

ABSTRACT

This work discusses the development of a compact Tunable Diode Laser Absorption Spectrometer (TDLAS) for gas phase mixing ratio and temperature measurements of condensible vapors, in particular H_2O and D_2O, in supersonic flows.

Through extensive pressure trace measurements and mass balances on the incoming species, the expected mixing ratio and temperature profiles of the condensible species along the supersonic nozzle have been characterized.

Using a Tunable Diode Infrared laser operating in the 8 μm region, the possibility of nonintrusively measuring the gas phase mixing ratio and the temperature (even simultaneously) in a supersonic nozzle is demonstrated.

The acquired spectroscopic data and the pressure trace measurements are compared and the results suggest the possibility to improve the instrument set-up and to improve the quality of the measurements. Also, the interpretation of our initial experimental results and the comparison with the pressure traces measurements suggest reasons to further investigate the condensation behavior of D_2O and H_2O.

ACKNOWLEDGEMENTS

Many people have given a substantial contribution to this work. It is my pleasure and honor to mention them in this following big list, and I hope they won't mind if my style is not very orthodox, but this is how I like it.

First I would like to thanks my advisor, Professor Barbara Wyslouzil, because of professional and private reasons. The professional ones are easy to guess for anyone who worked with her: she is the most talented and skillful researcher I ever met. Now, after spending this time in her group, I understand from her example how an engineer can turn into a scientist, and what nice gratification can come from the research work.

The private reason is immediate as well: she transformed a difficult task into an exciting journey and her kindness and understanding have always made my work easier and enjoyable, even in the most challenging moments. She is a fantastic person and I would never stop to be deeply grateful to her for all she did for me.

I am very grateful to Roberto Carpaneto, GianMaria Manfredini, Paolo Lombardo, Marco Cremonini, and to many other persons from D'Appolonia S.p.A. in Genova, for giving me the opportunity to pursue this important result.

Deep Thanks to Dr. Yury Zvinevich, to whom we referred as my "second advisor", because working with him into this project I learned a great deal of science, and hopefully used it. He has been a great researcher to work with, always competent and never impatient, despite the hard time I am sure I gave to him.

My Thanks to Dr. Yoo Jeong Kim. She always helped me in my research and very often much beyond it. Rarely is given a labmate with whom is so fantastic to share such experiences like it has been with Yoo Jeong. Thanks as well to the others members of the Aerosol Laboratory Group: Andrew Roberts, Dr. Kiril Streletzky, Murad Gharibeh and Carla Corbitt. With my good pal Andy and his roommates Mike and Ivo I had many nice and enjoyable activities and I have a very good memory of the interesting talks with Kiril.

Thanks to Dr. Mark Zahniser, Dr. David Nelson and Dr. Joanne Shorter of Aerodyne Research, for the endless number of times I asked and received their help. Also thanks to all the WPI students, technicians and professors who helped me many times in many occasions.

I owe a particular thanks to Francesco Pancheri, Javier Mosquera and Chung ling Ma. *Grazie Fra'*, *Gracias Javier*, *Thank you Horsie*: you are great and fantastic friends, and believe me, I know how important has been your friendships in the way to get here.

Lastly, but only in the random order of this list, I would like to thanks my Parents, Fabrizio and Lucia, to whom is dedicated this result. I feel my success is, in the end, mainly merit of their continuous and strong support during all my academic life.

TABLE OF CONTENTS

LIST OF TABLES

LIST OF FIGURES

LIST OF FIGURES (CONTINUED)

1 INTRODUCTION

An aerosol is an assembly of liquid or solid particles suspended in a gaseous medium long enough to be observed and measured [1]. These particles range typically in size from 0.003 microns to several tens of microns (conventionally, the upper size limit is considered to be about 100 μm). Both natural phenomena and human activities can generate aerosols: volcanoes, dust storms and wood or grassland fires are the most common natural causes, while the burning of fossil fuels is the main human contribution. Averaged over the globe, anthropogenic aerosols currently account for a large fraction of the atmospheric aerosol, and most are concentrated in the Northern Hemisphere, especially downwind of industrial sites, slash-and-burn agricultural regions, and overgrazed grasslands [2].

Aerosols have a large number of physical properties that are important for a wide variety of phenomena in nature and in technical applications. For example, the reflection and scattering of light in the atmosphere impacts the global climate and the ability of particles to collect electric charges is an important aspect of pollution control since many filtering devices exploit this characteristic. Nanometer-sized particles can also exhibit quantum effects that may be of vital importance for future electronic and medical devices [3]. Finally, the interactions between an aerosol and its environment are strong functions of the aerosol size distribution, concentration, composition, and the internal structure of the constituent droplets or particles.

In our laboratory, we study the formation, growth, and structure of pure and multicomponent nanodroplets using supersonic Laval nozzles and a variety of experimental techniques.

Laval nozzles are a particular kind of nozzle invented by the Swedish engineer Carl de Laval in 1883. They have a converging – diverging profile and are designed so that the flow can be treated as one dimensional, and that the expansion process details can be obtained by knowing the conditions at the inlet and by measuring one state variable as a function of position along the nozzle. When a gas flows through the nozzle without condensing, the pressure, density and temperature fall isentropically and the cooling rates are on the order of 10^6 K/s [4]. During a typical nozzle experiments, a condensible vapor forms a dilute gas mixture with a non-condensible carrier gas and expands as it flows through the nozzle. As the expansion progresses, the flow quickly becomes supersaturated and suddenly particles begin to form by homogeneous nucleation. Heat is released into the flow by droplet growth and the pressure, density, and temperature of the gas mixture deviate from their isentropic values. In our laboratory we define the onset of condensation as that point in the flow where the state variable temperature differs by 0.5 K from its isentropic value. Alternatively, onset can be defined as that point in the flow where the light scattered by the aerosol is first detected [4].

The dynamics of the condensation process are illustrated schematically in Figure 1, where the profiles of pressure, percentage of mass vapor condensed and the vapor phase molar mixing ratio are expressed as a function of the position along the nozzle.

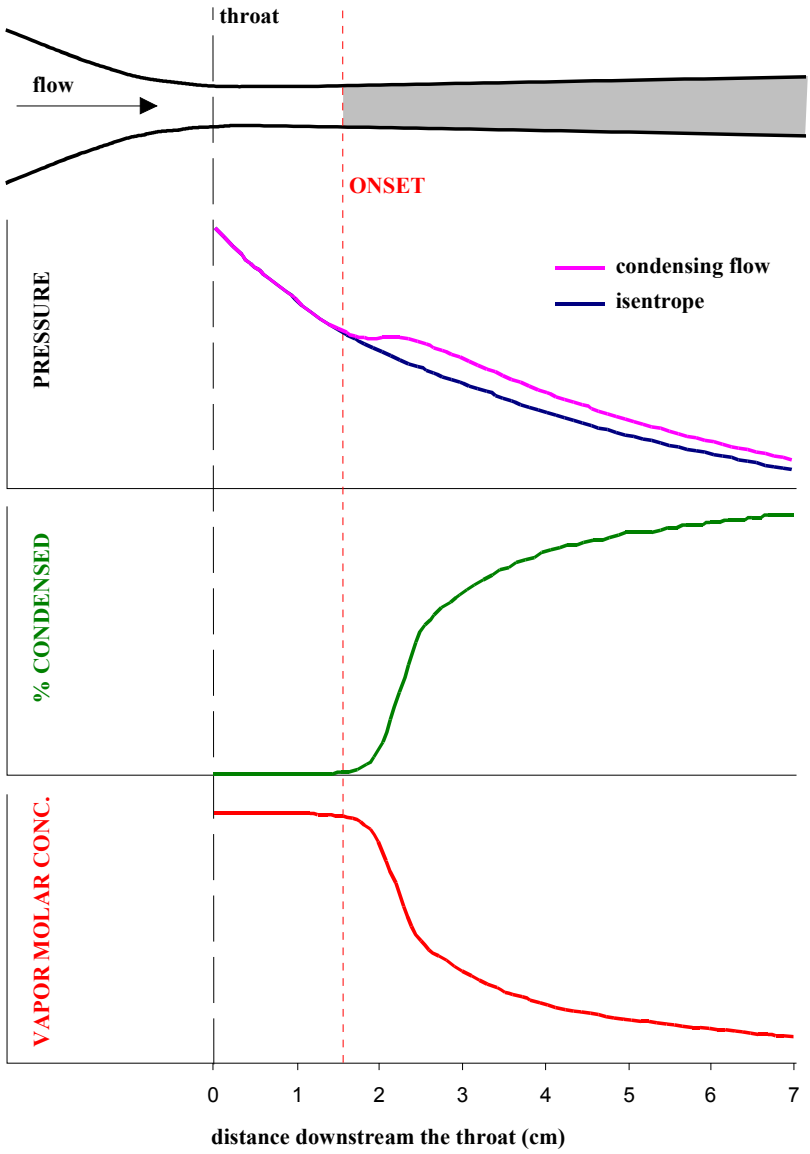

Figure 1.1 - Schematic representation of condensation dynamics in a supersonic nozzle

Not only do experiments in nozzles match the high cooling rates, high supersaturation and high nucleation rates typical of important industrial applications such as aerodynamic

and turbomechanical flows, but they produce nanodroplet aerosols with a high enough number density to make techniques like small angle neutron scattering (SANS) feasible. To date our research group has used supersonic nozzles to investigate the formation and structure of nanodroplets, to develop a deeper understanding of the phase transition phenomena that occur under conditions that are far from equilibrium [5-8], and to determine the parameter of the droplet size distribution and the internal structure of multicomponent nanodroplets using SANS [9-12]. In addition, simultaneous analysis of the SANS and the pressure trace data help to assess acceptable models of nucleation and droplet growth [8] and makes it possible to directly measure the nucleation rate [12].

During a supersonic nozzle experiment, the composition of the incoming gas mixture is set by the N_2 and condensible mass flowrates. If all the material condenses, then the overall composition of the final aerosol equals that of the incoming condensible vapor. Unfortunately there can be a large uncertainty on the overall composition of multicomponent droplets when less than 100% of the incoming material condenses. Although modeling studies suggest that close to 95% of the material should condense by the exit of the nozzle during most experiments, inverting the pressure trace data suggests that only about 70-80% of the vapor condenses [9]. Thus, for multicomponent condensation the uncertainty in the droplet composition can be unacceptably large. For SANS experiments from multicomponent droplets, the neutron scattering length density of the aerosol is a strong function of composition, and uncertainty in composition

translates directly into uncertainty in determining the droplet number density and internal structure.

The goal of this thesis is to develop a technique that will enable us to determine the overall composition of the aerosol inside the nozzle. Direct sampling is not an option - the nanodroplets exist only because the gas is moving rapidly and the temperature is low. Any attempt to capture the droplets would require slowing the flow. This would, in turn, raise the temperature and the droplets would rapidly evaporate. Thus, we require a non intrusive technique.

Historically, a variety of techniques are available for obtaining useful information about aerosols, and since approximately the 1950s, advances in aerosol measurement have been motivated by many kind of investigations [1]. In this thesis we want to use infra read spectroscopy to follow changes in the gas phase and by mass balance infer the composition of the condensed phase.

Infrared (IR) spectroscopy is an absorption method widely used in both qualitative and quantitative analysis. The infrared region of the spectrum includes wave numbers ranging from about 12,800 to 10 cm^{-1}. The IR range can be separated into three regions: the near-infrared (12,800-4,000 cm^{-1}), the mid-infrared (4,000-200 cm^{-1}), and the far-infrared (200-10 cm^{-1}). Most analytical applications fall in the mid-infrared region of the spectrum and IR spectroscopy has primarily been focused in assisting to identify organic compounds.

IR spectroscopy is extensively employed in quantitative techniques of analysis and detection of industrial pollutants in the environment. Unlike UV and visible spectroscopy, which uses larger energy absorbance from electronic transitions, IR spectroscopy relies on the much smaller energy absorbance that occur between various vibrational and rotational states. The only requirement for using IR methods is that the molecule should have an infrared line-spectrum which is resolvable at the Doppler limit. In practice this includes most molecules with five or fewer atoms together with some larger molecules [13].

The FTIR technique has been successfully used in supersonic Laval nozzles to determine onset of UF_6 clustering [14], in free supersonic jets for monitoring NO_x atmospheric traces [15] and in slit nozzles to observe clusters containing SF_6 [16]. The same sulphur hexafluoride clusters have been also investigated using a CO_2 laser [17] and High Resolution Diode Laser Spectroscopy [18]. In this last work the authors coupled the spectroscopic experiment with classic static pressure measurements determining the concentration of SF_6 monomers for the very first time.

Diode laser spectroscopy methods of measurements of gas-dynamic properties have also been used to investigate in a variety of flowfields, generally relevant to combustion, propulsion and aerodynamic facilities [19-22].

Among all the spectroscopic techniques, Tunable Diode Laser Absorption Spectroscopy, TDLAS, is the most advanced with respect to resolution and sensitivity. The principle of TDLAS is to carefully measure the intensity and shape of a single

isolated absorption line of the species. This is done by varying the frequency of the IR source ("tuning") and since the TDLs typically have a line width of 10^{-4} cm^{-1}, they are the instrument capable of giving the best possible resolution in the IR region [22]. Other IR techniques, such as FTIR, cannot reach such very high spectral resolution because of the very strong absorption that creates interference between species or between different lines of the same species. This is true despite some very recent improvements in developing high resolution FTIR systems [23, 24]

As previously discussed our interest is focused in developing a new nonintrusive technique for monitoring concentration and temperature in supersonic nozzles, as a function of the position, to validate and integrate results from other techniques. We are particularly interested in following the vapor mixing ratio in order to determine the droplet composition in multicomponent nucleation. To this end we purchased a Tunable Diode Laser Absorption Spectrometer and have coupled it to our supersonic Laval nozzle that is machined from aluminum with CaF_2 windows in the sidewall (see Appendix A for details). N_2 is used as carrier gas and we add the condensible component to the gas stream by vaporizing the desired species. We work in the mid-infrared (8 μm) region to measure the gas phase concentration and the temperature of the condensible vapors - in particular H_2O and D_2O.

The work is organized as follows: in the experimental section the equipment is described (the supersonic nozzle apparatus and the TDL system) and the pressure trace and TDL techniques are introduced. The governing principles are discussed, as well as

the interpretation of the data (pressure traces, absorption spectra) and the theoretical framework for obtaining the desired information from the absorption spectra.

These resulting information are presented and discussed in the following Chapter 3, where also pressure trace results are compared with results from spectroscopy investigations. In Chapter 4 eventually we summarize our work and present some concluding remarks.

2 EXPERIMENTAL

2.1 APPARATUS

These experiments use a conventional Laval nozzle with a nominal opening angle of 1.77° and a nominal throat area of 63.5 mm^2. The other basic design parameters of the nozzle are the same as those of the nozzle used by Heath [6, 7], Dieregsweiler [9] and Khan.[12]. The major difference is that the sidewalls contain 2 mm thick CaF_2 windows with an anti-reflective coating rather than Si windows. A complete description of the current nozzle is given in Appendix A.

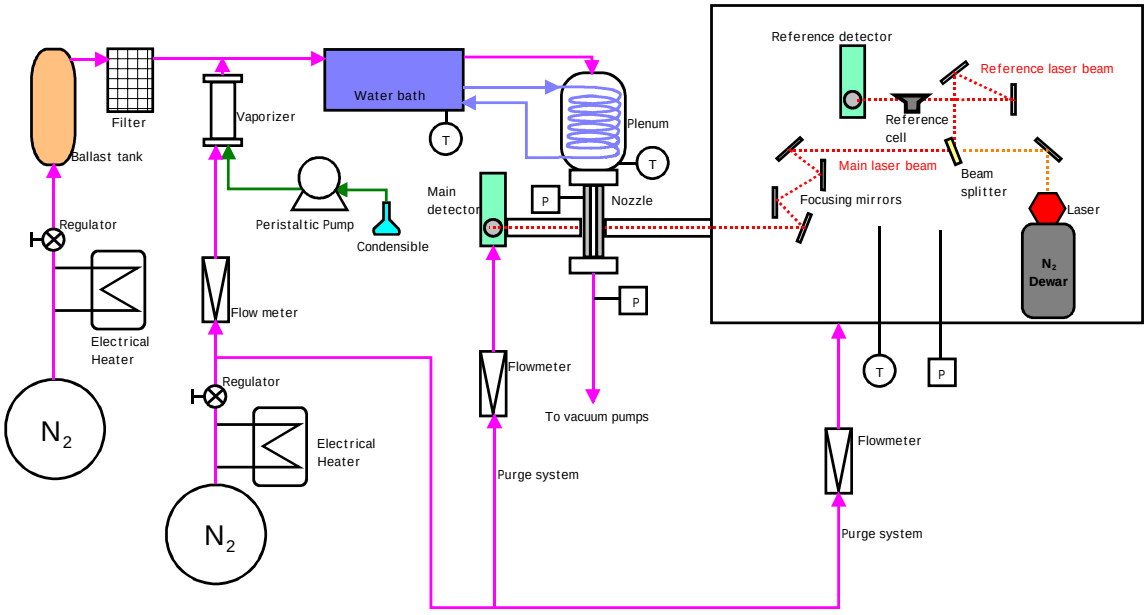

Figure 2.1 - The experimental setup integrates the IR spectroscopy with the supersonic nozzle flow system.

The experimental setup used to conduct the IR experiments is composed of two independent sub-systems: the Supersonic Nozzle System [6, 9, 12] and the Tunable Diode Laser Absorption Spectrometer (TDLAS) [25, 26]. A schematic diagram of the experimental setup is illustrated in Figure 2.1, and each sub-system is described in detail below.

2.1.1 Supersonic Nozzle System

All the experiments were conducted using the supersonic nozzle setup illustrated in Figure 2.2. This setup differs slightly from those described by Heath, Dieregsweiler, and Khan, [6, 7, 9, 12], and the changes implemented here have simplified and greatly improved both the pressure and temperature control. The main differences between the current setup and the earlier versions are that (1) the main flow of the carrier gas (N_2) is now supplied by only two rather than three high pressure liquid nitrogen dewars, (2) one of the main sources of pressure loss in the system has been reduced by replacing the finned heat exchanger with two electrical heaters, (3) the new flow regulators used on the dewars are specifically designed for drawing gas from a liquid N_2 dewar., and (4) the pressure loss between the main dewar and the ballast tank has been reduced by replacing the 1/4" OD polyethylene tubing with a 3/8" OD - 0.040" thick polyethylene tubing. Because both liquid nitrogen dewars are on balances (Cardinal Scale Inc., Arlyn Scale) the amount of nitrogen used can be measured for each pressure trace experiment. As in

the earlier work, the 0.1 m^3 ballast tank and a high volume filter, downstream of the main dewar and its electrical heater, is still required to damp out small pressure oscillations.

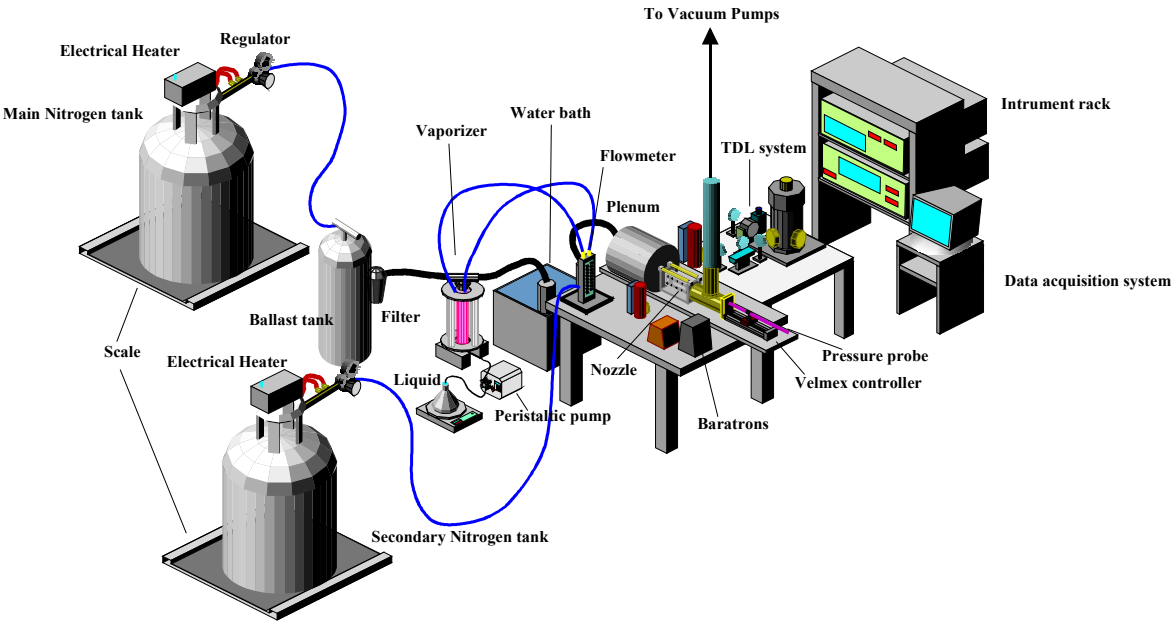

Figure 2.2 - 3 dimensional view of the experimental apparatus.

In the vapor generation system, located between the ballast tank and the water bath, liquid is pumped into the vaporizer using a peristaltic pump (Masterflex Pump Model 7523-20), and the mass flow rate of the condensible material is measured by weighing the liquid dispensed during the course of an experiment using a balance. N_2, supplied by the second dewar, flows through two flow meters and into the vaporizer. Heating tapes raise the temperature of these two nitrogen streams to 45-50 ^oC. One of the N_2 streams breaks the liquid up into a fine mist, while the second dilutes the gas stream and adds enough

additional heat to rapidly evaporate all of the droplets. The total energy added to the gas streams is approximately equal to 3 – 6 times the theoretical heat of vaporization of the liquid.

The stream rich in the condensible vapor mixes with the gas from the ballast tank and the combined gas mixture flows through copper cooling coils placed in a water bath (VWR model 1156 - with digital controller). This provides the primary temperature adjustment for the mixed gas stream. The flow then enters the plenum, a 0.335 m long ISO 200 stainless steel nipple containing additional finned copper cooling coils through which water from the bath recirculates. This provides the final temperature adjustment. The stagnation temperature T_0 is measured using a high accuracy RTD (Omega Engineering, fine diameter - 1/16" - platinum RTD) housed in a Teflon flow straightener and located in the center of the flow stream, inside the plenum itself.

After leaving the plenum, the gas flows through the nozzle and is then discharged to the atmosphere through 75 mm tubing by two rotary vane vacuum pumps (Busch Model RC0160 and RC0250) that provide up to 0.13 m^3/s pumping capacity.

2.1.2 Tunable Diode Laser Absorption Spectrometer System

A simplified block diagram of the Tunable Diode Laser (TDL) instrument is shown in Figure 2.3. There are two main modules in the instrument: the optical module and the electronic module.

The main part of the optical module is built on a 58×89 cm optical table and is enclosed by a plastic box. The box protects the TDL dewar, the detectors, transfer and focusing optics and the reference cells (see Figure 2.4) from dust and lets us purge the optical path, if desired. In an alternative configuration, part of the focusing optics are placed after the nozzle in order to refocus and separate the main signal from the signal due to fringes and to cut the latter off the beam pathways before reaching the detector;

The electronic module consists of a fast computer (Intel 1.0 MHz Pentium III processor) with two data acquisition boards and a dual laser control unit.

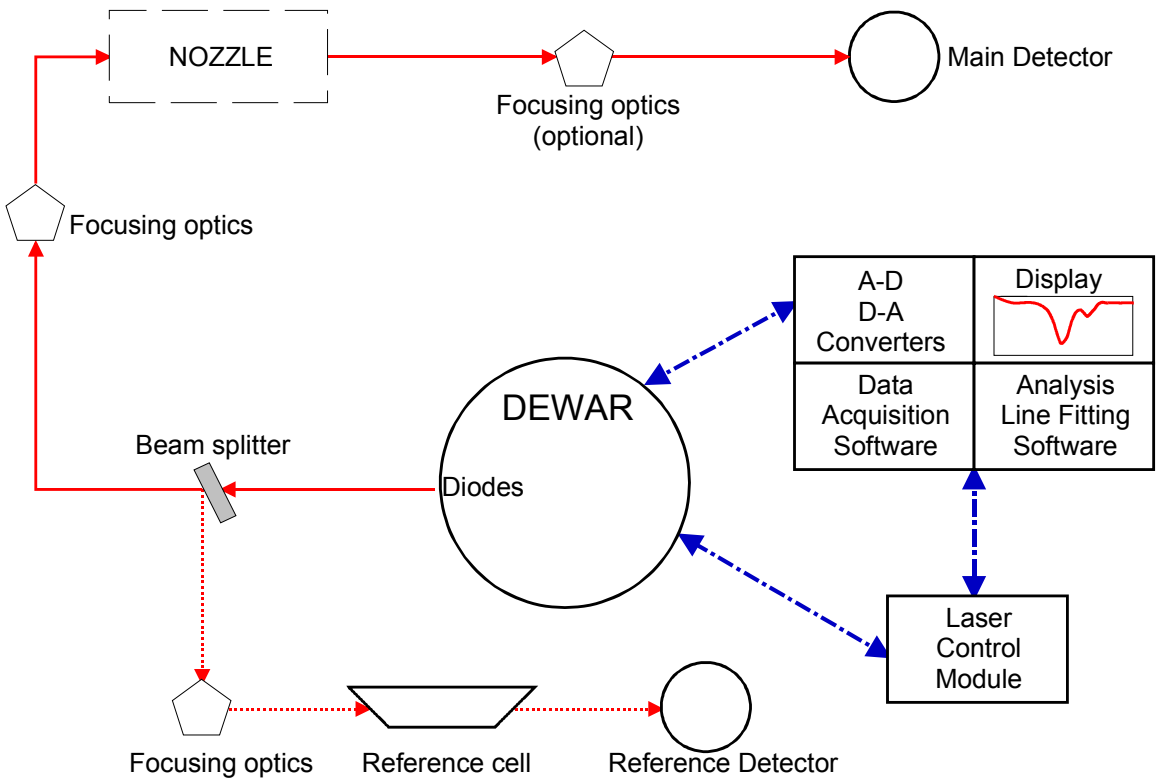

Figure 2.3 - Block diagram of the TDL system

The purpose of the optical module is to produce light of the correct wavelength from the infrared laser diode, to focus the beam with a series of optical mirrors, to direct the light through the supersonic nozzle windows (where the sampling takes place) and onto the detector. The main peculiarity of this assembly is the absence of a low volume long path length optical absorption cell or "multipass cell" containing the sample and this aspect, as will be explained in detail later, presents one of the greatest challenges in this work.

We worked with several optical configurations that differed only slightly from each other. The main differences among the configurations comprise the way the laser beam is focused (before, after, or in the middle of the nozzle) and by the kind of detector used (with or without a lens, with or without annexed focusing mirrors). Also, three different kinds of CaF_2 windows (clear, opaque, and with antireflective coating) were tested. Tests were performed using different combinations and arrangements and eventually led to the following conclusions.: (1) It was better to focus the sampling beam onto the main detector. Tests conducted with the focus in the middle of the nozzle, that then tried to re-focus the beam after getting rid of fringes, gave poor results. (2) The best way to reduce the fringes that are due to reflections of the beam between the two parallel windows is to use CaF_2 windows with an antireflective coating. (3) It is important to re-focus the sampling beam after the nozzle, before reaching the detector. (4) Each time the configuration of the pathway is altered, results may change slightly because of small

differences in the way the beam is focused and the fringes act on the detector. Thus, after any major change in configuration (and in general every time a new set of experiments is started) it is important to "calibrate the TDL system" (see Appendix D).

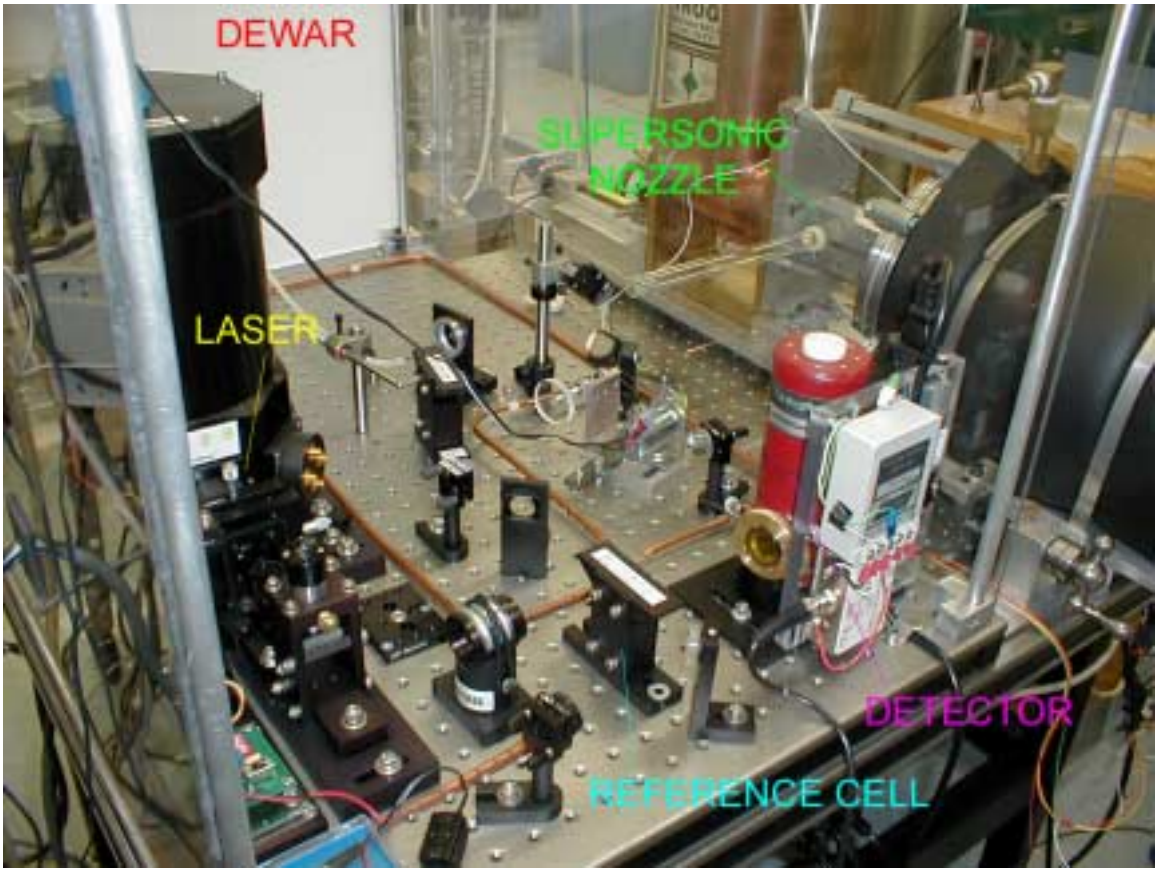

Figure 2.4 - Optical module of the TDL system

In addition to the main optical path, a portion of the laser beam is sent through a short (5 cm) "reference" cell containing a relatively high concentration of a gas of interest. This can be the same gas being monitored in the nozzle or an alternate gas. The signal

from the reference leg helps in the setup of the laser and allows us to lock the peak position during the experiment.

The electronics module controls the laser diode frequency, and processes the detected absorption signals to yield the gas mixing ratios. Both of these functions are controlled by the data acquisition and analysis software (TDLWintel, see Appendix C). The computer sends commands to the laser controller, which in turn adjusts the laser diode temperature and average current as well as providing a fast ramp that sweeps the laser frequency across the trace gas absorption feature. The laser light is detected and converted to electrical signals that are digitized by the data acquisition board.

The analysis program calculates the change in absorption as the laser frequency is swept across the spectral feature of interest. The absorbance is fit to a calculated lineshape, based on tabulated spectral parameters from the HITRAN spectral database [27-30], and on the measured temperature and pressure, using the procedures described in Paragraph 2.3 to yield an absolute gas concentration [25].

2.2 PRESSURE TRACES MEASUREMENTS

The supersonic Laval nozzles used here are designed so that the flow can be treated as one-dimensional. We can, therefore, obtain the entire history of the expansion by measuring the initial stagnation conditions and one state variable as a function of position along the nozzle.

Typically we measure the pressure along the length of the nozzle using a movable probe. The static pressure probe (HTXX-20-TW, Small Parts, Inc.) is a 762 mm long, 0.89 mm O.D. stainless steel tube with 4 equally spaced holes drilled 311 mm downstream from the tip. The probe is sealed at the upstream tip and the downstream end is connected to a high accuracy pressure transducer (MKS 120AA Baratron absolute capacitance manometer) via Tygon tubing and a vacuum tight fitting.

To ensure that the probe travels down the centerline of the nozzle, two sets of crosshairs are placed at the entrance and the exit of the nozzle and the probe is always held by both crosshairs even when it is in the furthest downstream position.

As illustrated in Figure 2.5, the probe is attached to a small positioner (VELMEX inc., MA1500, 1.5" wide, travel range up to 6") whose lead screw is rotated using a stepping motor controller (VELMEX inc., NF90 with three motor drives). The unislide assembly is controlled through a dedicated software interface on a normal PC. With this arrangement it is possible to resolve the position of the probe much better than 0.1 mm. A more detailed description of the main features of the positioner and the controller, as

given by the vendor, is provided in Appendix B and the complete command summary and setup instructions are available in the NF90 User manual [31].

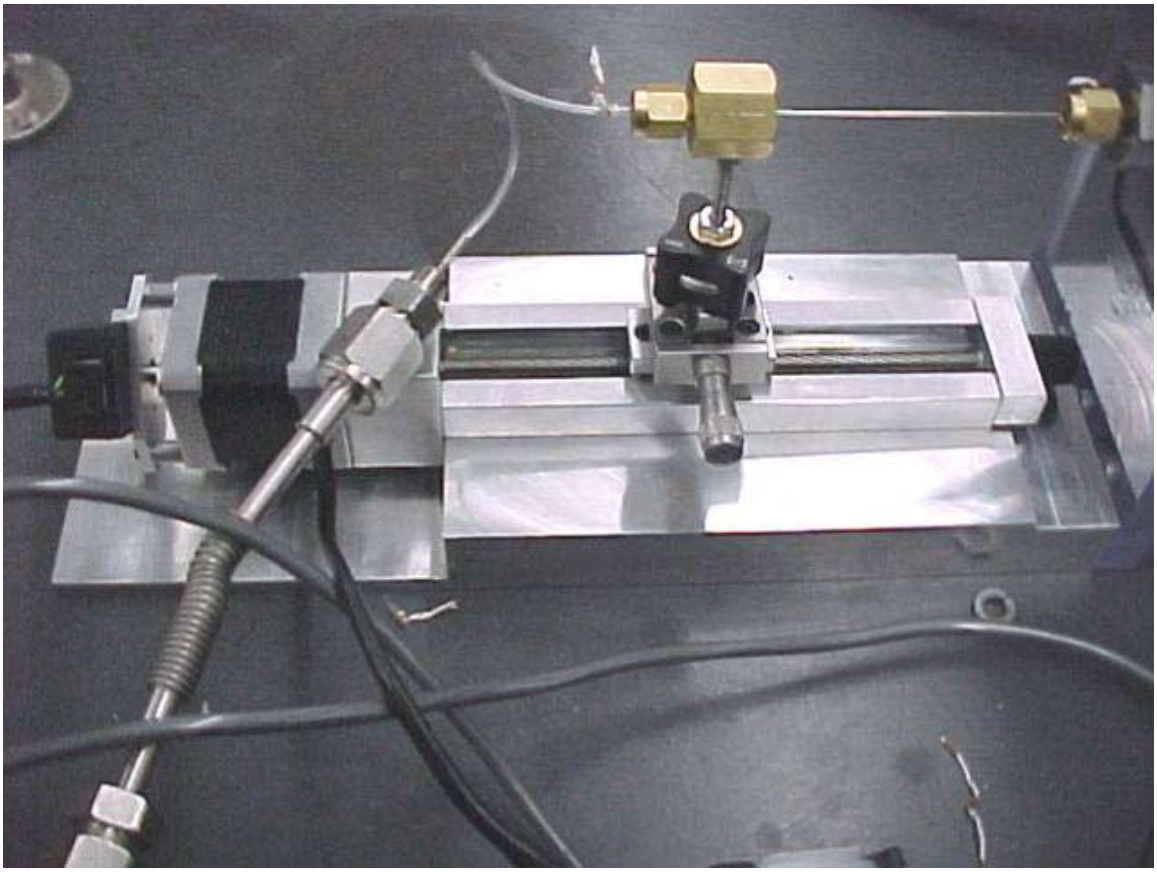

Figure 2.5 - Pressure probe and Velmex positioner assembly

2.2.1 Measuring and interpreting pressure profiles

Once the system reaches stable operating conditions, the static pressure at each location *p(x)* is measured along the centerline of the nozzle. Several pressure measurements are made in the subsonic region (straight and converging sections of the

nozzle), near the throat and then downstream of the throat. Measurements are taken with 0.1 mm resolution near the throat and 1 mm resolution elsewhere.

During a pressure trace experiment we typically record the following information (all the experiments with nozzle H have been conducted using Train B. If Train A is used, an additional measure for the relative humidity is taken and recorded using an RH probe located just before the plenum): static Pressure profile $p(x)$, stagnation Temperature T_0, stagnation Pressure p_0, weight of the main Liquid Nitrogen (LN2) dewar, weight of the secondary LN2 dewar, weight of the liquid dispensed through the vaporizer (this measure is taken manually recording the initial and the final weight of the flask containing the liquid and the time), the date and time of each measurement.

The data are recorded using a digital to analog board and a PC. The source code for the pressure data acquisition software, as well for all the others, is given in Appendix C. Usually a burst of 21 measurements are taken for each variable in less than 1 s via direct memory access mode and the average value of each variable and its corresponding standard deviation are computed and saved in a separate file.

Because of the boundary layers that develop along the walls and some play in the nozzle assembly, the effective area ratio of the nozzle differs from that of the design (see Appendix A). Therefore, before running a condensible flow experiment, the effective shape of the nozzle at the desired T_0 and p_0 is determined by measuring the "dry" pressure trace flowing only the carrier gas N_2 and using the relationships for an isentropic

expansion. The Mach number is obtained from the pressure ratio by the following equation:

$$M^2 = \left(\frac{u}{a}\right)^2 = \frac{2}{\gamma - 1} \cdot \left[\left(\frac{p}{p_0}\right)^{\left(1-\gamma/\gamma\right)} - 1\right] \qquad (1)$$

where:

M = local Mach number;

u = local velocity;

a = local speed of sound. This can be computed from the local temperature as $a = \sqrt{\gamma \cdot R \cdot T / \mu_i}$, where R is the universal gas constant and μ_i is the molecular weight of the inert carrier gas (N_2).;

γ = ratio of constant pressure and constant volume heat capacities;

p, p_0 = static pressure and stagnation pressure.

The area ratio is obtained from the Mach number using:

$$\frac{A}{A^*} = \frac{1}{M} \cdot \left[\frac{2 + (\gamma - 1) \cdot M^2}{\gamma + 1}\right]^{\frac{\gamma+1}{2\gamma-2}} \qquad (2)$$

where:

A = local cross sectional area;

A* = area of the throat.

The dry pressure trace is followed by experiments with the desired gas mixtures. The composition of the gas stream in presence of a condensible is directly determined from the mass flow measurement:

$$y = \frac{\dot{m}_v / \mu_v}{\dot{m}_v / \mu_v + \dot{m}_i / \mu_i} \tag{3}$$

where:

y	=	molar fraction of condensible vapor in the stream;
$\dot{m}$	=	mass flow rate;
μ	=	molecular weight;
v, i	=	subscripts for "condensible vapor" and "inert carrier gas", respectively.

The previous equation (3), in the hypothesis of $\dot{m}_i / \mu_i >> \dot{m}_v / \mu_v$, can be simplified to give:

$$y^0 = \frac{\dot{m}_v / \mu_v}{\dot{m}_i^0 / \mu_i} \tag{4}$$

Where $\dot{m}_i^0$ is the mass flow rate of the carrier gas nitrogen through the nozzle at the desired p_0 and T_0, determined during the "dry" pressure trace. Wyslouzil et al. [6] showed that an improved estimate for the molar fraction of the condensible vapor can be found by subjecting equation (3) to the following first order correction:

$$y = \frac{y^0}{1 - y^0 \cdot d} \tag{5}$$

The correction factor "d", using Nitrogen as a carrier gas (heat capacity ratio $\gamma = 1.4$), becomes [6, 9, 12]:

$$d = \frac{1}{2} \cdot \left(\frac{\mu_v}{\mu_i} - 1 + 0.743 \cdot \frac{\overline{C}_{pv} - \overline{C}_{pi}}{\overline{C}_{pi}} \right) \tag{6}$$

where:

$\overline{C}_p$ = average molar heat capacity.

To determine the conditions at the onset of condensation, the properties of the condensing flow are compared to the expansion that would have occurred in absence of condensation. For a given mixing ratio, the value of p/p_0 at the throat is given by:

$$\frac{p}{p_0} = \left[\frac{1 + \gamma_m}{2} \right]^{\gamma_m / (1 - \gamma_m)} \tag{7}$$

where, for a thermally perfect gas, the ratio of the heat capacities for the mixture is given by:

$$\gamma_m = C_{pm} \Big/ \left(C_{pm} - R \right) \tag{8}$$

and

$$C_{pm} = \sum_j y_j \cdot C_{pj} \tag{9}$$

where:

C_{pm} = molar heat capacity at constant pressure of the mixture;
y_j = mole fraction of component j;
C_{pj} = molar heat capacity at constant pressure of component j.

To derive the other properties of the condensing flow (local gas velocity *u*, temperature *T*, density ρ, condensate mass fraction *g*) from the dry and condensing flow pressure traces, we integrate the diabatic equations in a form with pressure and area ratio as the know quantities [6]. The source code of the program used to perform the diabatic equations integration is reported in Appendix C.

To directly compare the pressure trace results with the TDLAS measurements, we calculate the vapor mixing ratio (M.R.) in parts per billion of volume (ppbv) from the condensate mass fraction as a function of the position along the nozzle *g(x)* as:

$$\text{M.R.}(x) = 10^9 \cdot \frac{\left[\dot{m}_{v0}/\mu_v - \left(\dot{m}_{v0}/\mu_v\right)\cdot\left(g(x)/g_\infty\right)\right]}{\left[\dot{m}_{v0}/\mu_v - \left(\dot{m}_{v0}/\mu_v\right)\cdot\left(g(x)/g_\infty\right) + \dot{m}_i/\mu_i\right]} \qquad (10)$$

where:

M.R.(x) = vapor mixing ratio as a function of position along the nozzle;
$\dot{m}_{v0}$ = initial mass flow rate of the condensible;
$\dot{m}_i$ = mass flow rate of the carrier gas;
g(x) = condensate mass fraction as a function of position along the nozzle;
g_∞ = ratio of initial flow of vapor to total initial flowrate;
μ = molecular weight;
v, i = subscripts for "condensible vapor" and "inert carrier gas", respectively.

2.3 LASER ABSORPTION MEASUREMENTS

During a TDLAS experiment, the light absorption is measured along the length of the nozzle. One measurement is made in the stagnation region before the beginning of the converging section, and subsequent measurements are in the supersonic region with spatial resolutions up to 1 mm. The supersonic nozzle system (plemum, nozzle and vacuum tubing) is mounted on a sliding device attached to a linear translation stage. A lead screw mounted on the side of the plenum provides the translational movement and is rotated manually. This arrangement is attached to an optical counter, has a working range of about 20 cm and provides a way to resolve the position of the laser beam with respect to the nozzle better than 0.02 mm. The optical counter is calibrated in order to show the zero position in between the small and the big CaF_2 windows, and the entire length of both windows is available for the measurement.

A schematic of the optical arrangement was given earlier in Figures 2.1 and 2.4. The beam from the TDL housed in the cold dewar is first collimated and then directed by a sequence of mirrors (normal and focusing) through the nozzle and onto the cooled main detector (detector A). Part of the beam is split off and directed through a line-locking/reference cell and then onto the cooled reference detector (detector B). A visible He-Ne laser beam is combined with the invisible infrared beam to assist in alignment.

Detector A is placed into a dedicated closed box outside the optical table, while detector B is placed inside the main box containing the optical mirrors and the laser. The total pathlength of the sampling laser beam ranges from 105 to 130 cm, depending upon

the optical arrangement. Inside the box, on the optical table, an RTD measures the temperature along the laser pathway, while the atmospheric pressure during the experiment is monitored using a pressure transducer connected to the box via ¼ NSF PE tubing.

The data acquisition method is based on rapid sweep integration over the full infrared transition line shape. This is accomplished by scanning the laser frequency under computer control and at the same time measuring the transmitted infrared light intensity. The spectral information is analyzed in real time with a nonlinear least squares fitting routine which returns both the spectral line profile and laser power spectrum. The area under the absorption line, together with the absorption coefficient for the line is used to calculate the mixing ratio of the species being observed [26].

In a typical experiment, the laser temperature is held constant while the current through the laser is modulated by the computer to sweep the output frequency across the entire spectrum. The modulation is achieved in 50 to 200 discrete steps with a digital to analog converter. The infrared line is swept across at a rate of approximately 10 kHz. During approximately ten per cent of the sweep the laser current drops below the lasing threshold to provide a precise measurement of zero light intensity.

The signal voltage from the infrared detector is amplified by a low noise preamplifier, passed through a low pass filter and directed to the input of a National Instruments data acquisition board. The signal voltage is monitored differentially to minimize common mode pickup. A 12 bit analog to digital converter (ADC) on the National Instruments

board provides a numerical representation of the signal amplitude. The conversion time for the ADC is 200 nanoseconds. The result of each conversion is transferred to the extended memory of the PC using double buffered direct memory access (DMA). This process is fast enough to maintain a continuous 1 MHz data stream with 100% duty cycle.

2.3.1 Principles of TDLAS

The principle of TDLAS is absorption spectroscopy of radiation with frequencies between 4000 and 400 cm^{-1} (wavenumbers) - i.e. IR spectroscopy - using a single isolated absorption line of the species. TDLAS is a valuable technique for vapor phase measurements, mainly because being a high resolution spectroscopic technique it is virtual immune to interferences by other species. The ability to provide unambiguous measurements leads to the use of TDLAS as a reference technique against which other methods are often compared. Moreover it is a general technique, and the same instrument can easily be converted from one species to another by changing the laser and using different reference cells.

On the other hand TDLAS instruments are often complex and expensive. Moreover, the diode lasers themselves can be unreliable and each laser is unique, leading to the need to recharacterize the instrument whenever a new laser is installed.

In terms of fundamental principles, the transmission of a probe beam of monochromatic light through a uniform absorbing medium follows the Lambert-Beer Law [13, 19, 20]:

$$\ln\left(\frac{I(\upsilon)}{I_0(\upsilon)}\right) = -\alpha(\upsilon)\cdot L \qquad (11)$$

where:

$I(\upsilon)$ = intensity of monochromatic radiation of frequency υ transmitted through an absorbing species;

$I_0(\upsilon)$ = transmitted intensity in the absence of an absorbing species;

L = optical path length;

$\alpha(\upsilon)$ = absorption coefficient;

I/I_0 = Transmittance (T);

$\alpha \cdot L$ = Absorbance (A).

The absorption coefficient $\alpha(\upsilon)$ is related to the absorption cross-section $k(\upsilon)$ by:

$$\alpha(\upsilon) = k(\upsilon)\cdot C \qquad (12)$$

where:

C = concentration of the absorbing species in molecules per unit volume. Since in the practice is convenient to deal with logarithms to the base 10, often the Lambert-Beer Law is used in the form $\log(I/I_0) = -\varepsilon \cdot C \cdot L$, where $\varepsilon = k/2.303$.

A given absorption line is characterized by its integrated line strength S_T, which is independent of pressure and depends only of Temperature:

$$S_T = \int_0^{\infty} k(\upsilon) d\upsilon \tag{13}$$

The dimensions of S_T are thus the dimensions of the absorption cross section times the dimensions of frequency (or wavelength) and the relation between $k(\upsilon)$ and the line strength is called the line shape factor:

$$k(\upsilon) = S_T \cdot f(\upsilon - \upsilon_0) \tag{14}$$

where υ_0 is the central frequency of the unperturbed transition. Thus $f(\upsilon - \upsilon_0)$ relates the frequency-integrated absorption amount (i.e., line strength) to the specific absorption at distance $(\upsilon - \upsilon_0)$ from the line center. This gives a line shape which depends on temperature and also on pressure. The line shape can be described by (see Figure 2.6):

- Lorentz function (at atmospheric pressure, where collision broadening dominates).
- Gauss function (at low pressure, < 1 torr, where Doppler broadening dominates).
- Voigt function (at intermediate pressures): is a convolution of Lorentzian and Gaussian profiles. The Voigt profile tends to the Lorentzian profile at high pressure and to the Doppler at low pressure and is, therefore, the general form of the lineshape.

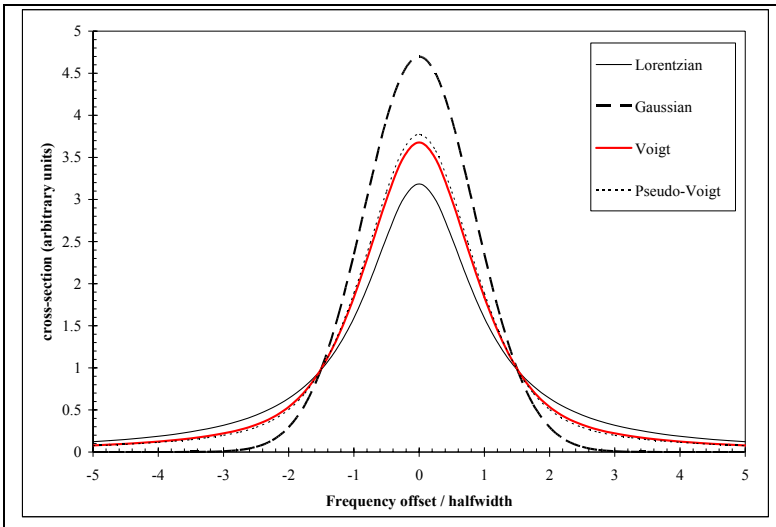

All the profiles are for the same values of S_T and halfwidth at half maximum (HWHM).

The Voigt profile corresponds to the pressure at which $\gamma_L = \gamma_D$.

The pseudo-Voigt profile corresponds to a weighted sum of Gaussian and Lorentzian profiles with a weight factor of 0.611 for the Lorentzian contribution (i.e. to the pressure at which $\gamma_L = \gamma_D$).

Lorentzian:

$$k_L(\upsilon) = \frac{S_T}{\pi} \cdot \frac{\gamma_L}{(\upsilon - \upsilon_0)^2 + \gamma_L^2} \qquad \gamma_L = \gamma_{L0} \cdot \left(\frac{p}{p_0}\right) \cdot \left(\frac{T_0}{T}\right)^{1/2}$$

In this formulas:
γ is the halfwidth at half maximum;
υ_0 is the line-centre frequency;
μ is the molecular weight;
c is the velocity of light.

Gaussian:

$$k_D(\upsilon) = \frac{S_T}{\pi} \cdot \left[\frac{\ln 2}{\pi}\right]^{1/2} \cdot \exp\left[-\frac{(\upsilon - \upsilon_0)^2 \cdot \ln 2}{\gamma_D^2}\right] \qquad \gamma_D = \left[\frac{2 \cdot k \cdot T \cdot (\ln 2)}{\mu}\right]^{1/2} \cdot \frac{\upsilon_0}{c}$$

Voigt (Brassington approximation):

$$k_V(\upsilon) = k_V(\upsilon_0) \cdot \left\{(1-x) \cdot e^{(-0.693 \cdot y^2)} + \frac{x}{(1+y^2)} + 0.016 \cdot (1-x) \cdot x \cdot \left[e^{(-0.0841 \cdot y^{2.25})} - \frac{1}{(1+0.021 \cdot y^{2.25})}\right]\right\}$$

$$y = \frac{|\upsilon - \upsilon_0|}{\gamma_V} \qquad x = \frac{\gamma_L}{\gamma_V} \qquad \gamma_V = 0.5346 \cdot \gamma_L + (0.2166 \cdot \gamma_L^2 + \gamma_D^2)^{1/2}$$

$$k_V(\upsilon_0) = S_T / [2 \cdot \gamma_V \cdot (1.065 + 0.447 \cdot x + 0.058 \cdot x^2)]$$

Pseudo-Voigt: weighted sum of Lorentzian and Gaussian profiles

Figure 2.6 - Lorentzian, Gaussian and Voigt lineshapes.

In the pressure range in between 10 Pa (0.1 torr) and atmospheric pressure (usually we operate our system at pressures in between 10 and 60 kPa) the lineshape can be described as a convolution of Lorentzian and Doppler profiles known as the Voigt profile. This can

be expressed in terms of a complex error function but it is often convenient to use approximations. Probably the most known is the one developed by Brassington [13, 32], however a simple pseudo-Voigt function expressed by a weighted sum of Gaussian and Lorentzian profiles also represent the profile to a very good accuracy (see Figure 2.6).

In modern systems like ours the sweep rate achieved is fast enough for the absorption spectrum to be averaged at rates of more than 10 kHz. In our system, the sweep rate can be as fast as 20 kHz for a 150 point spectrum, fast enough to strongly suppress the effect of 1/f noise. Use of these higher averaging rates raises the effective frequency at which the signal is measured to values where laser noise is considerably reduced [13].

Once the absorption spectrum has been acquired it can be fitted, using non-linear least squares methods, to a combination of a Voigt line profile and a polynomial to represent the variation in the baseline due to the wavelength-variation of the laser power. This means that if the strength of the line being monitored is known, in theory an absolute measurement is possible without need for any calibration source.

For normal measurements, where there is no need to subtract any undesired background contribution from the sample measure, the fitting procedure can be accomplished in real time. If background subtraction is required, or if the fitting conditions are changing during the experiment so that becomes unfeasible to perform a real time fit, the absorption spectra are saved and then post processed.

Exploiting the characteristics of the TDL systems, a mole fraction (or volume fraction) measure is immediately feasible along a uniform property path. In addition to that, the

absorber's temperature is obtainable by means of probing a pair of its absorption transitions [19-21, 46].

In practice, the strategy for measuring the temperature of the absorber gas, is based on the intensity ratio (R) of two absorption lines (line 1 and line 2), which is given in the following [13, 19, 46]:

$$R = f(T) = \frac{S_{T_0,1}}{S_{T_0,2}} \cdot \exp\left[-\left(\frac{h \cdot c}{k} \right) \cdot \left(E_1'' - E_2'' \right) \cdot \left(\frac{1}{T} - \frac{1}{T_0} \right) \right] \qquad (15)$$

where:

h = Planck's constant;
c = speed of light;
E" = lower state energy of the transition;
T_0 = reference temperature (usually 296 K);
k = Boltzmann's constant.

For a given pair of lines the previous ratio R is a function of temperature only, therefore measuring R spectroscopically it is immediately possible to derive the temperature of the absorbing gas.

2.3.2 Setup and measurements

Once the system is ready to operate (i.e. laser and detectors are cooled down and the nozzle system reaches stable operating conditions), the laser and the heater are turned on and the operating set points are loaded from the configuration file or are set manually. A

control is provided to access the values for the laser current set point, limit and range as well as to the temperature set point and range plus several other parameters.

Tunable diode lasers are tuned by varying the temperature of the active region. This can be done either by varying the temperature of the cold stage on which the diode is mounted or by varying the laser drive current, which varies the Ohmic heating of the active region. Varying the base temperature will tune the laser over its entire range but this procedure is slow. Varying the drive current gives a more restricted tuning range, of perhaps 20 wavenumbers, but allows high frequency modulation of the laser frequency [13]. In practice we use the two methods in combination. Depending on the set points chosen for laser current and temperature, different modes of operation of the laser can be obtained and consequently different absorption lines can be used for each species.

There are several factors involved in choosing the absorption line: (1) the line should be strong enough to give high sensitivity but should not be so strong that non-linear effects become important. Because of the nature of our experiment, the line must have relatively high strength at both high and low temperature. A lower state energy parameter meets this requirement. (2) Because the tuning range of a diode laser is not always continuous - the laser can undergo a mode jump - a particular absorption line may not be accessible. As we verified, even when a diode is initially able to operate at a particular wavelength, its characteristics can change over time. It is therefore important, wherever feasible, to choose a wavelength with several strong lines within the tuning range of the laser (sometimes just a few wavenumbers) so that there is a high probability

that at least one strong line will always be accessible. (3) The line can be isolated from other lines of the same species, but this is not a requirement. The TDLWintel software fingerprints method works well in presence of multiple absorption lines, even if they overlap each other. (4) The line should be isolated from interfering lines due to other trace species. As will be discussed below, monitoring H_2O causes the most problems because it is a relatively abundant atmospheric constituent and thus even weak lines produce significant background absorption. (5) If a temperature measurement is desired, the line should be chosen near a second absorption line with a different ground state energy, in order to perform the intensity ratio of the two absorption lines.

We worked with two different diode lasers - named Laser A and Laser B for convenience - with different frequency ranges and different performance characteristics, and with different setups for the optical arrangement. The main features for both lasers are reported in Table 2.1 [25].

We conducted experiments working with several absorption lines (see following Table 2.2), focusing mainly on the D_2O absorption lines with molecular transition frequencies equal to 1321.29 and 1321.64. Table 2.2 summarizes the main line characteristics used by the TDLWintel software reported from the HITRAN database [27-30] or, as for the D_2O case, from the available literature [33].

Table 2.1 - Diode Laser Performance

	LASER A	LASER B
Date shipped [(a)]	July 10, 1997	December 15, 1993
Frequency range (guaranteed)	1250 to 1275 cm^{-1}	1295 to 1310 cm^{-1}
Polarity	Positive	Positive
Maximum allowed current	500 mA	500 mA
Maximum operating temperature	100 K	99 K
Operating conditions:	1253 cm^{-1}	1333 cm^{-1}
at	166 mA	274 mA
and	83 K	86 K
Power (multimode)	0.44 mW	0.57 mW
at	166 mA	306 mA
and	83 K	86 K
Threshold conditions	1233 cm^{-1}	1089 cm^{-1}
at	115 mA	1 mA
and	80 K	20 K
Tuning rate	559 MHz/mA	1073 MHz/mA
at	203 mA	306 mA
and	83 K	86 K
Tuning range	1.20 cm^{-1}	2.35 cm^{-1}
at	203 mA	306 mA
and	83 K	86 K

[(a)] to Aerodyne Research Inc.

Once the line is visible in the defined working range, the Laser Tuning Rate is determined to convert each channel number in the acquired spectrum to a relative frequency value in order to be able to execute fingerprint fits (i.e. fits based on a spectral template typical of the species). This can be done manually, but in practice the tuning rate is determined using TDLWintel's tuning rate utility which automatically calculates the tuning rate by analyzing a frequency scan acquired with an etalon inserted in the beam path. The etalon used here had a free spectral range of 0.0483 wavenumbers.

Table 2.2 - Line transition characteristics. Water refers to H_2O with the natural abundance of H and D, while D_2O was fully deuterated water with better than 99.9% deuteration.

	Mol.	υ_{ij}	S_{ij}	R_{ij}	γ_{AIR}	γ_{self}	E"	n	δ
LASER A	Water	1268.38222	5.527E-22	3.018E-02	0.0843	0.3810	1050.15770	0.65	-0.003580
	Water	1271.78782	1.876E-21	4.844E-03	0.0871	0.3900	648.97870	0.74	-0.006230
	D_2O	1271.443400	4.980E-20[(b)]	N.A.	0.098[(a)]	N.A	74.14200	0.79[(a)]	N.A.
LASER B	Water	1316.97240	3.251E-21	1.543E-01	0.0643	0.3130	1255.16670	0.65	0.003950
	Water	1337.90873	2.945E-22	2.008E-01	0.0120	0.1700	1806.67000	0.40	-0.002830
	Water	1339.14848	2.884E-21	2.654E-01	0.0296	0.1550	1394.81420	0.70	-0.004710
	D_2O	1321.29220	1.660E-21[(b)]	N.A.	0.0470[(a)]	N.A.	1084.3648	0.80[(a)]	N.A.
	D_2O	1321.29410	3.310E-21[(b)]	N.A.	0.0470[(a)]	N.A.	1084.3648	0.80[(a)]	N.A.
	D_2O	1321.64030	3.100E-20[(b)]	N.A.	0.1010[(a)]	N.A.	206.2769	0.79[(a)]	N.A.

υ_{ij} Frequency in cm^{-1}
S_{ij} Intensity in $cm^{-1}/(molecule \times cm^{-2})$ at 296 K
R_{ij} Weighted transition moment-squared in Debyes
γ_{AIR} Air-broadened halfwidth in cm^{-1}/atm at 296 K
γ_{self} Self-broadened halfwidth in cm^{-1}/atm at 296 K
E" Lower state energy in cm^{-1}
n Coefficient of temperature dependence of air-broadened halfwidth
δ Air-broadened pressure shift of line transition in cm^{-1}/atm at 296 K
(a) This parameter have been derived *a posteriori* from the fitting itself since the information was not available. It is possible to vary the value by ± 50% according to the observations without violating any fundamental physical principles [34].
(b) These intensities are calculated [33]. An error ranging from 0% to 21% has been observed experimentally for selected lines [33] and therefore is to be expected an equivalent uncertainty in applying this data.

In the earlier versions of the TDLWintel software the original approach to this problem modeled the tuning rate (TR) with a nonlinear three parameter analytical function [26], as in equation (16)

$$TR(ch) = x + y \cdot e^{(-z \cdot ch)} \tag{16}$$

where:

x = linear tuning rate (cm^{-1}/channel);

y = nonlinear tuning rate (cm^{-1}/channel);

z = decay constant (dimensionless parameter which determines the range of influence for the nonlinear effect);

ch = channel number.

In the newest versions of the software (as the one used in the present work) the option to use a numerical lookup table created by fitting the extrema in a spectrum, acquired with the etalon inserted in the optical path, has been added to the analytic model.

In the new model the positions of these extrema are then fit using cubic spline interpolation [34, 35]. In the TDLWintel software the resulting cubic spline function is evaluated at each data point in the spectrum to produce a relative frequency lookup table.

Although both old and new model are accurate in capturing the tuning rate function, the new model is more flexible and relies on all the extrema, while the old model works only on the minima of the etalon spectrum. In the present work, eventually the new spline interpolation method has been used. Figure 2.7 illustrates an example fit performed using the two models.

Once the tuning rate is defined and the fitmarkers (for the fit procedure) are positioned, one measurement is made in the small window and further measurements are made with the desired spatial resolution in the main window. Generally the resolution

used is 300 ramp points, 20 of them dedicated to the ramp shut-off, corresponding, in the best situation, to a little more than 1 cm^{-1}.

CUBIC SPLINE INTERPOLATION METHOD	THREE PARAMETER ANALYTICAL FUNCTION METHOD
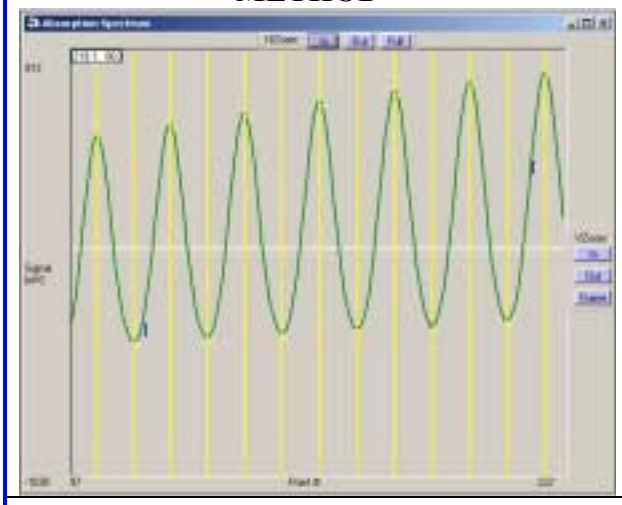	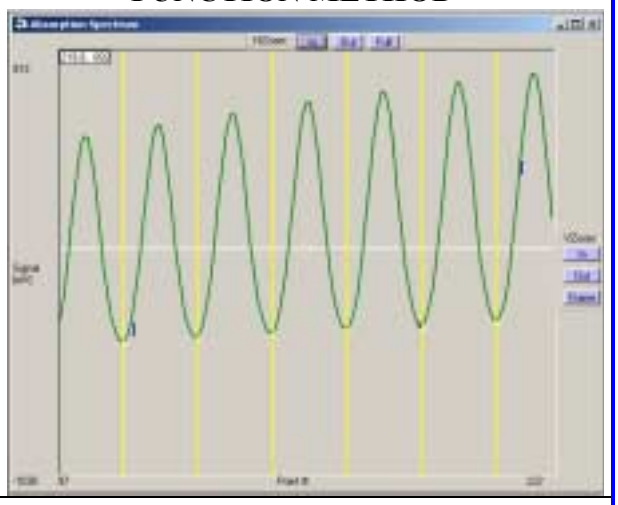

The white carats (symbol ^) show the location of the extrema as determined by the software. These positions are input to the fit. The yellow lines show the positions of the extrema calculated from the resulting spline fit. The agreement is excellent for both methods, the new method is however more accurate and flexible.

Figure 2.7 - Screen shot of determination of nonlinear laser tuning rate function by fit to etalon spectrum.

For each position several spectra are recorded under both the sampling condition, i.e. flowing condensible in the system, and under the background conditions, flowing only the carrier gas N_2. The sample and background measurements are taken within a very short time interval to minimize the effect of the instruments natural drift. Real systems are subject to thermal drift, so that in the time between taking the sample spectrum and the background spectrum the absorption signals will have drifted and cancellation will

not be perfect. Therefore the success of background subtraction depends firstly on the thermal and mechanical stability of the system and secondly on the rapidity with which sample and background spectra can be alternated. Researcher that analyzed this problem [13] found that the sample and background spectra should be acquired within a total period of 60 s for optimum results.

In these experiments the limiting factor is the stability of the system, since after starting and/or stopping the condensible flow, several seconds are require to restore the desired stagnation pressure and to ensure steady state. It is, therefore, not feasible to reduce the time necessary to acquire a sample/background set of spectra to less than 40-45 s.

During the experiment the program executes a nonlinear least squares fitting routine and determine the integrated absorption intensity for the absorption spectrum from each channel. The result of the fitting routine is displayed on the computer screen as a function of time so that trends in the trace gas concentration are immediately apparent, however this result has no meaning other than an informal check on the status (sample/background), because the correct pressure and temperature of the flow cannot be set directly during the sampling.

Individual spectra are saved to the hard disk at the desired time resolution. Usually we use a data update time of slightly less than 0.3 s and one spectra out of four averaged spectra is saved, thus we write one spectra every about 1.2 seconds - this is just a rule of thumb, in practice any reasonable time resolution is acceptable, as long as the whole set

of spectra for each point is recorded in within 45-60 seconds, i.e. a time period over which no appreciable drift of the laser mode occurs. In addition, as a log of the experiment, a concentration stripchart is saved on the hard disk in a "*.str" or stream file. The file names are encoded with the year, date, hour, minute and second that the file was opened; this is true for stream files as well as spectral files [26].

The procedure just described is independent of the optical arrangement used. We tested several different optical arrangements during our experiments, each one with different features. As a "rule of thumb", we verified that the most important characteristic to have exact measures and reproducibility is to focus the laser beam on the detector exactly, no matter how complex the pathway of the laser beam itself is.

The main problem in these experiments arises from the fringes that occur as a consequence of the light reflection between the two windows on the sidewalls of the nozzle. The measurements taken downstream of the onset of condensation are of much more difficult to interpret because the background subtraction operation does not give good results. The reason is mainly related to the conditions inside the nozzle that change in between the sampling and the background measure, due to the occurrence of the condensation in one case and not in the other. This is primarily a problem during the spectroscopic temperature measurements. In this case, the ratio of the line strengths of the absorption lines can be influenced (or even altered) by the sinusoidal shape of the baseline that is the result of incomplete background subtraction. One of the very last improvement tested on the system has been the attempt to compensate for the change in

pressure and temperature inside the nozzle when condensation occurs, trying to flow a "blank" substance whose fluidodynamic behavior is similar to the substance under investigation but the spectroscopic characteristic totally different, so that the TDL experiment can remain unaltered. The results of this attempt, preliminary but promising at this stage, have been added as Appendix F.

2.3.3 Data analysis

From the TDLAS experiment we obtain both sample and background absorption spectra, for many different positions along the nozzle. In addition we obtain a concentrations stripchart from the preliminary on-line fitting. The most useful aspect of the on-line fit is to confirm that the species of interest is present or absent. We also record manually the beginning time at which the sample and the background spectra are taken at any position. This is also automatically recorded along with the spectra. The purpose of the manual time record is merely to help in finding the set of spectra for each position in the software folder where all the spectra (usually thousands) are saved during the experiment.

For each position 5-10 spectra taken under stable conditions are loaded together, to yield a representative averaged spectrum. If a background subtraction is needed, the background spectra are loaded in the same way and they are subtracted from the sample spectrum, in the way described in section 2.3.3.1.

The "net" sample spectra absorption lineshape is fit to Voigt profiles using a nonlinear least squares approach (Levenberg-Marquardt - [35]) implemented in the TDLWintel software. The result returned by the fit includes one or more mixing ratios or concentrations for the molecules that are responsible for the absorption spectrum. A detailed description of the Fitting procedure is provided in section 2.3.3.2.

The diode laser power spectrum is represented as a slowly varying polynomial of adjustable order; typically a quadratic or cubic polynomial is used. The program is capable of fitting a spectrum with contributions from up to three molecules. In addition, the spectrum from each molecule can be composed of as many as 100 individual spectral lines. The mixing ratio of each substance is simultaneously fit together with the diode laser polynomial baseline. The absolute accuracy of the area under the peak returned by the fit is a few percent [26].

2.3.3.1 Background subtraction

There are two different issues, both leading to the same problem, when measuring the absorption of light using TDLAS in our system. The first is that any optical element along the beam pathway (mirrors, windows, etc.) absorbs or diffracts light, and alters the measurement. Secondly, more than 99% of the beam's pathlength is in the open atmosphere. As a consequence, absorption from atmospheric substances must be taken into account when interpreting the results.

In our system there are two orders of magnitude difference in between the sample pathlength inside the nozzle (1.26 cm) and the total beam pathlength (115 to 160 cm, depending upon the different optical configuration used). Consequently, the contribution from any absorption coming from the external pathway (i.e. external to the nozzle) is about 100 times more significant than the absorption from the same substance at the same concentration in the nozzle. In order to measure only the concentration inside the nozzle, it is necessary to get rid of this external contribution by subtracting the background signal from the sample spectra. This is particularly difficult for species like H_2O that are both abundant in the atmosphere and whose concentrations are not necessarily stable over the course on an experiment.

When, however, substances not naturally present in atmosphere (like D_2O) are investigated, the previous problem is not pertinent, but the background subtraction has to be performed anyway. The reason is that the laser beam passes through a series of devices and is reflected many times before reaching the detector. In fact, we verified that the detector itself is a source of backscattering. Thus, in order to discern that part of the signal that is due to absorption by the substance of interest, a "blank" measure has to be performed and its contribution subtracted from the sample signal.

For a perfectly stable system, a background spectrum would display the same fringes as the sample spectrum and subtraction of this background spectrum would remove the fringes completely. Real systems however are subject to thermal drift, so that in the time between taking the sample spectrum and the background spectrum the fringes will have

drifted and cancellation will not be perfect. Thus, the success of background subtraction depends both on the thermal and mechanical stability of the system and on the speed with which the sample and background spectra can be alternated [13].

The figure below is the Sample measure raw data signal. The absorption is by D_2O in gas phase inside the nozzle and by any gas present in the open atmosphere along the pathway of the laser beam.

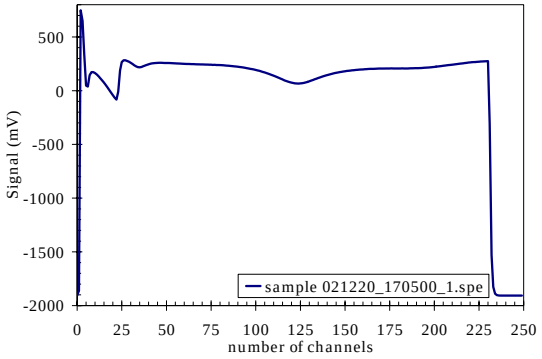

The figure below is the Background measure raw data signal. The absorption is given only by the gases present in the open atmosphere along the pathway of the laser beam.

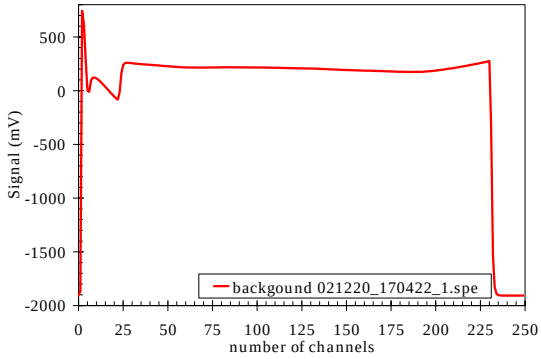

The figure below is the Net data signal, after spectroscopic subtraction (i.e. ratio of the two raw data signal) of the background signal from the sample measure. The absorption is now given only by the D_2O in gas phase inside the nozzle.

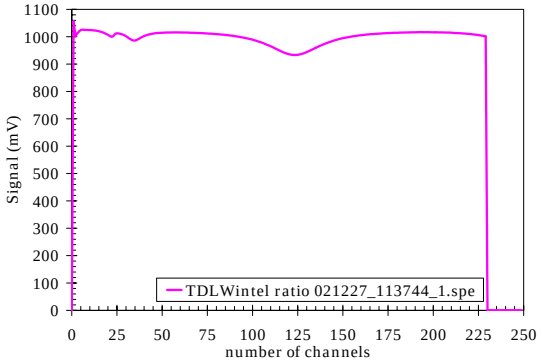

$$z = 1000 \cdot \left(\frac{\frac{x + |x_{min}|}{|x_{min}|}}{\frac{y + |y_{min}|}{|y_{min}|}} - 1 \right) + 1000 \qquad 0 < \text{channel \#} < \text{cutoff}$$

$z = 0$ channel # = 0 ; channel # ≥ cutoff

x = intensity of sample spectrum at any point;

y = intensity of background spectrum at any point;

z = intensity of ratio spectrum at any point;

x_{min} = minimum intensity of sample spectra;

y_{min} = minimum intensity of background spectra.

Figure 2.8 - Background subtraction procedure.

Sample and background spectra should be acquired within a total period of 60 s for optimum results [13, 34]. In our system, for each point sampled, we record the sample spectra and the background spectra within a 45 s time period.

Basically the background subtraction operation is a ratio between the sample spectrum and the background spectrum, both normalized to its lower absorption intensity value, in order to have only positive values centered around 1, where unity corresponds to a perfect match between sample and background (i.e. no sample absorption). All values are then displayed by TDLWintel in a one-thousand scale. The operation is applied to all spectrum points except the first point and the cutoff points, where the 0 value is set by default. Figure 2.8 illustrates the main steps of the background subtraction process.

2.3.3.2 Fitting the spectra and estimating the mixing ratio

There are three steps required to define a spectral fit. (1) fit markers must be placed on the spectrum, then (2) the species specific fitting parameters and the operating conditions (p, T, pathlength) must be defined, and eventually (3) the laser tuning rate must be defined (for fingerprint fits).

Fit markers are placed on the spectrum to define the types of fits desired and the locations for those fits. Each fit must have a marker which defines the beginning of the fit and a marker which defines its end. Other markers are used to define the regions between spectral peaks (baseline regions), the positions of peaks and the region where the

laser is turned off (zero). A detailed and exhaustive description of the procedure for defining a valid set of fit markers is given in the TDLWintel manual [26].

Fingerprint fits are the preferred method for fitting spectral data in TDLWintel. These fits use Voigt line profiles where the Voigt lineshape parameters are fixed and are determined from first principles (the tuning rate, the spectroscopic parameters, pressure and temperature) but are not parameters of the fit. Fingerprint fits take full advantage of and require complete knowledge of the species spectroscopy (for example from the HITRAN database[27-30]). At the start of a fingerprint fit, the program calculates a spectral template for each species in the fit. This template can be quite complex, consisting of up to 100 individual lines each described by a Voigt line profile. The calculation of this template requires knowledge of the temperature, the pressure and the tuning rate function for the laser. The unknowns in the fit are simply the mixing ratios of each species and the definition of the frequency scale - that is the absolute frequency of any one point in the spectrum.

The laser tuning rate must be defined to execute fingerprint fits, and this can be done in the way described previously, using TDLWintel tuning rate utility (see equation (16)) In general, to execute an effective and reliable fit, the baseline should be as wide as possible, in order to have more points in between the beginning and the end of the fit for the procedure; in addition, the polynomial used for the fit should be adequate to simulate the baseline (there are instances for which a polynomial of 4^{th} or 5^{th} degree is required).

If the baseline is simulated effectively, and the fitmarkers are well placed, the fit automatically returns the mixing ratio of the absorption species.

Generally TDLAS systems are limited in sensitivity not by laser or detector noise but by optical fringes superimposed on the measured spectrum [13]. These fringes result from unwanted etalons formed by reflections and scattering in the optical system and take the form of an approximately sinusoidal variation of the background signal with a period equal to the free spectral range (FSR) of the etalon. Sometimes these fringes can be reduced by careful optical design and adjustment, but it is usually a difficult and challenging step, as we verified testing many different optical arrangements. This is why the net spectrum (i.e. after the background subtraction) sometimes presents a baseline that is not flat, and therefore requires a higher degree polynomial.

2.3.3.3 Estimating the temperature

Based on the principles illustrated earlier in paragraph 2.3.1, in order to estimate the temperature of the absorbing gas, a pair of distinct absorption lines must be available in the working mode range of the laser.

Table 2.2 summarized the characteristics of the D_2O and H_2O absorption lines on which we focused our attention. In particular the D_2O lines with frequency equal to 1321.29 (two overlapping lines) and 1321.64 have been made available in the same working mode and display frequency range during our experiments by fine tuning the current intensity and the operating temperature of the diode laser. This is, unfortunately,

a procedure that has to be performed each time, because of the natural working drift of the instrument.

In order to spectroscopically measure the temperature following the proposed procedure, we performed a fit on each absorption line of the pair, taking care to compensate for the change in the base line due to mutual inference of the two lines, by creating two fictitious parameter files (*.hit files) containing only the line under investigation in the TDLWintel software. Next, a normal fit was performed using the same procedure detailed earlier in this paragraph.

Having fit both lines, the temperature (which is normally imposed from calculations based on inversion of the pressure traces measures) was varied until both fits gave the same mixing ratio (the mixing ratio has to be exactly the same, since the measure taken by the two lines is concurrent). This was possible because the TDLWintel software was able to simulating one substance (D_2O), but perform two different fits, with separate fitmarkers and using two different *.hit files, thus virtually implementing two distinct fits for two distinct substances. The process is illustrated in Figure 2.9, where a snapshot of the TDLWintel software is provided.

The temperature calculated this way was directly used to calculate a new mixing ratio (this is implicit in the procedure) and different results arise than from a normal (single absorption line) TDL experiment. However, as will be shown in the following, these new values are extremely close to the previous ones, even when the spectroscopic predicted temperature is significantly different from the pressure trace data inversion estimation.

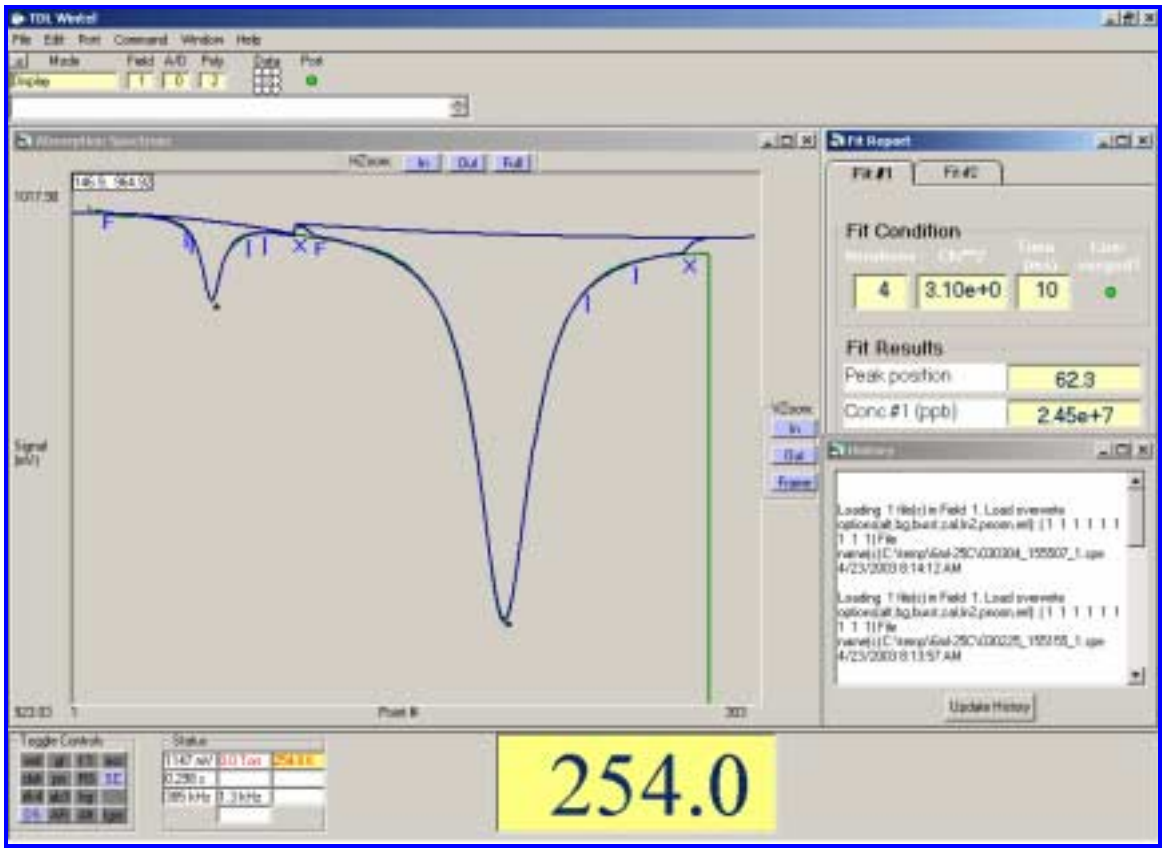

Figure 2.9 - TDLWintel (revision 5.27) - Temperature estimation procedure.

3 RESULTS AND DISCUSSION

3.1 PRESSURE TRACE RESULTS

Many experiments were conducted with different assemblies of the same nozzle. We used clear and opaque (rough-surface) windows and antireflective coated windows, and every time, in order to replace them, the nozzle has been disassembled and reassembled, in some cases using different sidewalls (the CaF_2 windows are very fragile and since they are glued to the sidewalls the procedure to detach them is usually very uncomfortable. For this reason it has been preferred to prepare specific sidewalls for each kind of window). The nozzle used in this experimental work (see Appendix A) was designed to match our standard nozzle (Nozzle A) that has been widely used in pressure traces, light scattering and SANS experiments by our group. Although the desired expansion ratio was carefully defined, the expansion rate changed for each set of sidewalls.

Figure 3.1 illustrates the nozzle profile measured for the assembly with antireflective coating on the windows. This is the assembly used for the pressure trace and TDL experiments that are discussed in this chapter. Tables 3.1 and 3.2 summarize the stagnation and onset conditions obtained from the pressure trace experiments for H_2O and for D_2O, respectively. In both cases experiments were carried out at two different stagnation temperatures with T_0 corresponding to 25 ± 0.05 ^oC and 35 ± 0.05 ^oC, while the stagnation pressure used, p_0, was always set equal to 60.4 ± 0.07 kPa.

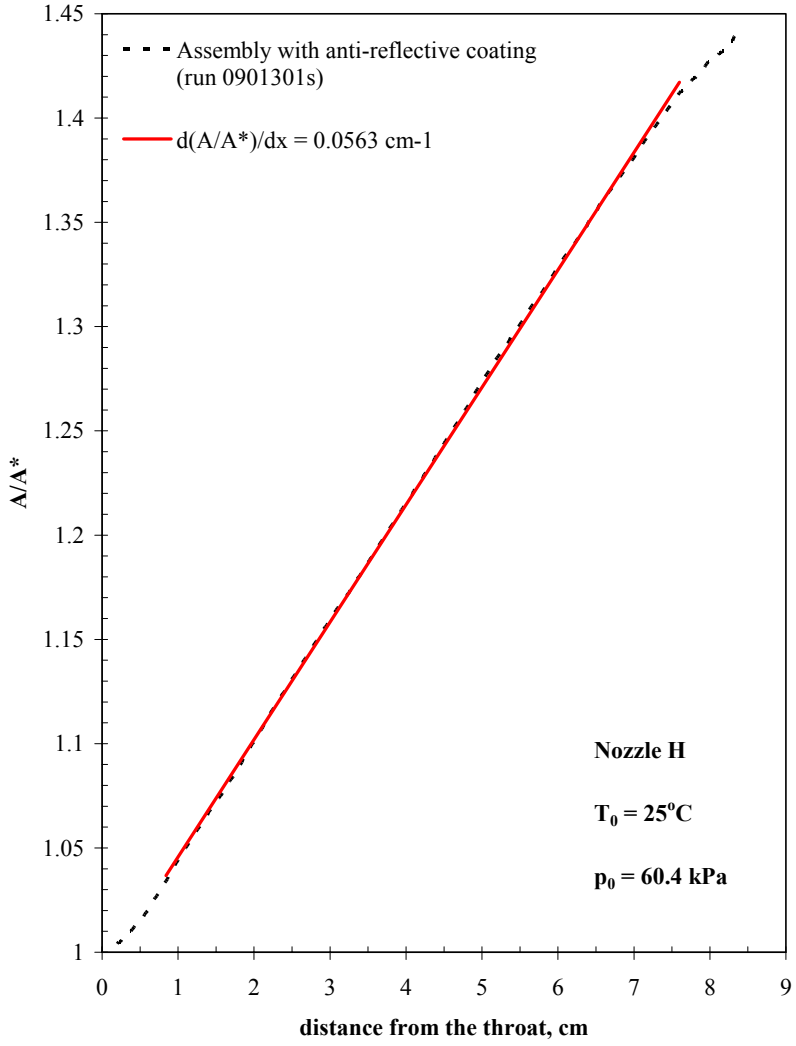

Figure 3.1 - Expansion ratio for the nozzle assembly with antireflective coating

Table 3.1 - Stagnation and onset conditions for the H_2O experiment.

Stagnation Conditions				Onset Conditions			
p_0, kPa	T_0, °C	$\dot{m}_v$, g/min	p_{v0}, Pa	p_v, Pa	T_{on}, K	x_{on}, cm	File name
	dry				dry		1001301s.txt
60.44	25.03	2.653	523.26	158.67	212.49	2.5	1001302s.txt
60.41	25.03	3.322	654.88	213.54	216.94	2.0	1001303s.txt
60.42	25.00	3.969	782.67	269.06	220.22	1.7	1001304s.txt
60.42	25.02	5.271	1039.33	393.85	226.45	1.2	1001305s.txt
60.43	25.01	5.254	1036.25	393.85	226.63	1.1	1001306s.txt
60.45	25.02	6.554	1292.96	526.10	231.10	0.8	1001307s.txt
60.44	25.01	9.164	1807.66	827.76	238.98	0.4	1001308s.txt
	dry				dry		1301301s.txt
60.41	35.05	2.640	539.32	142.03	211.00	3.6	1301302s.txt
60.44	35.04	3.319	678.30	193.18	215.77	3.0	1301303s.txt
60.44	35.02	3.970	811.45	242.57	218.77	2.6	1301304s.txt
60.45	35.03	5.268	1076.87	351.10	224.28	2.0	1301305s.txt
60.45	35.04	6.551	1339.18	469.60	229.01	1.6	1301306s.txt
60.39	35.04	9.105	1859.45	724.26	236.02	1.0	1501308s.txt
	dry				dry		0901301s.txt
60.40	25.03	1.342	263.99	65.69	200.83	4.1	0901302s.txt
60.41	25.02	2.005	394.51	111.23	208.11	3.1	0901303s.txt
60.40	25.00	2.662	523.70	160.36	213.06	2.4	0901304s.txt
60.40	25.02	3.975	782.06	272.08	220.98	1.6	0901305s.txt
60.43	25.01	5.296	1042.42	401.10	227.43	1.1	0901306s.txt
60.42	25.02	7.908	1556.23	688.81	236.69	0.5	0901307s.txt
	dry				dry		1501301s.txt
60.42	35.04	1.423	278.31	60.56	199.77	5.4	1501302s.txt
60.45	35.04	2.054	401.90	97.94	206.35	4.3	1501303s.txt
60.39	35.04	2.684	524.69	138.06	210.93	3.6	1501304s.txt
60.41	35.04	3.957	773.80	230.19	218.47	2.6	1501305s.txt
60.42	35.03	5.244	1025.62	333.45	224.09	2.0	1501306s.txt
60.42	35.04	7.806	1526.55	562.21	232.25	1.3	1501307s.txt

The data presented in this work were measured during several different sessions, but the experimental setup and the procedures correspond to those discussed in the previous chapters. To summarize the onset data, it is useful to present them in a log p vs T plot (Wilson Plot), as it is done in Figure 3.2 for both H_2O and D_2O.. The same H_2O data are also presented in Figure 3.3, together with other data from a number of supersonic nozzle experiments performed over the years by many different authors. Despite the time gaps

and in many cases the different techniques used, all of the points show a substantial agreement as they clearly appear tightly clustered around the same curve [5, 12, 36-40].

Table 3.2 - Stagnation and onset conditions for the D_2O experiment.

Stagnation Conditions				Onset Conditions			
p_0, kPa	T_0, °C	$\dot{m}_v$, g/min	p_{v0}, Pa	p_v, Pa	T_{on}, K	x_{on}, cm	File name
		dry			dry		2301308s.txt
60.41	25.03	1.417	253.41	67.66	204.90	3.5	2301302s.txt
60.41	25.02	2.103	376.13	112.84	211.83	2.6	2301303s.txt
60.47	25.02	2.797	500.69	161.95	216.42	2.1	2301304s.txt
60.44	25.03	4.188	749.33	274.22	224.20	1.3	2301305s.txt
60.41	25.04	5.575	996.93	405.59	231.08	0.8	2301306s.txt
60.41	25.00	8.287	1482.20	685.72	239.64	0.4	2301307s.txt
		dry			dry		2401301s.txt
60.44	35.04	1.429	262.67	60.17	202.73	4.9	2401302s.txt
60.45	35.04	2.119	389.59	101.54	210.35	3.8	2401303s.txt
60.47	35.04	2.813	517.33	145.49	214.98	3.1	2401304s.txt
60.46	35.04	4.201	772.50	244.41	222.34	2.2	2401305s.txt
60.45	35.05	5.578	1025.53	354.02	227.98	1.7	2401306s.txt
60.43	35.04	5.585	1026.49	355.10	228.11	1.7	2401307s.txt
60.42	35.03	8.325	1529.99	595.00	235.89	1	2401308s.txt
		dry			dry		0301301s.txt
60.41	25.01	2.933	522.22	172.75	217.81	1.9	0301304s.txt
60.42	25.02	5.842	1040.87	432.56	232.48	0.8	0301302s.txt
60.43	25.01	8.723	1553.97	733.11	240.98	0.3	0301303s.txt

Data presented in Figure 3.2 and in Tables 3.1 and 3.2 show onset in between 0.3 and 5.4 cm downstream from the throat, for both H_2O and D_2O. The observed onset temperatures ranges from about 199 to about 240 K and over this short range the onset pressure is clearly an exponential function of the temperature, and the curves for H_2O and D_2O are almost parallel.

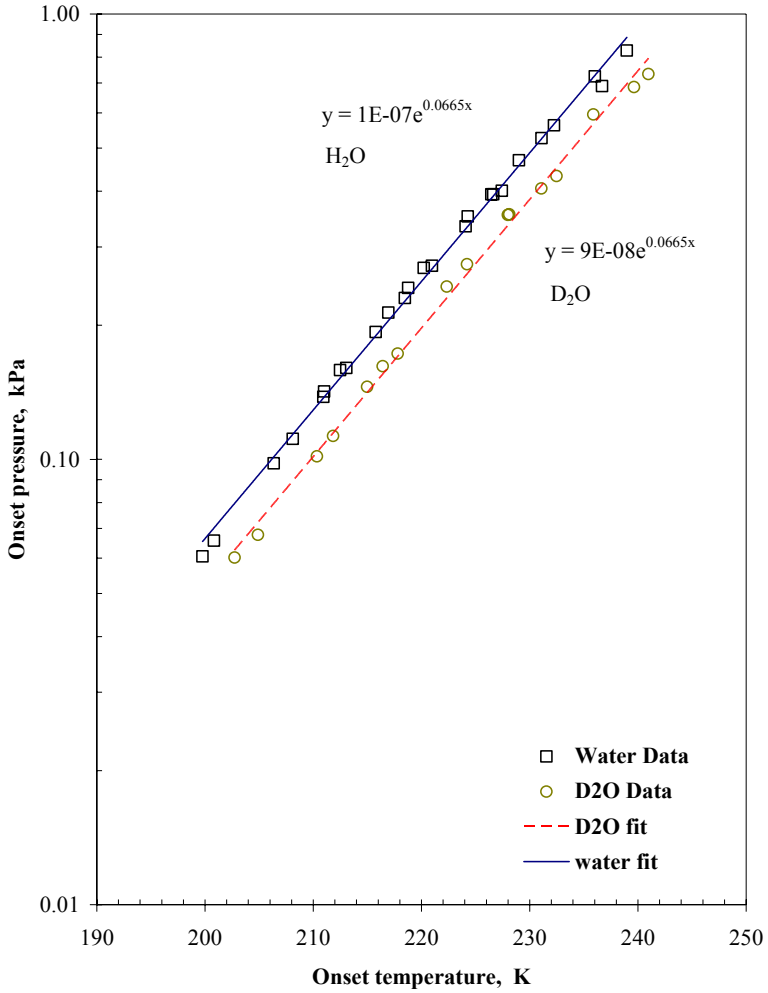

Figure 3.2 - Wilson plot of onset data of H_2O and D_2O for a constant p_0.

Figure 3.4 illustrates some of the pressure traces taken for the D2O experiments discussed above. The initial conditions correspond to the conditions used for the TDL experiments.

The specific position of the onset is one of the crucial parameters to validate and test by means of the TDL experiment. We observe that maintaining T_0 fixed, the onset

occurs earlier as the amount of condensible increases. If the condensible flowrate is maintained fixed, we observe that the position of the onset shifts downstream as the temperature increases. This makes sense since at higher temperature the supersaturation is lower, given a fixed amount of condensible material. At higher temperature the density of the carrier gas is also lower, therefore the same amount of condensible represent a bigger fraction of the total stream. This would push the position of the onset upstream, but it has a much smaller effect.

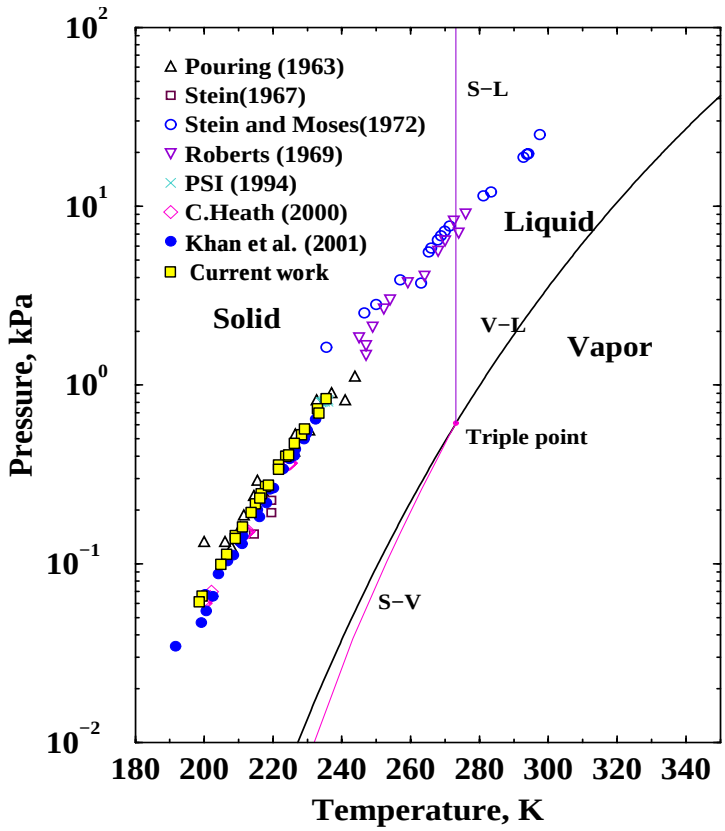

Figure 3.3 - Wilson plot of onset data of H_2O from supersonic nozzles experiments [5, 12, 36-40].

The goal for the pressure trace experiments were to determine the condensible mixing ratio profile along the nozzle: this allows us to directly compare the mixing ratio measurements taken with the TDL instrument to those derived from the pressure observations.

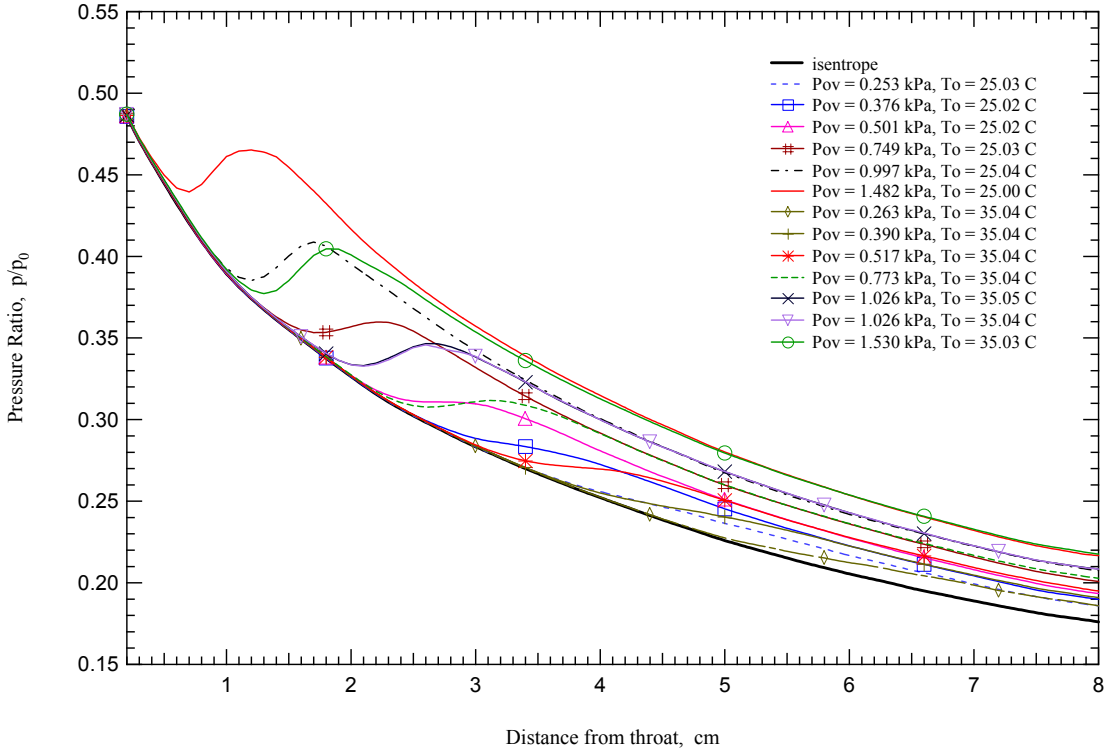

Figure 3.4 - Pressure traces for D_2O experiments.

3.1.1 Vapor phase mixing ratio

The vapor phase mixing ratio can be calculated as a function of the position along the nozzle from the pressure trace observations and the quantities derived, as discussed in the experimental section. The concentration is expressed as a mixing ratio in parts per billion

in volume. Here are presented the same flowrates used in the TDL experiment. As will be detailed in the following chapters, we worked at 2 different temperatures and 3 different flowrates.

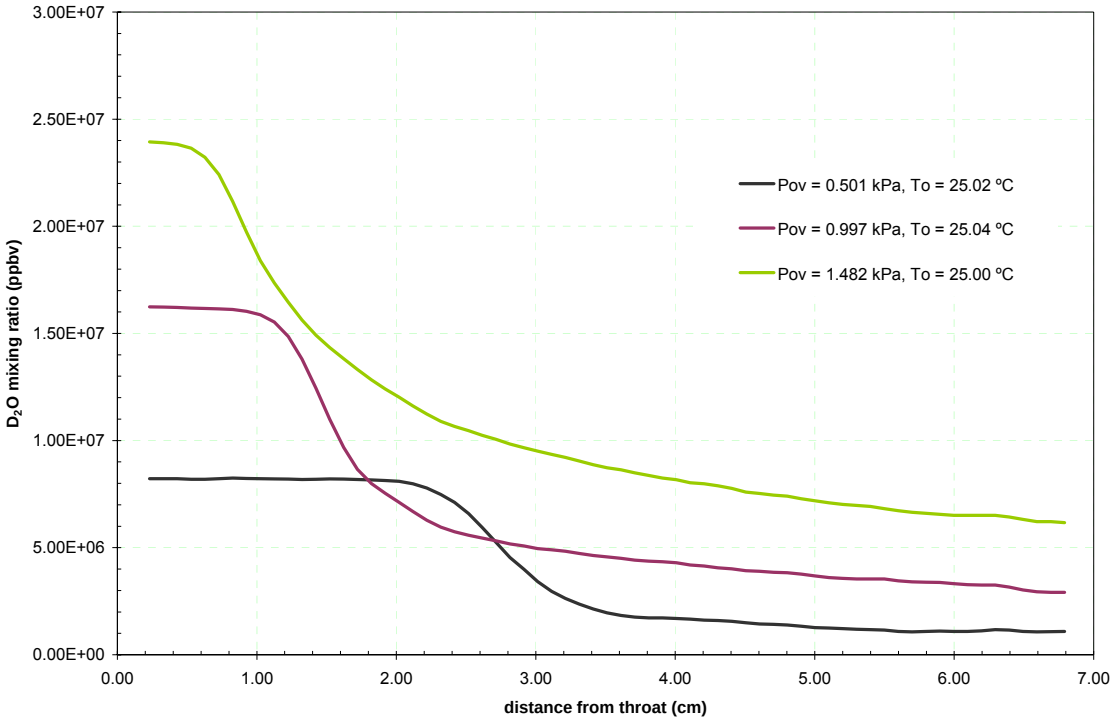

Figure 3.5 - D_2O mixing ratios derived from the pressure traces for the T_0 = 25 ^oC case.

Figures 3.5 and 3.6 show the calculated mixing ratios for the 25 and the 35 ^oC runs respectively, for the 3 different flowrates useful to compare the results with the TDL experiments.

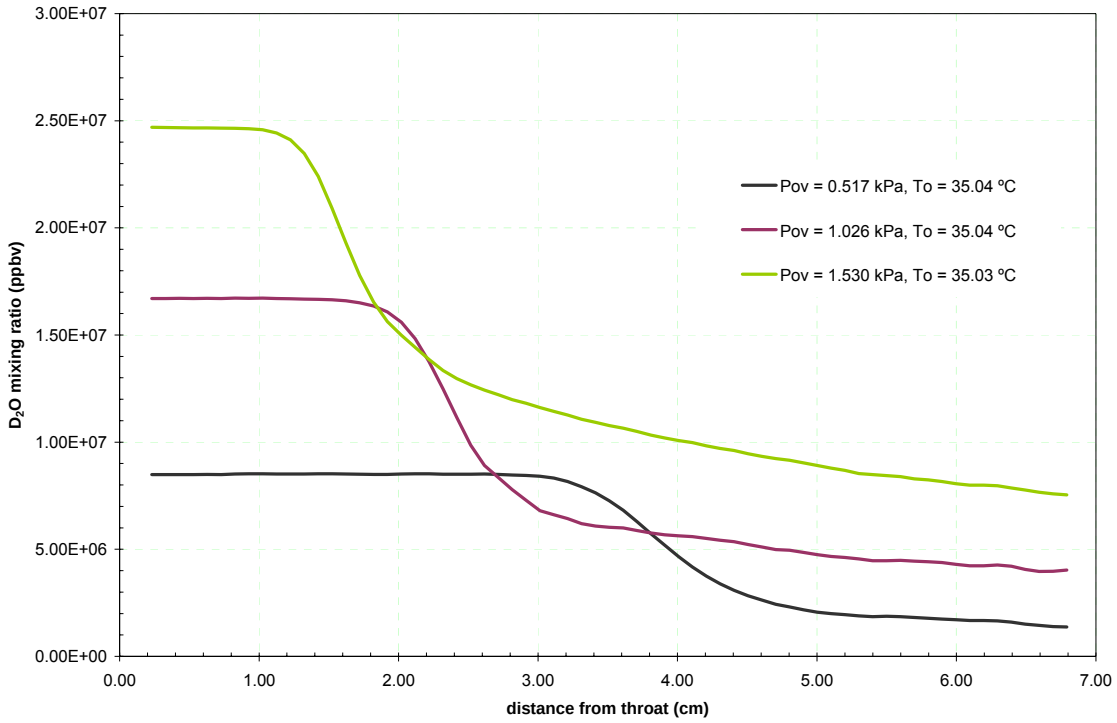

Figure 3.6 - D_2O mixing ratios derived from the pressure traces for the T_0 = 35 ^oC case.

The two sets of experiments (at 25 and 35 ^oC) have been developed at fixed flowrates of the peristaltic pump: 1, 1.5, 2, 3, 4 and 6 ml/min, corresponding to mass flowrates of 1.4, 2.1, 2.8, 4.2, 5.6, 8.3 g/min respectively (see the peristaltic pump calibration factors in Appendix D). The resulting initial vapor pressure P_{v0} of the condensible is slightly different due to the difference in temperature.

The possibility to closely control the condensible flowrate and the initial conditions ensure the reproducibility of the results and the correct interpretation of the TDL experiments conducted using the same equipment. Normally, as shown in Tables 3.1 and

3.2, the temperature control system used allows us to keep the temperature differences between any two experiments to less than 0.05 K. The pressure control is very good as well, and normally the stagnation pressure difference with the set point is kept below 0.07 kPa (less than 0.2% of the nominal value).

3.2 LASER ABSORPTION RESULTS

As discussed in the previous sections, the main goal of the present work is to measure the gas phase mixing ratio of the condensible vapor. This target, important as it is by itself, is only a piece of a bigger puzzle which includes the possibility to predict the conditions required to initiate phase transitions, the rate at which transition occurs and the structure of the final droplets.

The theoretical approach has been discussed in the experimental section. In the following, the results of the application of this new TDL technique to the problem of monitoring gas mixing ratios in the nozzle are presented.

3.2.1 Vapor phase mixing ratio

Following the approach presented in Paragraph 2.3, the D_2O mixing ratio is obtained from the background-subtracted spectra fitted to a Voigt lineshape function. Figures 3.7 and 3.8 show the results of the fitting procedure and the returned values for the mixing ratio, in the T_0 = 25 and 35 ^oC case, respectively. These results are compared with the values predicted by the data inversion of the pressure traces data for the same stagnation conditions and condensible flowrates. Table 3.3 summarize the set of runs performed.

All the experiments discussed here were performed using Laser B and looking at the absorption line with molecular transition frequency equal to 1321.64 cm^{-1}, a strong D_2O absorption line within the working range of our TDL instrument. The spectroscopic

information for this particular absorption line have been derived from reference 33 and the values have been calibrated according to the procedure described in Appendix D.

Prior to condensation, the D_2O mixing ratios obtained from the TDL experiment show very good agreement with the data derived from the pressure trace measurements. The onset of condensation for the TDL experiments is shifted somewhat downstream of equivalent pressure trace experiments, especially for the higher condensible flow rate experiments, and the agreement becomes progressively worse farther downstream. The reason for poor agreement far downstream is the appearance of fringes caused mainly by the fact that the pressure and temperature in the sample (with condensation) are different than those in the background (no condensation).

Most important, the values of mixing ratio derived from the TDL experiments systematically show a higher degree of condensation after the onset (or a lower residual gas phase concentration).

All the previous remarks are clearly depicted in Figures 3.9 and 3.10, where the ratio of the mixing ratios derived from the TDL experiments and the pressure trace experiments are plotted as a function of the distance from the throat. Before the onset of condensation the ratio is very close to the unity, and the error is confined inside a ± 5% boundary (dashed lines). After the onset of condensation we have a little peak (caused by the "shift" discussed above) and then the values of the mixing ratios from the TDL experiments fall down to about 35-40% of the values predicted by the pressure traces.

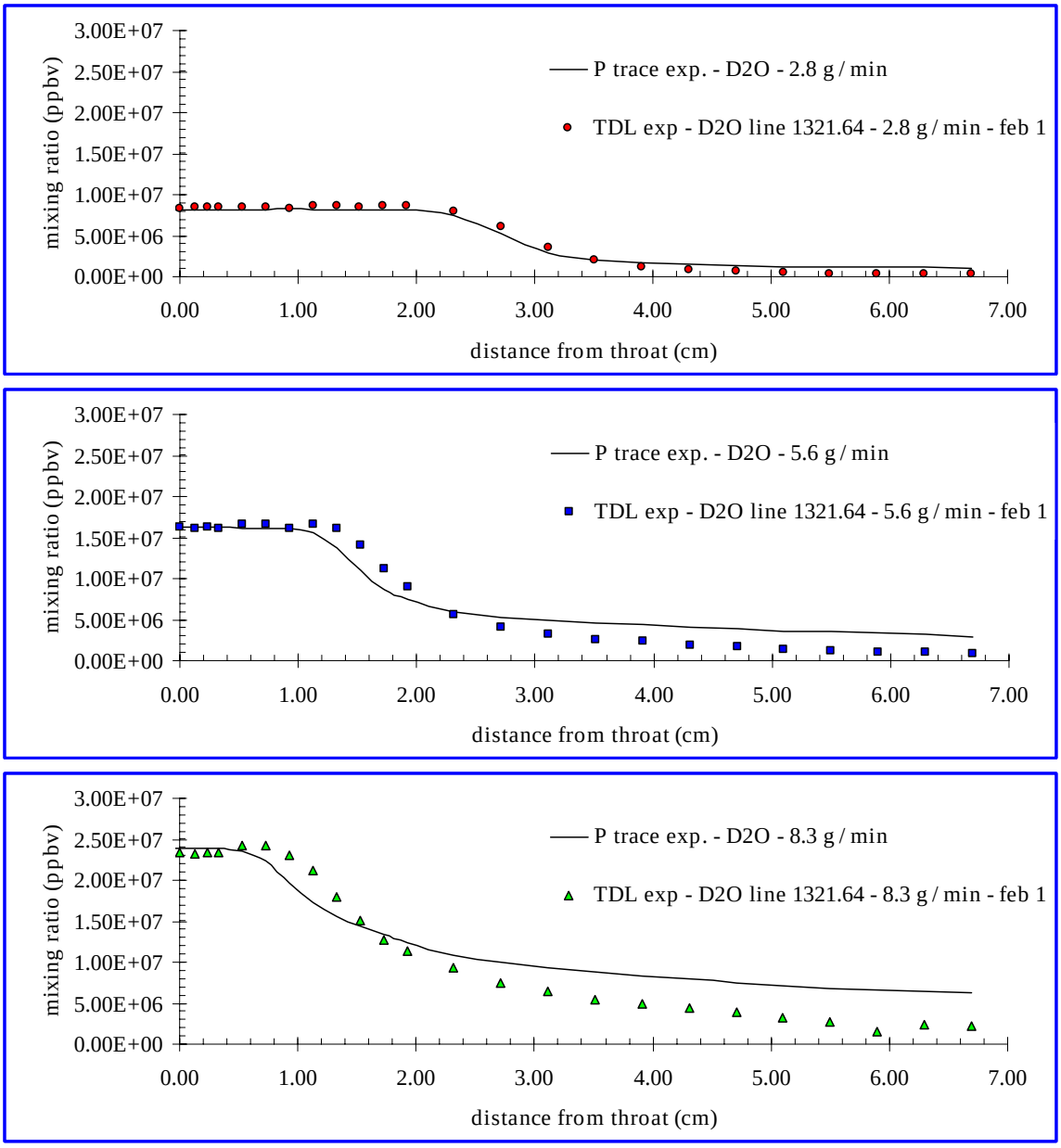

Figure 3.7 - D_2O mixing ratios derived from the TDL experiment and comparison with the corresponding mixing ratios from the pressure traces for the T_0 = 25 ^oC case.

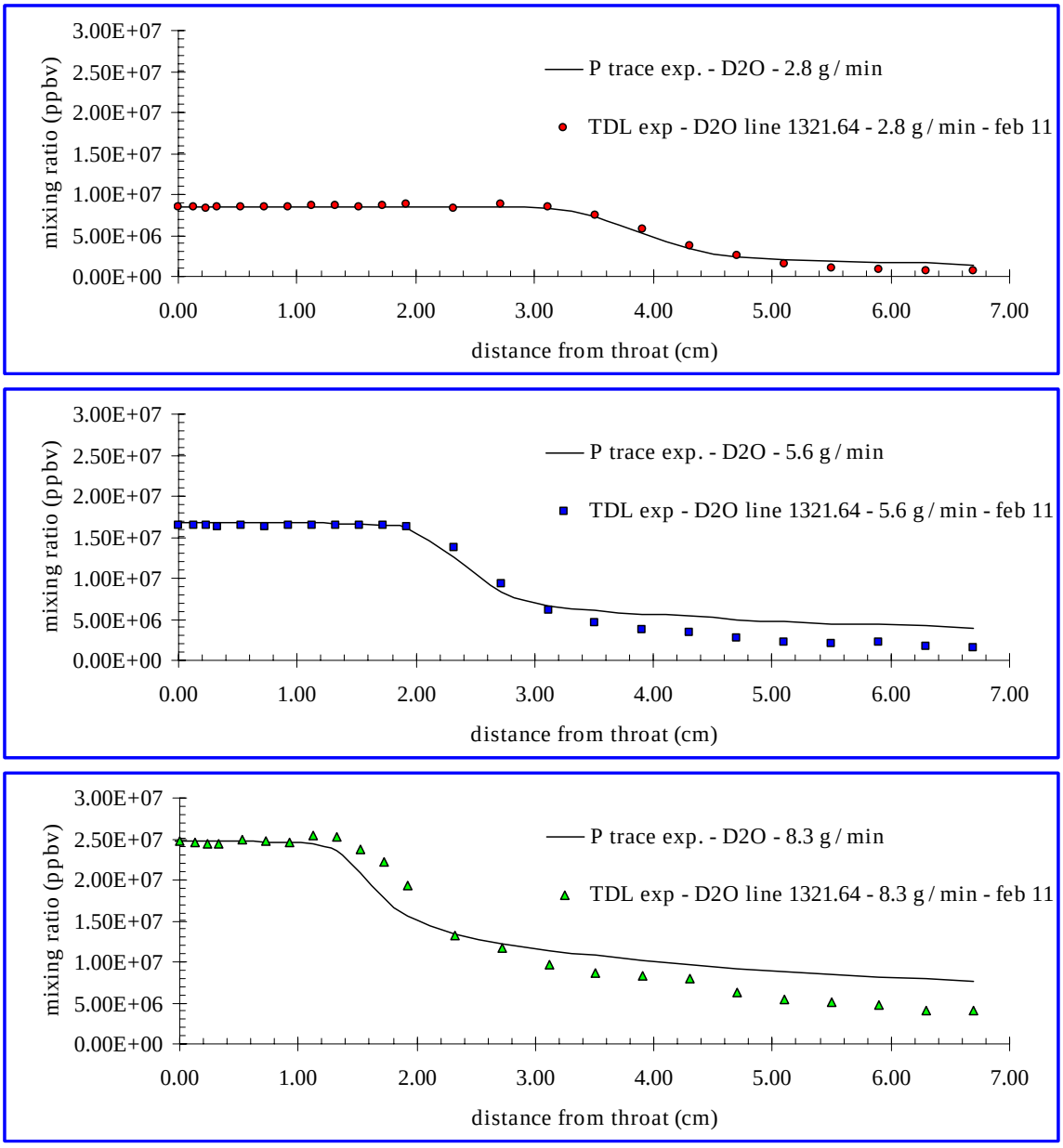

Figure 3.8 - D_2O mixing ratios derived from the TDL experiment and comparison with the corresponding mixing ratios from the pressure traces for the $T_0 = 35\ ^oC$ case.

Table 3.3 - Pressure traces and TDL experiments summary

pressure trace experiment	Initial mixing ratio (ppbv)	run id.	TDL experiment	Initial mixing ratio[(a)] (ppbv)	run id.
Pov = 0.501 kPa, To = 25.02 ºC	8.21E+06	2301304s.txt	TDL exp - D_2O line 1321.64 - 2.8 g/min - feb 1	8.48E+06	020103_2ml
Pov = 0.997 kPa, To = 25.04 ºC	1.62E+07	2301306s.txt	TDL exp - D_2O line 1321.64 - 5.6 g/min - feb 1	1.63E+07	020103_4ml
Pov = 1.482 kPa, To = 25.00 ºC	2.39E+07	2301307s.txt	TDL exp - D_2O line 1321.64 - 8.3 g/min - feb 1	2.38E+07	020103_6ml
Pov = 0.517 kPa, To = 35.04 ºC	8.48E+06	2401304s.txt	TDL exp - D_2O line 1321.64 - 2.8 g/min - feb 11	8.54E+06	021103_2ml
Pov = 1.026 kPa, To = 35.04 ºC	1.67E+07	2401307s.txt	TDL exp - D_2O line 1321.64 - 5.6 g/min - feb 11	1.64E+07	021103_4ml
Pov = 1.530 kPa, To = 35.03 ºC	2.47E+07	2401308s.txt	TDL exp - D_2O line 1321.64 - 8.3 g/min - feb 11	2.49E+07	021103_6ml

(a) Calculated as average over the values registered before the onset of condensation, using the calibrated spectroscopy parameters (see Appendix D).

Some hypothesis have been formulated about the reasons for the appearance of the "shift" of the onset position. Most likely the differences in between the conditions at which the TDL experiments is carried out with respect to the pressure trace experiment are responsible. These are not operating conditions (which are very accurately reproducible), but intrinsic conditions, such as the presence or absence of the probe inside the nozzle. The presence of the probe reduces the cross sectional area (altough in minimal part) and therefore, during a TDL experiment, the same amount of condensible is more diluted and this in theory shift the onset downstream. Moreover, the expansion ratio also changes, giving virtually for the two experiments a slightly different nozzle [ref. 12]. An exhaustive study of the way these small differences affect the position of

the onset requires both more experiments and a more complete analysis and these are out of the main scope of this work.

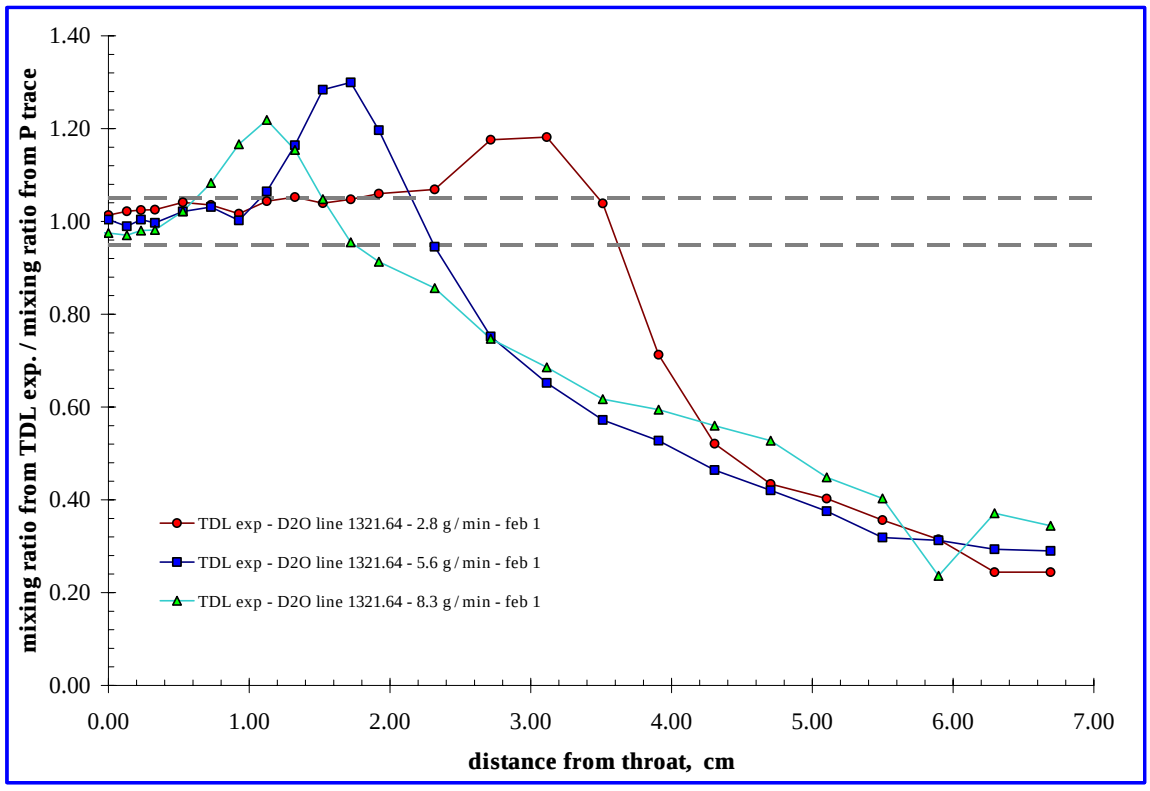

Figure 3.9 - ratios of D_2O gas phase mixing ratios from the TDL experiments to gas phase mixing ratios from the pressure trace experiments as a function of the position along the nozzle, for the $T_0 = 25^oC$ case.

The final values of mixing ratio observed during a TDL experiment are about 35-40% of the values derived from the pressure trace experiments. This trend is observed consistently in all of the experiments (using either D_2O or H_2O and for several different

absorption lines), and it is, therefore, necessary to investigate further the reason of such disagreement.

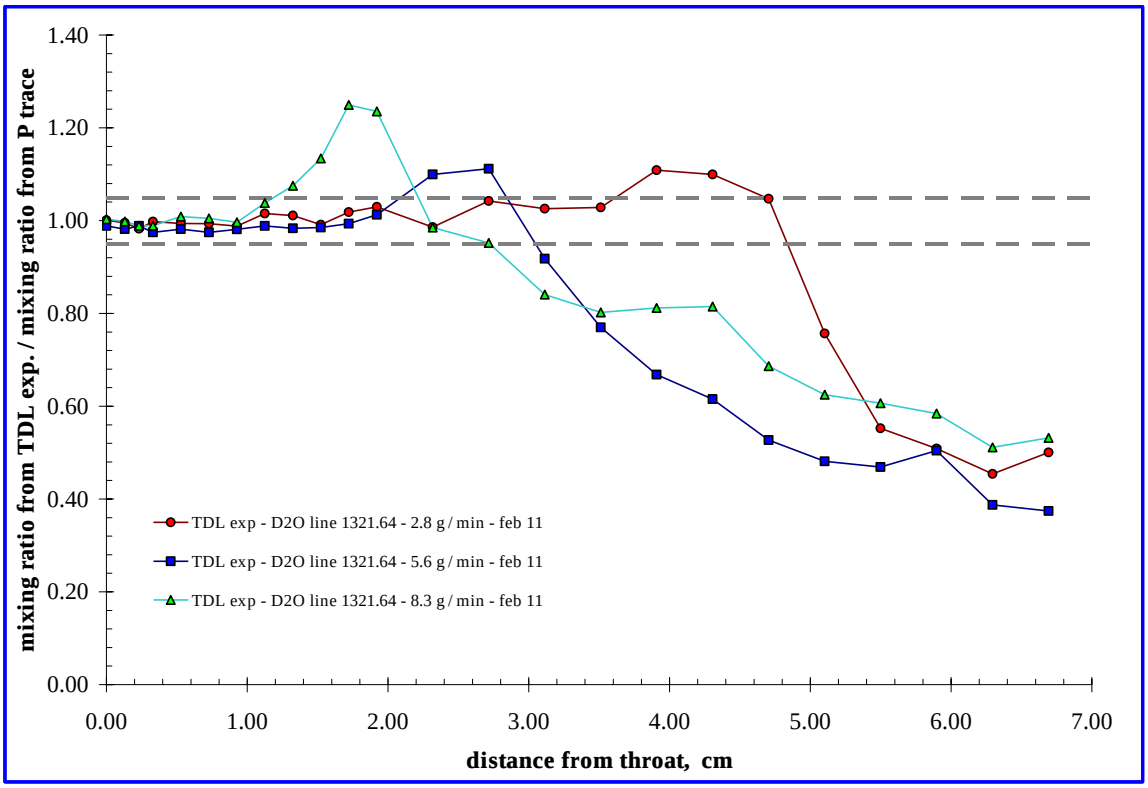

Figure 3.10 - ratios of D_2O gas phase mixing ratios from the TDL experiments to gas phase mixing ratios from the pressure trace experiments as a function of the position along the nozzle, for the $T_0 = 35^oC$ case.

As often described in the previous sections, the transition from vapor to liquid is accompanied by the latent heat release to the flow, thus the deviation of the state variables from the isentropic values. Of all the state variables, we measure the pressure by means of the pressure trace. From the pressure profile inside the nozzle we derive the unmeasured properties of the condensing flow using the diabatic flow equations (that are

integrated in a form with pressure, area ratio, stagnation pressure and temperature as the known quantities [6]) and doing this, we need to know the value for the latent heat at the phase transition conditions. This value for the latent heat [9, 41] presents a certain degree of uncertainty for substances like H_2O and D_2O, in our temperature range far below 0 ^oC.

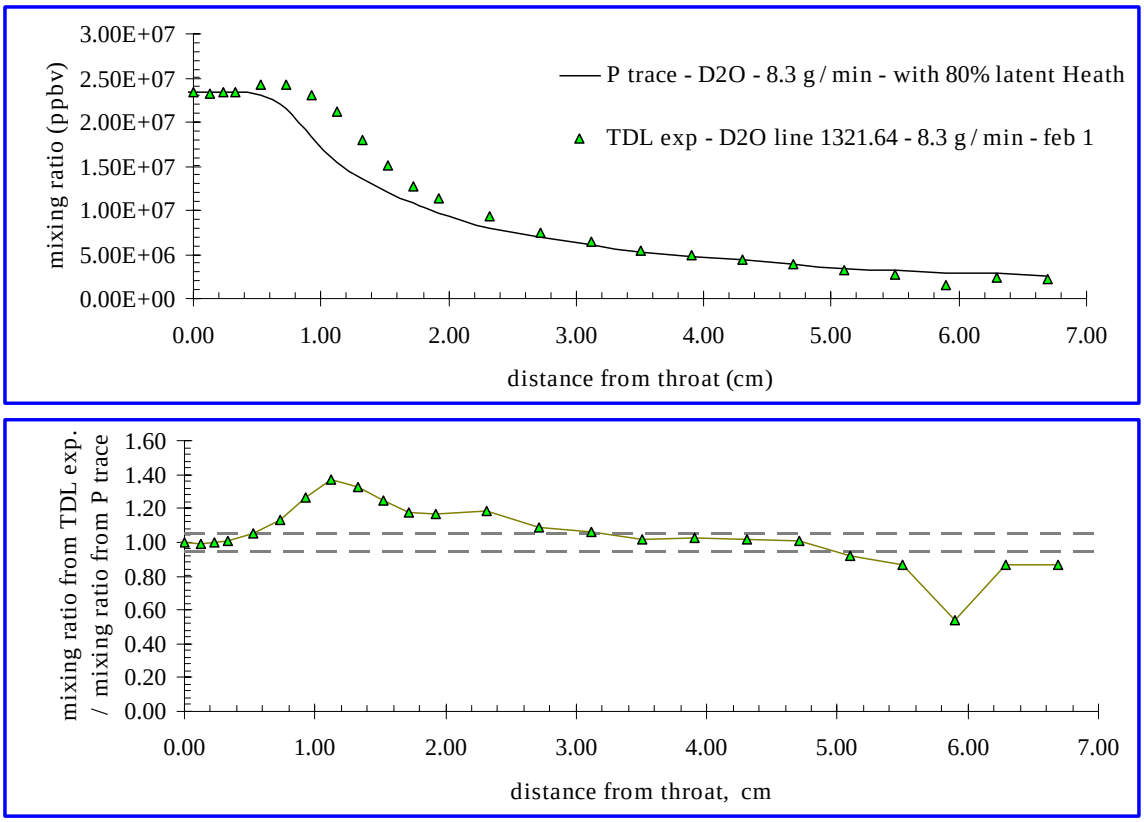

Figure 3.11 - D_2O mixing ratios derived from the TDL experiment and comparison with the corresponding mixing ratios from the pressure traces for the T_0 = 25 ^oC case, 8.3 g/min D_2O, using only 85% of the latent heat.

In fact, if we simply reduce the latent heat of D_2O to 85% of the value currently used in the data inversion program, the agreement between the TDL and pressure trace experiments is greatly improved. A typical results is shown in Figure 3.11 for the case 8.3 g/min D_2O, p_0 = 60.4 kPa, T_0 = 25 ^oC.

Although we have no firm proof that this is the actual reason, the TDL experiment can surely represent a valid instrument of investigation in this problem.

3.2.2 Temperature estimation

Using the technique described in Chapter 2, the very first direct spectroscopic measure of the D_2O vapor flow temperature in a supersonic nozzle was carried out. The strategy for measuring the temperature of the gas phase is based on the direct comparison of the intensity of two absorption lines, whose ratio, for a given pair of lines, is a function of temperature only [19].

Figure 3.12 illustrates the temperature inferred for the T_0 = 25 ^oC case for 2.8, 5.6 and 8.3 g/min of D_2O. Figure 3.13 reports the results for the T_0 = 35 ^oC case. In both cases, before and just after the onset of condensation agreement between the TDL and pressure trace experiments is quite good. Further downstream, the TDL experiments predict higher values for the temperature, and the values are much more scattered. This is in part due to the complications in performing a good fit that follows the appearance of strong fringes in the absorption spectrum and weak absorption by the D_2O as the vapor is depleted from the gas stream.

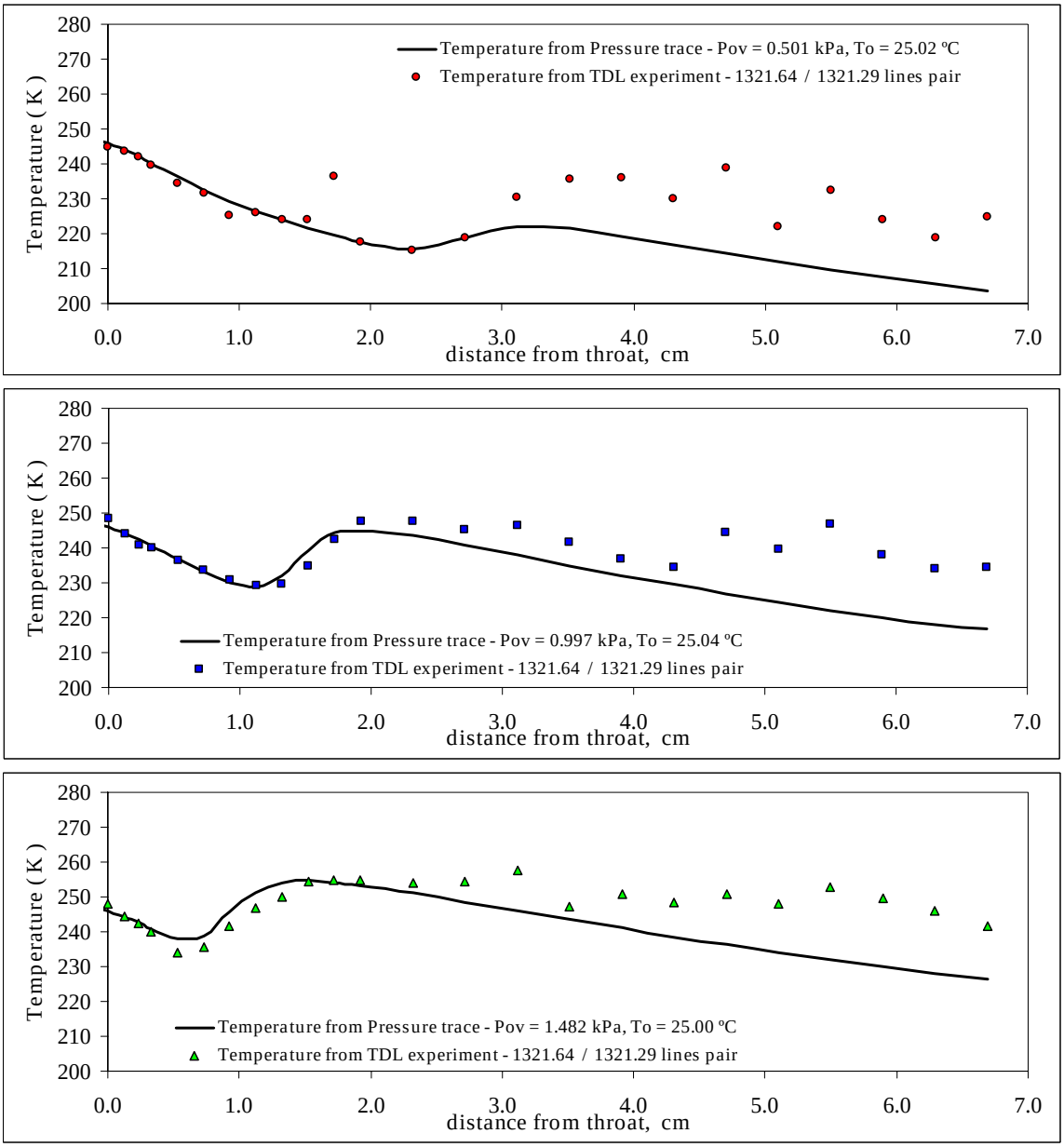

Figure 3.11 - Temperature versus distance from throat calculated from Pressure trace and TDL experiment, T_0 = 25 ^oC case.

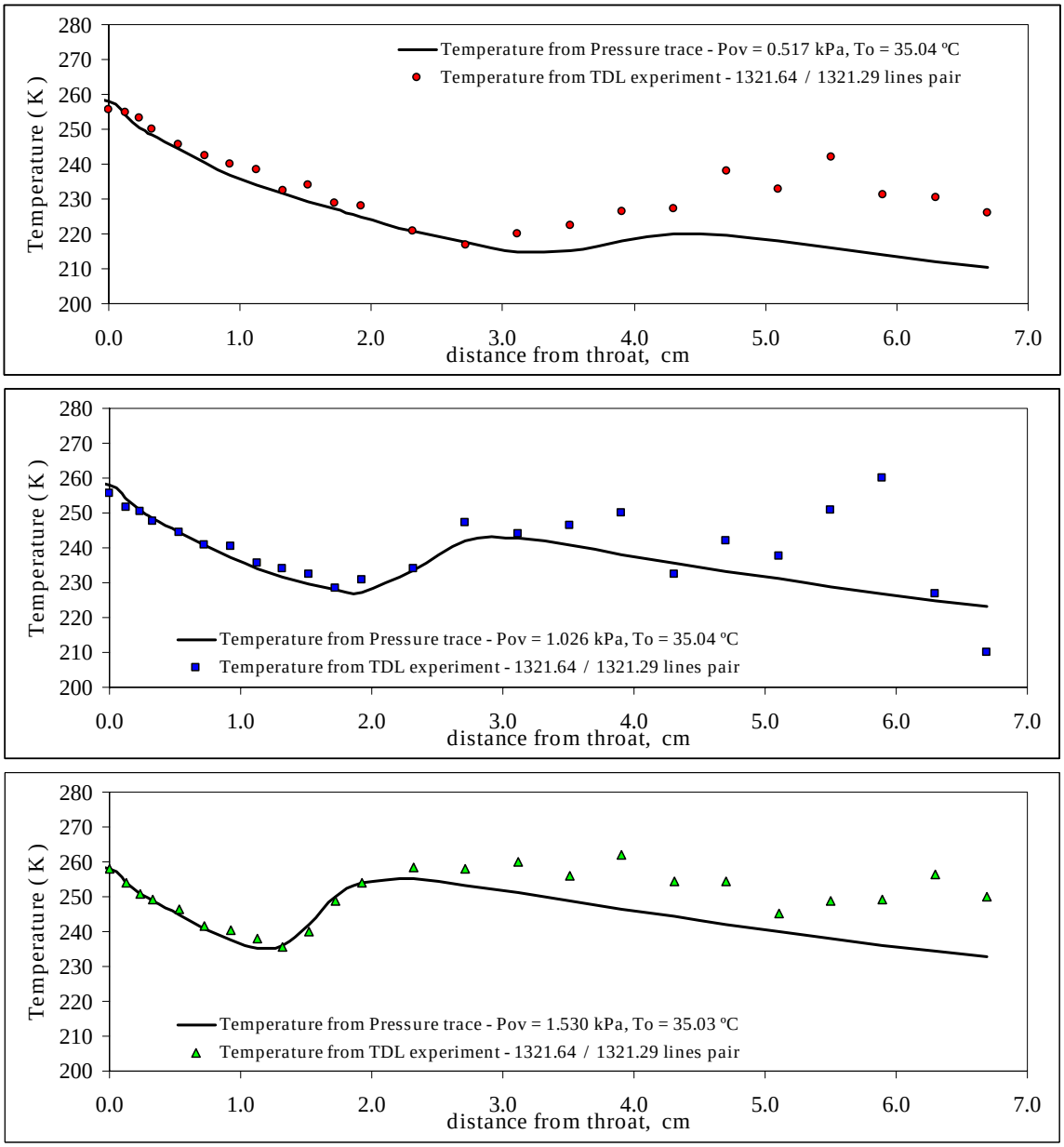

Figure 3.12 - Temperature versus distance from throat calculated from Pressure trace and TDL experiment, T_0 = 35 ^oC case.

The difference between the temperature derived from the TDL experiment and the temperature derived from the pressure trace is shown in Figure 3.13. Here is possible to

see that the difference increases after the onset to more than +5% in most cases, but is always less than +20%.

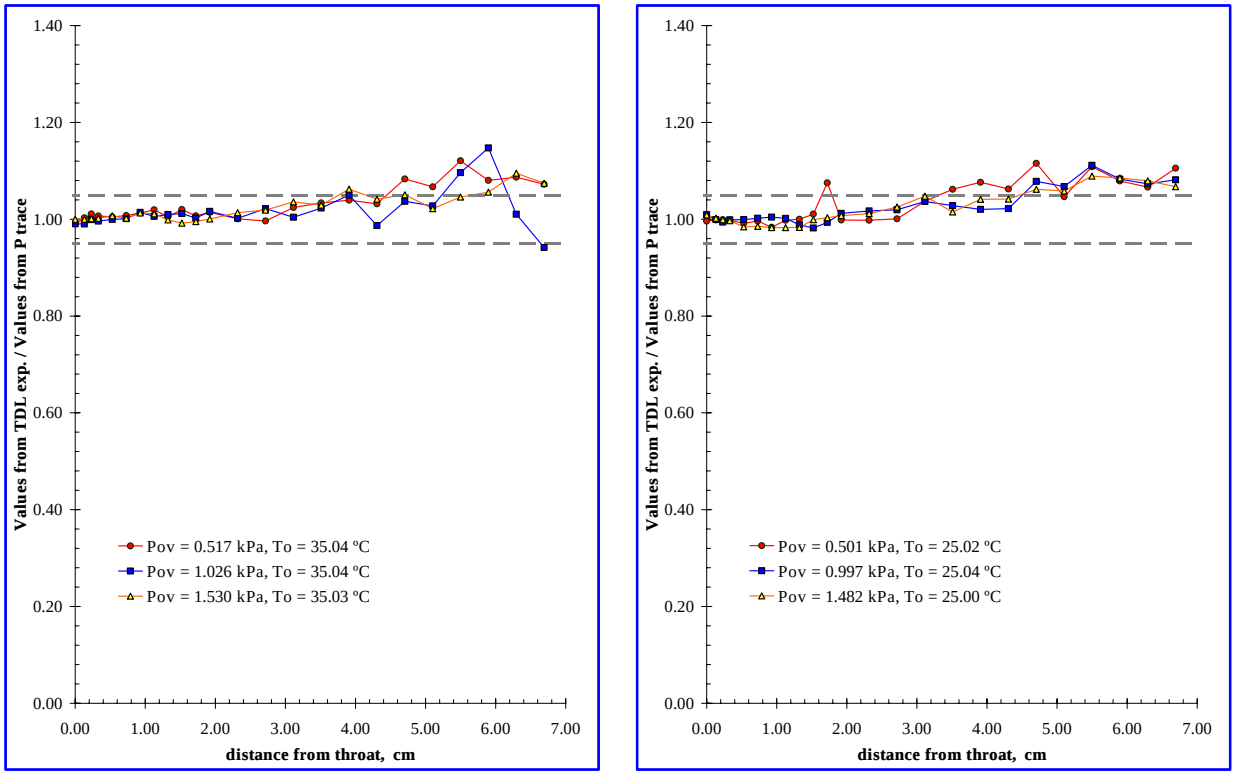

Figure 3.13 - Ratios of Temperature calculated from Pressure trace and TDL experiment for D_2O at selected flowrates versus distance from throat.

After deriving the temperature from the TDL experiment, it is possible to input this calculated temperature to obtain the mixing ratio (the TDL Wintel software does actually this by default during the process of deriving the temperature). This procedure returns values for the mixing ratio that are only slightly different than those previously calculated using the temperature predicted from the pressure trace.

To better understand this, we note that the derived temperature values are dominated by the absorption line(s) with the biggest energy of the lower level of the transition (i.e. by the lines at molecular transition frequency equal to 1321.29 - see Table 2.2). Also we note that there is an order of magnitude difference in the linestrength between the absorption lines compared to derive the temperature. The more intense linestrength corresponds to the line with molecular transition frequency equal to 1321.64, which dominates the derived mixing ratios values, but is not very temperature sensitive.

Thus, even for relatively large changes in the temperature, the mixing ratio determined by using this line is not affected very much. This is obviously a problem due to the choice of absorption lines analyzed in this work. As remarked in Chapter 2, sometimes the possibility to work with a given pair of absorption lines is outside the direct control of the operator and depends on the peculiar characteristic of the Diode Laser.

The main problem, again, is given by the very complicated procedure of fitting a spectrum due to the fringes which occur at any position after the onset.

4 SUMMARY AND CONCLUSION

We have developed a nonintrusive technique to measure the vapor phase mixing ratio and temperature in supersonic flows based on high resolution absorption spectroscopy.

The system was tested using H_2O and D_2O to identify the problems and to develope a procedure to collect the data and calibrate the instrument. We observed depletion of the condensible species from the gas phase, and from the directly measured absorption spectra, we derived the temperature and gas phase mixing ratio.

Our results shows a very good agreement with data derived from pressure traces inversions up to the onset of condensation, after that, the spectroscopically predicted mixing ratio and temperature differ from the other techniques results significantly, and suggest new directions for future investigations.

Developing the system further, solving the issues that have been discovered and addressed, and eventually applying this procedure in conjunction with aerosol SANS can provide an opportunity to characterize the droplet composition, which is an essential step to clarify the complex multicomponent systems behavior.

5 REFERENCES

[1] Baron, P. A., Willeke, K., Aerosol Measurement - Principles, Techniques and Applications, Wiley & Sons, NY, 2001.

[2] NASA webpage: http://terra.nasa.gov/FactSheets/Aerosols/

[3] American Association for Aerosol Research webpage: http://www.aaar.org/

[4] Moses, C. A., Stein, G. D., "*On the growth of steam droplets formed in a laval nozzle using both static pressure and light scattering measurements*", Journal of Fluids. Engineering, Vol 100, 311, 1978.

[5] Wyslouzil, B. E., Wilemski, G., Beals, M. G., and Frish, M., "*Effect of Carrier Gas Pressure on Condensation in a Supersonic Nozzle*", Phys. Fluids, 6, 2845, 1994.

[6] Wyslouzil, B. E., Heath, C. H., Cheung, J. L., and Wilemski, G., "*Binary Condensation in a Supersonic Nozzle*", J. Chem. Phys.,113, 7317, 2000.

[7] Heath, C. H., Streletzky, K. A., Wyslouzil, B. E., Wölk, J, and Strey R., "*H2O-D2O condensation in a supersonic nozzle*", J. Chem. Phys., 117, 6176, 2002.

[8] Streletzky, K. A., Zvinevich, Y., Wyslouzil, B. E., and Strey, R., "*Controlling Nucleation and Growth of Nanodroplets in Supersonic Nozzles*" J. Chem. Phys. 116, 4058, 2002.

[9] Dieregsweiler, U. M., M.S. Thesis, Worcester Polytechnic Institute, 2001.

[10] Wyslouzil, B. E., Wilemski, G., Cheung, J. L., Strey R., and Barker, J., "*Doppler Shift Aniosotropy in Aerosol SANS*", Phys. Rev. Letters, 60, 4330, 1999.

[11] Wyslouzil, B. E., Cheung, J. L., Wilemski, G. and Strey, R., "*Small Angle Neutron Scattering from Nanodroplet Aerosols*", Phys. Rev. Letters, 79, 431, 1997.

[12] Khan, A., M.S. Thesis, Worcester Polytechnic Institute, 2001.

[13] Brassington, D. J., Tunable diode laser absorption spectroscopy for the measurement of atmospheric species, Imperial College of Science Technology and Medicine, 1995

[14] Okada, Y., Tanimura, S., Okamura, H., Suda, A., Tashiro, H., Takehuci, K., "*Vibrational spectroscopy and predissociation of UF_6 clusters in a supersonic Laval nozzle*", J. Mol. Struct., 410-411, 299-304, 1999.

[15] Luckhaus, D., Quack, M., "*High resolution FTIR spectra of NO_x (NO_2, N_2O_4) in Supersonic Jet Expansions and their rovibrational analysis*", J. Mol. Struct., 293, 213-216, 1993

[16] Barnes, J. A., Gough, T. E., "*Fourier Transform Infrared Spectroscopy of supersonic Jets: observation of clusters containing sulphur hexafluoride*", Chem. Phys. Letters, 130, 297-300, 1986.

[17] Melinot, P., Monot, R., Zellweger, J. M., *Van Den Bergh, H., "Infrared Laser action on the spatial, velocity and cluster size distribution in an SF_6 free jet*", Chemical Physics, 84, 345-358, 1984.

[18] Wu, B. J. C., Laguna, G. A., "*Gasdynamic and infrared spectroscopic measurements in a condensing flow of a sulfur hexafluoride-argon mixture*", J. Chem. Phys. 71, 2991-2999, 1979.

[19] Arroyo, M. P., Hanson, R. K., "*Absorption measurement of water-vapor concentration, temperature, and line-shape parameters using a Tunable InGaAsP diode laser*", Applied Optics, 32, 30, 1993.

[20] Allen, M. G., Kessler, W. J., "*Simultaneous water vapor concentration and temperature measurement using 1.31 μm Diode Laser*", AIAA Journal, 34, 3, 1996.

[21] Baer, D. S., Hanson, R. K., Newfield, M. E., Gopaul, N. K. J. M., "*Multiplexed diode laser sensor systemfor simultaneous H_2O, O_2 and temperature measurement*", Optics Letters, 19, 22, 1994

[22] Linnerud, I., Kaspersen, P., Jaeger, T, "*Gas monitoring in the process industry using diode laser spectroscopy*", Appl. Phys. B, 67, 297-305, 1998.

[23] McIntosh, A. L., Wofford, B. A., Lucchese, R. R., Bevan, J. W., "*High resolution Fourier transform infrared spectroscopy using a high temperature argon arc source*", Infrared Physics and Tech. 42, 509-514, 2001.

[24] Hu, S. M., Ulenikov, O. N., et al., "*High resolution Fourier Transform intracavity laser absorption spectroscopy of D_2O in the region of the $4\nu_1+\nu_3$ band*", J. Mol. Spectr., 212, 89-95, 2002.

[25] McManus, J. B., Nelson, D. D., Shorter, J., Zahniser, M. S., Dual Tunable Diode Laser System for D_2O - Laser Kit, Aerodyne Research Inc., 2001.

[26] Nelson, D. D. (prepared by), TDL Wintel, User's manual - Rev. 1.5.20, Aerodyne Research Inc., 2002.

[27] HITRAN webpage: http://www.hitran.com/

[28] McClathchey, R. A., et al, "*AFCRL Atmospheric Absorption Line Parameter Compilation*", AFCRL.TR-73-0096, Env. Res. Papers, No. 434, 1973.

[29] Rothman, L. S., et al, "*The HITRAN Molecular Spectroscopic Database and HAWKS (HITRAN Atmospheric Workstation): 1996 Edition*", 1996.

[30] Rothman, L. S., et al, "*The HITRAN Molecular Spectroscopic Database: Edition of 2000 including updates through 2001*", 2003.

[31] VELMEX Inc., NF90 SERIES - User's guide, Bloomfield, NY, 1999.

[32] Ida, T., Ando, M., Toraya, H., "*Extended pseudo-Voigt function for approximating the Voigt profile*", J. Appl. Cryst., 33, 1311-1316, 2000.

[33] Camy-Peyret, C., Flaud, J. M., Mahmoudi, A., Guelachvili, G., Johns, J. W. C., "*Line positions and intensities in the v_2 band of D_2O improvied pumped D_2O laser frequencies*", International J. of infrared and millimeter Waves, 6, 3, 1985.

[34] Zahniser, M. S., Aerodyne Research Inc., Billerica, MA, private communications, 2001-2003.

[35] Press, W. H., et al, Numerical Recipes in Fortran 77, Vol 1, Cambridge University Press, 2001.

[36] Pouring, A. A., Ph.D. Thesis, Yale University, 1963.

[37] Stein, G. D., Wegener, P. P., J. Chem. Phys. 46, 3685, 1967.

[38] Stein, G. D., Moses, C. A., J. Coll. Int. Sci. 39, 504, 1972.

[39] Roberts, R., "*A light scattering investigation of droplet growth in nozzle condensation*" Report No. 97, MIT, Gas Turbine Lab, Cambridge, MA, 1969.

[40] C. H. Heath, Ph.D. Thesis, Worcester Polytechnic Institute, 2001.

[41] Hill, P. G., MacMillan, R. D. C., Lee, V., J. Phys. Chem. Ref. Data, 11, 1, 1982.

[42] Stein, G. D., Ph.D. Thesis, Yale University, 1968.

[43] Crystran Ltd website, **http://www.crystran.co.uk/caf2data.htm**, CaF_2 data sheet.

[44] Spectra-Tech, A.R.K. (Attenuated Total Reflectance Kit), User's manual, CaF_2 data sheet.

[45] Perry, R., H., Green, D., W., Perry's Chemical Engineer's Handbook, 7th ed., McGraw-Hill, 1999.

[46] Sanders, S., T., Wang, J., Jeffries, J., B., Hanson, R., K., "*Diode-laser absorption sensor for line-of-sight gas temperature distributions*" Applied Optics, 40, 24, 2001.

[47] Spectral System Inc., Hopewell Junction, NY, private communication, 2003.

[48] VELMEX Inc. webpage: http://www.velmex.com/

APPENDIX A

THE SUPERSONIC NOZZLE

The supersonic nozzle used for the purposes of this thesis work has been labeled as "NOZZLE H", following the sequence of names used for the previous supersonic Laval nozzles in our laboratory [9, 12, 40].

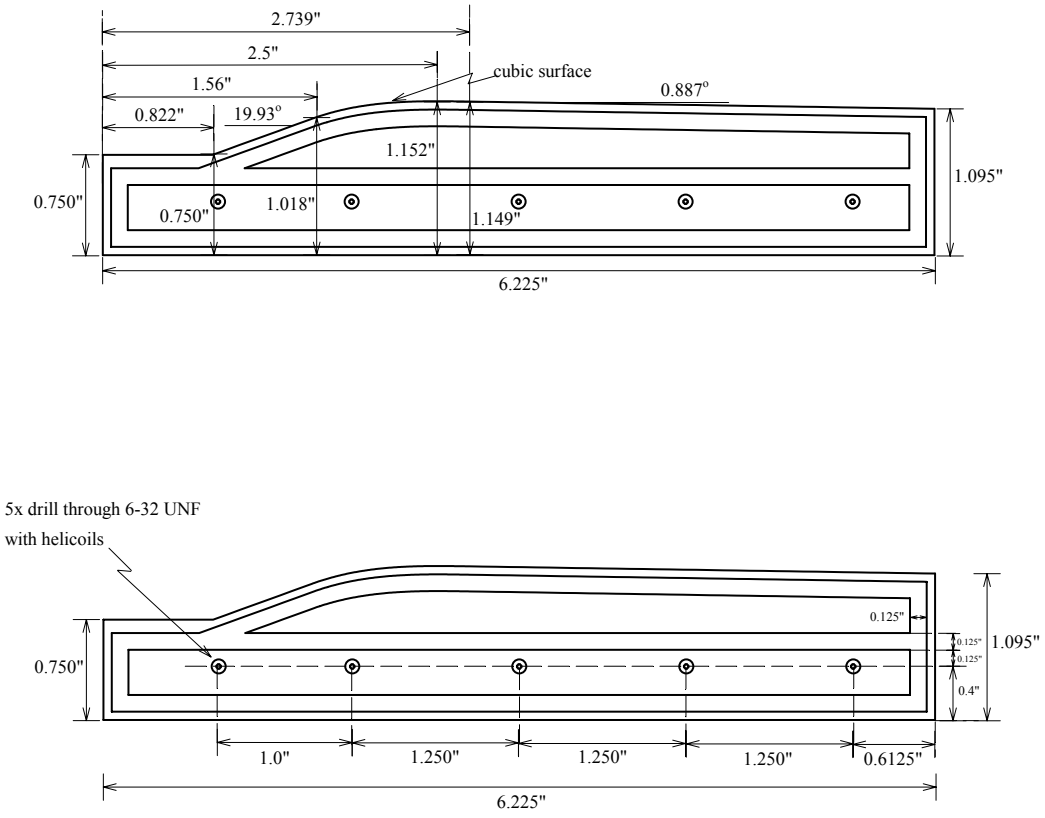

Figure A1 - Nozzle H, side view of top/bottom blocks

Nozzle H, as its predecessors, is machined from aluminum with straight side walls and with two symmetric converging-diverging blocks at the top and the bottom. The nozzle profiles of each block are symmetrically identical and the profile is given by an initial straight horizontal part and two straight converging and diverging sections joined by a cubic polynomial through the throat. The required degree of smoothness (that must be enough to avoid weak shocks in the flow downstream of the throat.) at the joints of different sections is ensured by making the nozzle contour continuous through the second derivative [42].

In Figures A1 to A5 are presented Nozzle H drawing designs, while the final appearance of the assembled nozzle is illustrated in Figures A6 and A7.

Table A1 - CaF_2 properties [43, 44]

Optical Properties		**Physical Properties**	
Transmission Range	0.13 to 10 μm	Density	3.18 gm/cm^3
Refractive Index	1.39908 at 5 μm	Melting Point	1360 °C
Reflection Loss	5.4% at 5 μm (2 surfaces)	Thermal Conductivity	9.71 Wm^{-1} K^{-1}
Restrahlen Peak	35 μm	Thermal Expansion	18.85×10^{-6}/ °C
dN/dT	-10.6×10^{-6}/ °C	Hardness	Knoop 158.3 (100)
Chemical Properties		Specific Heat	854 J Kgm^{-1} K^{-1}
Solubility at 20°C	0.0017 g / 100 g water	Dielectric Constant	6.76 at 1 MHz
Molecular Weight	78.08	Young's Modulus (E)	75.8 GPa
		Shear Modulus (G)	33.77 GPa
		Bulk Modulus (K)	82.71 GPa

The main purpose of this new nozzle design was to conduct IR laser absorption experiments, therefore the side walls of the nozzle have been equipped with two Calcium Fluoride (CaF_2) windows for each side walls upstream and downstream the throat.

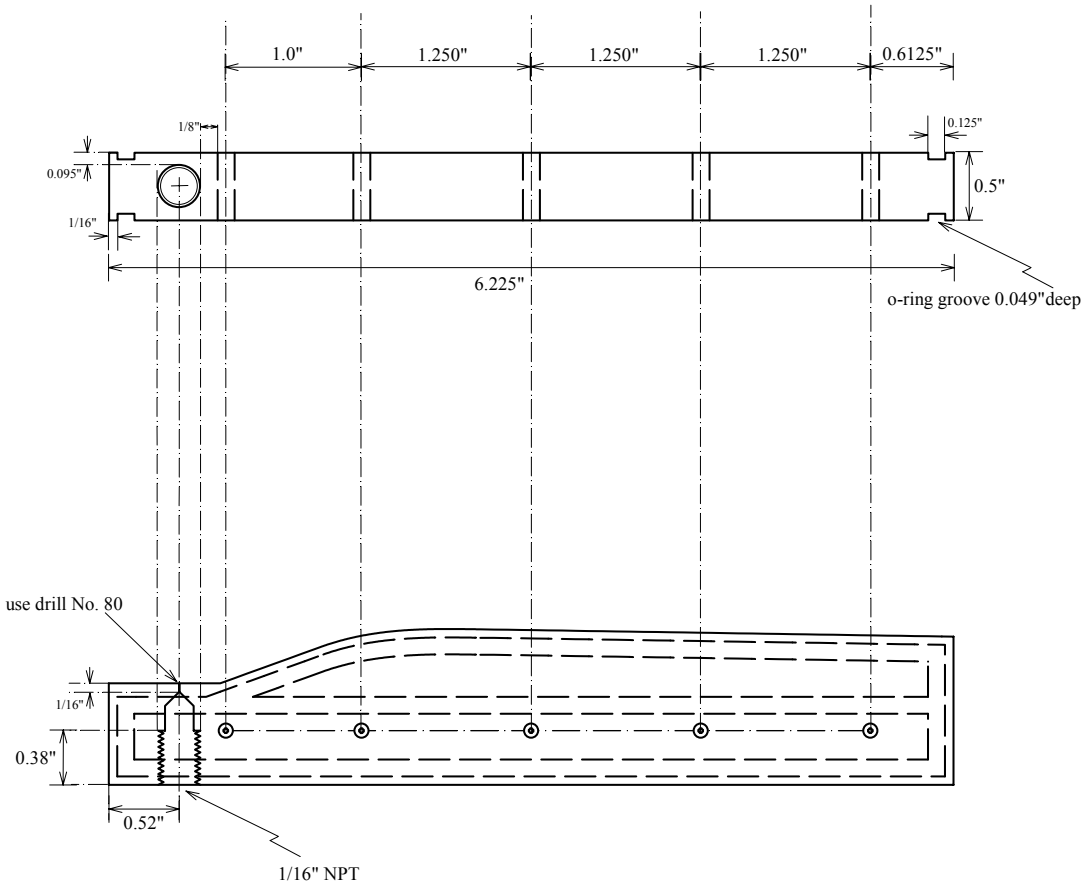

Figure A2 - Nozzle H, top view of top/bottom blocks and NPT connection details.

Currently there are over a dozen different infrared window materials to choose from, each one with its own characteristic properties. Main Factors to be considered in the

choice are the spectral range to be studied and the chemical properties of the sample versus that of the window [44].

Calcium Fluoride is one of the hardest materials, its composition is Single Cubic Crystal, with a melting point of 1633 K. It resists most acids and alkalides, it is non-hygroscopic at room and lower temperatures and is transparent to IR light in the region 1,025-50,000 cm^{-1}, as is possible to see in Figure A8. The main optical, chemical and physical properties of Calcium Fluoride are reported in Table A1.

An anti-reflective (AR) coating (Spectral System Inc.) has been provided to both sides of each window in order to reduce the amount of infrared light reflected from the lens and thus improve the clarity and get rid (at least partially) of the fringes that have been observed during preliminary tests. These fringes have greatly influenced the development of the present work and has been only partially solved by means of the AR coating. The AR coating used is a three-layer coating specifically designed to work at 8 μm wavelength. The first of the layers is a binder Sapphire layer used mainly to make the coating adhere to the Calcium Fluoride window. The interesting characteristic here is that the thickness of this layer is very small and guarantee the transmission of IR light up to the desired 8 μm, beyond the normal Sapphire cut-off (about 5.5 μm). The other two layers are mixed copyrighted materials (Spectral System Inc.) that provide the actual antireflective function [47].

To be able to seal the assembly without breaking the windows, shallow O-Ring grooves 3.2 mm (0.125") thick have been foreseen on each side of the nozzle blocks (as

illustrated in Figures A1 and A2) and rubber gaskets cut from supersoft Neoprene have been constrained into these grooves. Each window itself is then glued into an opposite groove machined on the internal part of the side walls (see Figures A3 and A4). The glue used for the purpose is silicone-based and each window can be removed, if necessary, without having to break it, raising slowly the temperature above 100 ^{o}C in order to reach the melting point for the glue but far away from any temperature and condition that could damage the windows. In fact, the maximum temperature CaF_2 can tolerate is about 800 ^{o}C in dry atmosphere but the material is sensitive to thermal shock.

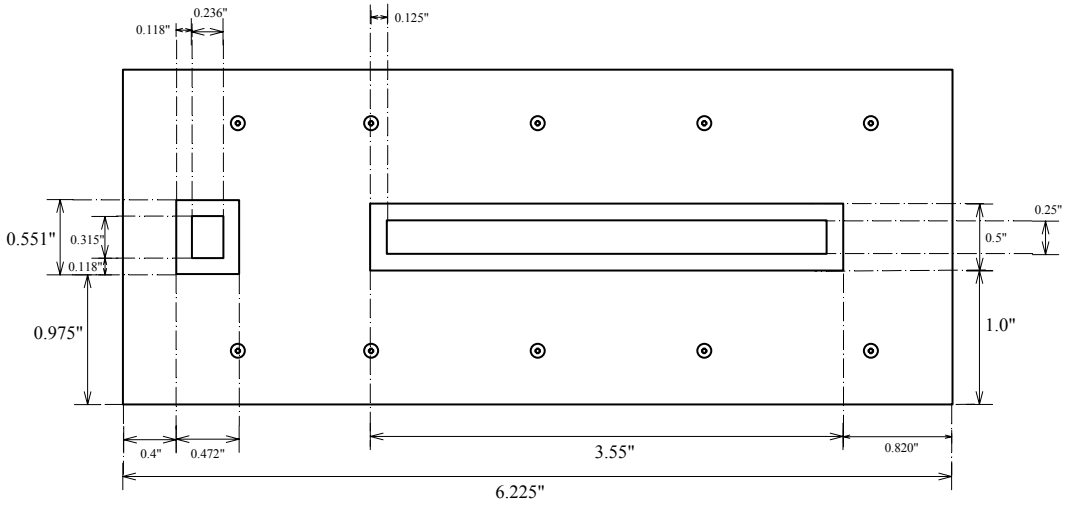

Figure A3 - Nozzle H, main dimensions of the side walls

The nozzle used in this experimental work has been designed to be fluidodynamically identical to another nozzle (Nozzle A) widely used in pressure traces, light scattering and SANS experiments in our group [9, 12].

The converging section of Nozzle H is 43 mm long (1.68") and the diverging section is 95 mm long (3.73"). The total opening angle of the supersonic region is 1.77^{o} in the linear region and the throat has been designed to be 12.7 mm wide (0.5") and 5 mm high (0.197"). The cross sectional area A* at the throat is therefore 63.5 mm^2 and the ratio of the area at the exit of the nozzle to the area of the throat is 1.58.

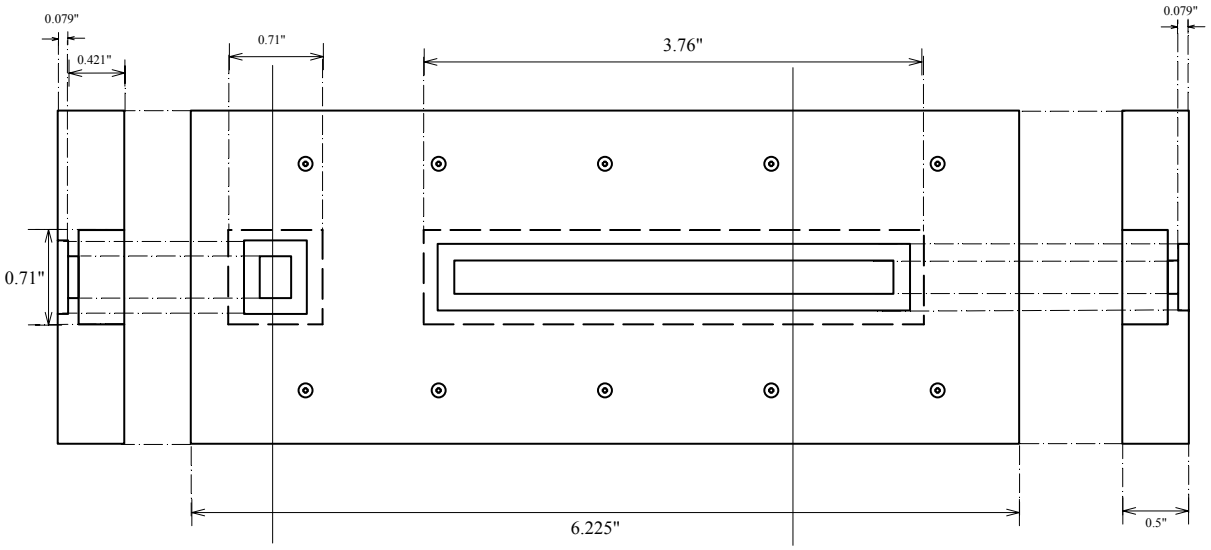

Figure A4 - Nozzle H, optional clearance of the window (external side). Different side walls have been machined for being used with different windows (transparent, opaque, with and without anti-reflective coating). Some of the side walls do not have the additional clearance on the external side.

The main significant difference between Nozzle H and Nozzle A (as well as for each other nozzle used in our group) is the presence of a straight section about 21 mm long in the undisturbed subsonic region, before the beginning of the converging section (see Figures A1, A2 and A6). In addition to provide a possibility to directly measure the static

pressure at the very beginning of the nozzle through an apposite pinhole drilled on the block 7.8 mm before the beginning of the converging section, this change also allowed us to place an additional small IR transparent window in the undisturbed region, for both calibration and validation purposes. In fact, in this part of the nozzle the pressure is directly measured and the temperature is know precisely since the flow comes directly from the Plenum, therefore this information plus the mass balance on the condensible and non condensible species make it possible to calculate what the expected vapor phase mixing ratio should be. This can be done as well in the upstream part of the main window, before the onset of condensation, knowing the pressure and temperature of the flow from the pressure trace experiment.

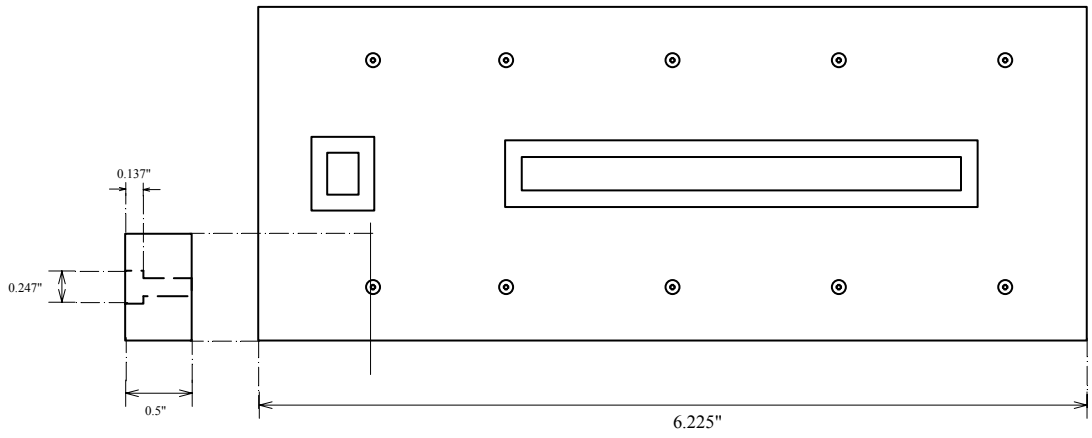

Figure A5 - Nozzle H, helicoils detail

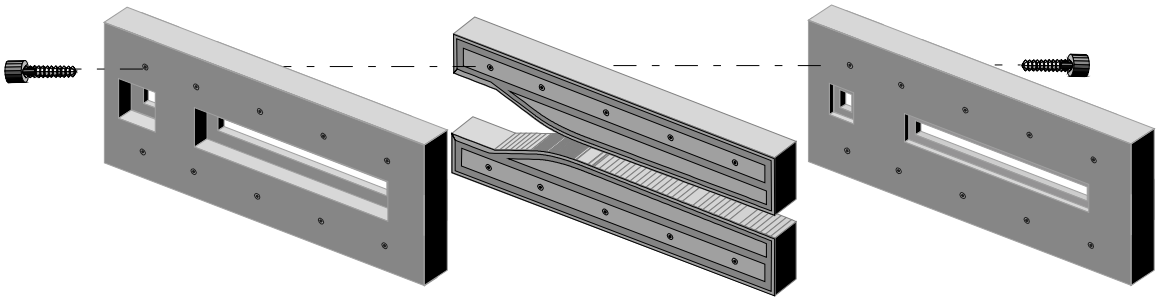

Figure A6 - Nozzle H, assembly

Due to the presence of the prolongation in the initial part, Nozzle H can be currently used only on TRAIN B of our experimental sets of equipments (see Figure 2.2), because it requires a custom-made holder to be connected to the vacuum and pressure probe systems.

Figure A7 - Nozzle H, assembled look· Here the side wall without window extra clearance is presented.

As a matter of fact, talking *a posteriori*, the nozzle design could be slightly improved in some of its features. First, the current o-ring groove design in the nozzle blocks was initially intended for not glued, rubber sealed, larger and thinner windows. This initial choice presented some unexpected problems due to the fragility of the glass, therefore the side walls have been successively modified and the windows size reduced cutting the height by half.

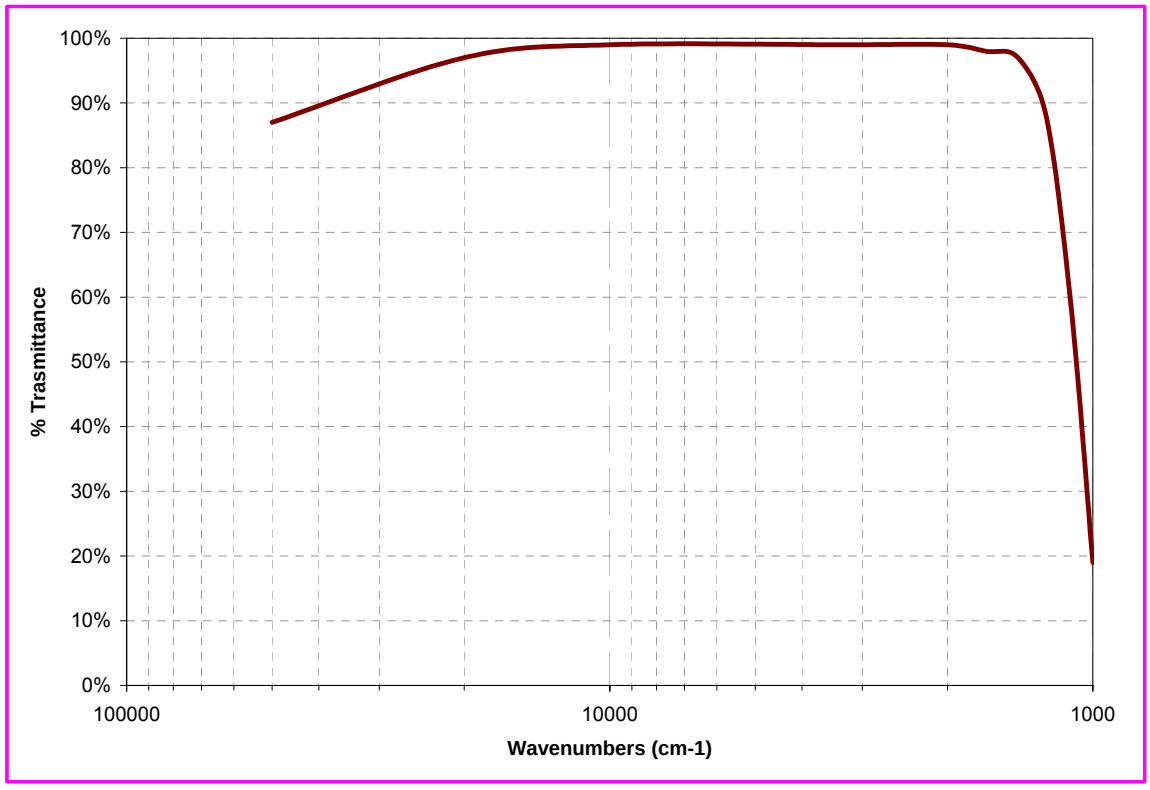

Figure A8 - Calcium Fluoride - Transmittance versus Wavenumbers [43, 44]

Since the blocks are result of a precision expensive machining and due to the fact that the rubber gaskets were already available, the o-ring groove design has been kept as originally. However, using glued smaller windows the same sealing effectiveness could be obtained simplifying the o-ring design to the outer contour only, which would make the preparation of the gaskets much faster and easier.

In addition, in case of an analogue new nozzle design for the IR experiment, it could be worthwhile to foresee a slightly longer small window in the straight part, in order to be able to undertake a bigger number of useful measures (Right now only 1 measure is taken in the small window, although the number could be increased to at least two or three at different spots, it would be interesting to have a still higher representative number of measures).

APPENDIX B

PRESSURE PROBE POSITIONER AND CONTROLLER [31, 48]

MA Base UniSlide Assemblies
A comparison of dovetail base style:

MB Style - the standard motorized UniSlide Assembly

-Includes protective internal limit switches, 1.
-Base is stiffer than the MA style reducing the deflection of unsupported sections.
-Added height allows most units to lie flat on a flat mounting surface.

MA Style - the low-profile design UniSlide Assembly

-A more compact design with reduced slide height and weight. Base lengths available to 12".
-Compatible with steppers, AC synchronous motors and PM motors only. Motors extend below slide base.
-Outboard limit switches suggested unless used with NEMA 17 low torque motors.


MB style


MA style
UniSlide Assembly Bases

Series MA1500

Series MA1500 Assemblies

Description

These small, low profile positioners are for light duty applications with light loads. The MA1500 is available in four lengths. The maximum recommended step rate is 1000 steps/sec. The base requires support along its full length except for the lightest loads (< 1 lb.). Way covers are not available. See page 6 of the Price List for MA1500 Series.

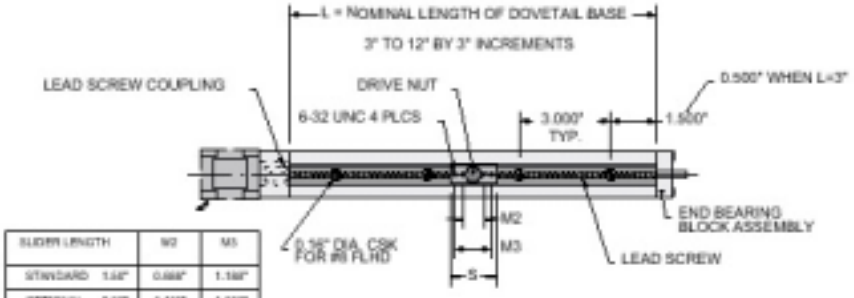

SLIDE LENGTH	M2	M3
STANDARD 1.44"	0.888"	1.188"
OPTIONAL 2.06"	1.188"	1.488"
OPTIONAL 3.06"	1.188"	2.688"

LEAD SCREW EXTENTIONS:
0.50" X 0.218" DIA. FOR B/P20 LEAD SCREW
" 0.231" DIA. FOR C/P40 LEAD SCREW
" 0.250" DIA. FOR K1,K2/Q1,Q2 LEAD SCREW

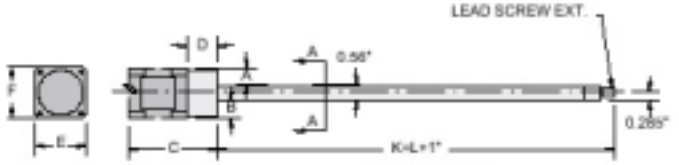

MOTOR TYPE	A	B	C	D	E	F
PITTMAN GM9000 SERIES	0.00"	0.14"	4.44"	1.12"	1.0"	1.375"

Model NF90 Controller

The NF90 is a low cost programmable stepping motor controller for running three motors, one-at-a-time. The Controller incorporates a single chip "Super Microprocessor" that has on-chip RAM. The RAM is available for temporary storage of a user-entered program and motion parameters.

Commands and data are entered through the RS-232 interface from a host computer, terminal, or programmable controller. Specialized Commands provide simple and efficient entry of a complex, yet compact, program.

Features

✓ A complete microprocessor-based Controller with motor drives for one, two, or three motors.

✓ Low cost and small size

✓ 400 steps per revolution (0.9° step angle) resolution

✓ Linear type motor and logic power supplies result in low Electromagnetic Interference (EMI).

✓ A Digitizing function can be utilized with a host terminal connected as a readout of motor position.

✓ A three wire RS-232 allows a host to enter Commands (ASCII characters) and Data, Poll for status, and Read Position information.

✓ The NF90 will run in an interactive or stand-alone mode.

✓ Acceleration/Deceleration settable from 2,000 to 100,000 steps/sec^2 in 2,000 step/sec^2 increments.

✓ Speed programmable from 1 to 6000 steps/sec. in 1 step/sec increments. NOTE: Most motors have low torque above 2000 steps/sec.

✓ Incremental Index distance is programmable from ±1 to ±1,048,575 steps.

✓ Programmable Return-to-Zero position.

✓ Six powerful Loop Commands provide from one to continuous repeat operations, performing simple functions like auto-reverse, raster scans and other complex XY matrix patterns.

✓ Programmable pauses from 100 milliseconds to 13 minutes.

✓ A User Output can be programmed to turn On and Off an external solid state relay, or interface to other logic level devices.

✓ A User Input can be utilized in a program as a WAIT for external switch or relay closure.

✓ Backlash Compensation can be set to automatically finish every index approaching from the positive direction.

✓ Run, Limit switch, Joystick, Output, Input, RS-232 and Motor connections are accessible at unpluggable connectors on the front panel.

✓ RS-232 baud rate settings are switch settable to 300, 1200, 4800, or 9600.

✓ Terminal, Diagnostic and BASIC, C, and Pascal Example Programs for PCs on diskette are included.

Features continued

✓ A User program can be put in EPROM by Velmex for a nominal fee.

✓ As many as 255 controllers can be "daisy-chained" together allowing the host to address each one from just one serial port.

✓ The NF90 can be set to signal the host when a limit switch has been encountered.

✓ Automatic Power Down reduces power consumption by de-energizing the motors when at a standstill.

✓ Single Step mode is provided for debugging a program or as a controlled interrupt.

✓ Completely wired and tested for direct connection to UniSlide Motors /Assemblies.

✓ The NF90 can be polled for its status at any time; additionally a prompt ("^") is automatically sent to the host when a program has finished.

✓ The NF90 can be programmed to send a pulse or character at preset distances without stopping or slowing the motor.

✓ Motor position can be read while motor is in motion.

✓ Limit Switches for CW and CCW directions are provided with plug-in connection to UniSlide limit switch assemblies. Limits can be used for "homing."

✓ Two year Limited Warranty.

SPECIFICATIONS

FUNCTIONAL

Packaged Controller/Driver, using Microcomputer control of stepping motors. Unipolar series resistance (L/R) driver. Operates one to three (dependent on model) motors, one-at-a-time.
Interactive limit switch inputs (TTL), (CW and CCW for each axis).
One User Input (0V to +3V min., -25V to +25V max.), and one User Output (0 or +5V, 10 mA sinking and 3 mA sourcing capability).
Programming through full-duplex RS-232-C; 300,1200,4800,9600 Baud (switch settable), 7 Data bits, Even parity, 2 Stop bits, ASCII; special configurations with 8 data bits, odd or no parity, are available.
User available RAM for program storage is 101 bytes.
Remote Run and Jog Inputs (TTL).
Eight foot motor and limit switch cables with connectors.

MOTOR COMPATIBILITY

1.8° PM 6 or 8 lead stepping motors, 4.7 Amp/phase max. Factory matched for a particular motor current, motors on each axis to be the same Amp/phase value.

PHYSICAL

Weight: 7.2 lbs. (3.2 kg)
Height: 5.0 inches (12.7 cm)
Width: 10.8 inches (27.4 cm)
Depth: 7.8 inches (19.8 cm)

ELECTRICAL REQUIREMENTS

90 to 130 VAC 50/60Hz, 150 watts
210-250V 50 Hz. available on request

ENVIRONMENTAL

35° to 95° F (2° to 35° C) Convection cooled

MODELS

Model # NF90-1 One motor version
Model # NF90-2 Two motor version
Model # NF90-3 Three motor version

OPTIONS

Remote Manual Push-button Control
19" Rack Mount Kit
15' Communication Cable for PCs (DB9 connector with DB9 to DB25 Adapter).

Command Summary

Command	Function
I*m*M*x*	Set steps to Index a motor CW (positive), *m*= motor# (1,2,3), *x*=1 to 1048575
I*m*M-*x*	Set steps to Index a motor CCW (negative), *m*= motor# (1,2,3), *x*=1 to 1048575
I*m*M0	Index a motor to absolute zero position, *m* =motor# (1,2,3)
S*m*M*x*	Set Speed of a motor, *m* = motor# (1,2,3), *x*=1 to 6000 steps/sec.
A*m*M*x*	Acceleration/deceleration, *m* = motor# (1,2,3), *x* =1 to 50
L0	Loop continually from the beginning
L-0	Sets the Loop-to-marker at the current location in the program
L*x*	Loop from beginning or Loop-to-marker *x*-1 times (*x* =2 to 255)
L-*x*	Loop from beginning or Loop-to-marker *x*-1 times, alternating direction of motor 1
LM-2	Loop once from beginning or Loop-to-marker reversing index direction of motor 2
LM-3	Loop once from beginning or Loop-to-marker reversing index direction of motor 1 and motor 2
P*x*	Pause *x* tenths of a second and output if output enabled (*x* =0 to 8191, 10 µsec pause when *x* =0)
U0	Wait for a "high" on the user input
U1	Wait for a high on the user input, holding the user output high while waiting
U2	Disable user output when pausing
U3	Enable output when pausing (reset state)
U4	User output "low"
U5	User output high
U6	Send "W" to host and wait for a "G" to continue
U7	Start of Continuous Index with pulse output
U8	Start of Continuous Index sending "@" to the host
U9	End of Continuous Index
B*x*	Backlash compensation, compensation on when *x* =1, off when *x* =0
O*x*	Indicate limit switch Over-travel to host, off when *x* =0, NF90 sends "O" when *x* =1 and a limit switch is encountered

Command	Function
Q	Quit On-Line mode (return to Jog/Slew mode)
R	Run program
N	Null (zero) motors 1,2,3 absolute position registers
K	Kill operation in progress
V	Verify Controller's status, NF90 sends "B" to host if busy, or "R" if ready
C	Clear program from memory
D	Decelerate to a stop (interrupts current index in progress)
E	Enable On-Line mode with echo on
F	Enable On-Line mode with echo oFF
G	Go after waiting or holding
H	Put Controller on Hold (single step mode)
X	Send position of motor 1 to host
Y	Send position of motor 2 to host
Z	Send position of motor 3 to host

The following are for NF90s that are daisy-chained together:

[*x*]	Send commands to the next NF90 in the "chain", *x* are any of the above commands
&	Enable multiple NF90s that are daisy-chained

APPENDIX C

DATA ACQUISITION AND DATA ANALYSIS SOFTWARE

C.1 TDLWINTEL

In this section an overview of the TDLWintel software is provided, remanding to the user manual [26] for a more detailed and exhaustive description.

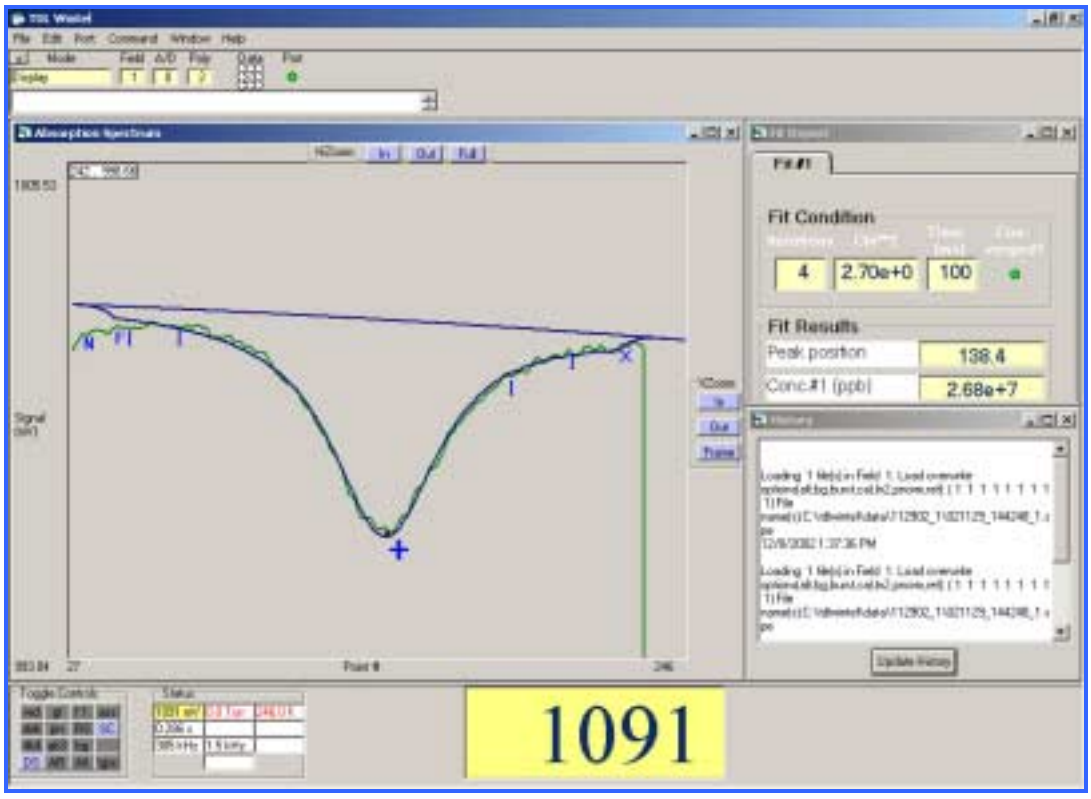

Figure C1 - TDLWintel (revision 5.27) - user interface

The TDL Wintel data acquisition program is a Windows-based program (see Figure C1) designed to frequency scan a tunable laser, acquire the resulting absorption spectrum and analyze it by performing an advanced type of sweep integration. The program has been developed at Aerodyne Research and is written in Microsoft Visual Basic.

The software sweeps over the full spectral transition or group of transitions, then integrates the area under the transitions using nonlinear least squares fitting to the known spectral line shapes and positions. It does not use frequency modulation (FM) techniques.

At the beginning of each scan the software turns the laser on and its frequency is swept across the desired transition frequency using a software generated voltage ramp. At the end of the scan the laser current is dropped below threshold to determine the detector voltage corresponding to the absence of laser light. The sweep rate can be as fast as 20 kHz for a 150 point spectrum.

Spectra are averaged in a background process while maintaining a 100% duty cycle. The resultant spectrum is fit to a set of Voigt line shape functions which are determined by the pressure and temperature. The baseline is treated as a slowly varying polynomial, from 0^{th} to 6^{th} order.

With this approach, absolute species mixing ratios are returned directly from the nonlinear least squares fits and therefore calibration is not required. The species mixing ratios are tied to absolute spectroscopic data from the HITRAN data base (or any other

available database). The time resolution for continuous mixing ratio measurements can be as small as 10 milliseconds.

TDLWintel requires the following components:

- A PC (running Windows), which runs the laser control and data processing program itself;
- A data acquisition board (National Instruments, PCI-6110E or PCI-6111E), which digitizes the detected laser signals and sends analog ramp and shutoff signals to the laser;
- A second (optional) data acquisition board (Measurement Computing, Inc., CIO-DAS08-AOH). This is used to monitor ambient temperature and pressure. These parameters are necessary for proper spectroscopic analysis. However, for use in a stable ambient like a laboratory, these parameters can be set to appropriate values in the software.

This software has been designed to interface particularly well with the Laser Components L5830 tunable diode laser controller. Aerodyne Research, Inc. provides an interface kit which allows TDLWintel to communicate with this laser controller. With this feature activated the diode laser temperature, current and other vital parameters can be monitored and modified using the TDLWintel program.

C.2 PRESSURE DATA ACQUISITION CODE

The source code of the program for the pressure data acquisition is reported below. With respect to previous works by Khan and Heath [12, 40], the only difference is given by the calibration factors for the instruments (see Appendix D) which have been re-calculated recently.

```
/*********************************************************************
 * File to aquire data using the DAS1602 board
 *
 * This program should acquire data from 3 different instruments
 * using a single interface (the little A/D D/A converter box.
 * Also, this program will determine the average and standard deviation
 * of data collected and save it to a specified file.  This file
 * can then be read by spreadsheet programs such as Lotus 1-2-3 for
 * further data analysis.
 *********************************************************************/

/* WARNING !!!!!!
 *        (In the following, the term *run* is defined as a single sweep
 *         of all the channels)
 *
 *        When using the timed input feature of this program, only 30
 *        runs of all channels can be receieved at one time.  Because
 *        the program is collecting data for standard deviation measurements
 *        while the program is being run, collecting more than 30 runs
 *        will cause an overflow error.
 *        If you wish to sample at such a high rate or for so long as you
 *        will go over this 30 run limit, use the version of this program
 *        that does not compute averages and standard deviations, since it
 *        has no such limitations.
*/

#include "math.h"
#include "stdio.h"
#include "conio.h"
#include "stdlib.h"
#include "time.h"
#include "dos.h"
#include "dasdecl.h"
#include "das1600.h"
#include <string.h>


DWORD   hDev1600;
DWORD   hDrv1600;
short   nErr;              /* Function return error flag */
DWORD   dwOUTval;
DWORD   dwINPval;
DWORD   dwSamples = 4;  /* Number of samples to aquire */
char    far  *szErrMsg;         /* Pointer to error message */
DWORD   hFrameAD1600;      /* A/D Frame Handle */
DWORD   hdev;
short   nStatus;           /* Used to monitor data transfers */
DWORD   dwTransfers;       /* Used to monitor data transfers */
WORD    wADval;            /* Strorage for A/D value */
void DisplayError(char *szFuncName, short nErr);

main(int argc, char *argv[])
{
 /* Define the file variables and set the run value (measure of run # in file)
*  to 0 */

  char *file1="ddmmyrr.TXT";
  int run=0;
  FILE *file_1;
  char *file2="ddmmyrrS.TXT";
  FILE *file_2;
  double val0, val1, val2, val3, val4, val5, val6;    /* converted value of the A/D
acquisision*/
  char colltype, testchar;
  int mperiod = 1;   /*  ADDED by CHEATH for convenience  */
  int datapoints = 20;  /*  ADDED by CHEATH for convenience  */
  float po;
  float points;
  int j=1,i;
  time_t t=0.00, *t_ptr=&t;
  struct time colltime, *ct_ptr=&colltime;
  char    *hr_ptr=&ct_ptr->ti_hour,    *min_ptr=&ct_ptr->ti_min,    *sec_ptr=&ct_ptr-
>ti_sec;
  double position, delP, delT, gamma=1.40, P, Pfit, Po2, PPo2, PPo2fit, T, Tfit;
  double strip;
  int iposition;
  int pos;
  double chan0[200];
  double chan1[200];
  double chan2[200];
  double chan3[200];
  double chan4[200];
  double chan5[200];
  double chan6[200];
  double avg[7];   /* AVERAGE OVER THE 5 CHANNELS */
  double sdev[7];
  double sum[7];
  double sumsq[7];

/* clear the screen, and print information about the program */
  printf ("□[H□[J \n\n");
  printf ("dataac03.exe\n\n");
  printf ("     A program to aquire data from multiple instruments using\n");
  printf ("a single interface (by means of an A/D converter box.)  All\n");
  printf ("signals will be acquired and printed to the screen as well as\n");
  printf ("written to a file specified.  In addition the average and \n");
  printf ("standard deviation of the data is stored in another specified\n");
  printf ("file.\n");
  printf ("Channel 1 -- Plenum Pressure Sensor MKS 690A53TRA\n");
  printf ("Channel 2 -- Stagnation Pressure Sensor 120AA-01000RBJ\n");
  printf ("Channel 3 -- Omega Temperature Deg. C\n");
  printf ("Channel 4 -- Relative Humidity\n");
  printf ("Channel 5 -- Cardinal Scale Weight lb\n");
  printf ("Channel 6 -- Arlyn Scale Weight lb\n");
  printf ("                ***************************************\n");
  printf ("                Note:   This program is still in beta\n");
  printf ("                       form....Report any errors!    \n");
  printf ("                ***************************************\n");
  printf ("Program will now initialize the board and the drivers.....\n");

/* FIRST STEP IS TO INITIALIZE THE HARDWARE/SOFTWARE */
  if (( nErr = K_OpenDriver("DAS1600", "das1600.cfg", &hDrv1600)) != 0) {
    DisplayError("K_openDriver", nErr);
    exit(nErr);
  }
  printf ("Initialization complete and succesful!!\n");

/* OPEN THE OUTPUT FILES */
```

```
  if(  (argc  !=  3)  ||  ((file_1=fopen(argv[1],"a+"))  ==  NULL)  ||
((file_2=fopen(argv[2],"a+")) == NULL)
     || (strcmp(argv[1], argv[2]) == 0) ){
   printf("\nCannot open the two output files for the raw and averaged summary
data,\n");
   printf("conventionally entered as ddmmyrr.TXT and ddmmyrrS.TXT,
respectively.\n");
   printf("dd = day, mm = month, y = last digit of year and the S is for summary
output file for nu programs\n\n");
   printf("%s ddmmyrr.TXT and ddmmyrrS.TXT",argv[0]);
   exit(1);
  }

/* ESTABLISH COMMUNICATION WITH THE DRIVER THROUGH A DEVICE
HANDLE */
  if ( ( nErr = K_GetDevHandle(hDrv1600, 0, &hDev1600) ) != 0) {
   putch (7); printf(" Error %X during K_GetDevHandle ", nErr ) ;
   exit(1);
  }

/* TO PERFORM ANY A/D OPERATIONS, YOU MUST FIRST GET A HANDLE
TO AN */
/* A/D FRAME (THE DATA TABLES INSIDE THE DRIVER PERTAINING TO
A/D OPERATIONS).*/
  if ((nErr = K_GetADFrame (hDev1600, &hFrameAD1600)) != 0) {
   DisplayError("K_GetADFrame", nErr);
   exit(1);
  }

/* SPECIFY THE INTERNAL TRIGGER.  I'M NOT SURE IF THIS IS NEEDED.*/
  if ((nErr = K_SetTrig (hFrameAD1600, 0)) != 0) {
   DisplayError("K_SetTrig", nErr);
   exit(1);
  }

/* ***************************************************************** */
/* LOOP FOR AVERAGED INPUT */
/* ***************************************************************** */
   time(t_ptr);
   printf("Date and time of this session: %s\n", ctime(t_ptr));
   fprintf(file_1,"\nDate and time of this session: %s", ctime(t_ptr));
   fprintf(file_2,"Position Ave 1 Std 1 Ave 2 Std 2  Ave 3 Std 3  Ave 4 Std 4  Ave 5
Std 5 Ave 6 Std 6 Time\n");
    do {
     printf("Integer multiple of 0.01sec period to collect samples e.g. 1: ");
     scanf(" %d", &mperiod);
     printf("Integer number (1-199) of samples to collect e.g. 21: ");
     scanf(" %d", &datapoints);
     printf("%d datapoints with %.2fsec period for %.2fsec collect time\n",
     datapoints,mperiod/100.0,((double)(datapoints)*mperiod/100.0));
     if(datapoints > 200) {
      printf("too many datapoints\n");
      fclose(file_1);
      exit(0);
     }
     do {
      /* HERE THE MAIN LOOP STARTS FOR TRIGGERING OF DATA
AQUISITION */
      printf("Enter probe position> ");
      scanf(" %d", &pos);
      printf("(q)uit, new (s)ample count, new (p)osition, or other key to continue\n");
      if(((testchar = getch())=='q') || testchar == 's'
        || testchar == 'p') { continue; }

      fprintf(file_1,"Position : %d\n", pos);
      printf("Run     Channel 1  Channel 2 Channel 3  Channel 4  Channel 5 Channel 6
Time\n");
      fprintf(file_1,"Run     Channel 1   Channel 2 Channel 3   Channel 4   Channel 5
Channel 6 Time\n");

      do {
       j++;
       if(j%(15*mperiod) == 0) {
        run++;
       }

       /* SAMPLE AND READ CHANNEL 1 AT GAIN 4 AND STORE SAMPLE
IN wADval */
       if ((nErr = K_ADRead (hDev1600, 1, 2, &wADval)) != 0) {
        putch(7); printf ("Error %X in K_ADRead operation.", nErr);
        exit(1);
       } /* STRIP LEAST-SIGNIFICANT 4 BITS AND DISPLAY wADval */
       if(j%(15*mperiod) == 0) {
        val1=((wADval >> 4) & 0xfff)*0.61035*0.99551036-0.39485913; /* cal02s
PP */
       }/* Theoretical of 0.61035 for 10000(DblTorr)/(4096*(4gain)) */
       /* SAMPLE AND READ CHANNEL 2 AT GAIN 1 AND STORE SAMPLE
IN wADval */
       if ((nErr = K_ADRead (hDev1600, 2, 0, &wADval)) != 0) {
        putch(7); printf ("Error %X in K_ADRead operation.", nErr);
        exit(1);
       } /* STRIP LEAST-SIG 4 BITS AND DISPLAY val cnvrtd from wADval*/
       if(j%(15*mperiod) == 0) {
        val2=((wADval >> 4) & 0xfff)*0.24414*0.99635249+0.05037511; /* cal02s
PP */
       }/* Theoretical of 0.24414 for 1000Torr/(4096*1(gain)) */
       /* SAMPLE AND READ CHANNEL 3 AT GAIN 1 AND STORE SAMPLE
IN wADval */
       if ((nErr = K_ADRead (hDev1600, 3, 0, &wADval)) != 0) {
        putch(7); printf ("Error %X in K_ADRead operation.", nErr);
        exit(1);
       } /* STRIP LEAST-SIGNIFICANT 4 BITS AND DISPLAY wADval */
       if(j%(15*mperiod) == 0) {
        val3=((wADval >> 4) & 0xfff)*0.024320522;
       }/* Theoretical of 0.0244140625=100DegC/(4096*1) */
        /* val3=((wADval >> 4) & 0xfff)*0.015205797; */
       /* SAMPLE AND READ CHANNEL 4 AT GAIN 4 AND STORE SAMPLE
IN wADval */
       if ((nErr = K_ADRead (hDev1600, 4, 2, &wADval)) != 0) {
        putch(7); printf ("Error %X in K_ADRead operation.", nErr);
        exit(1);
       } /* STRIP LEAST-SIGNIFICANT 4 BITS AND DISPLAY wADval */
       if(j%(15*mperiod) == 0) {
        val4=((wADval >> 4) & 0xfff)*0.012181949;
       }
       /* SAMPLE AND READ CHANNEL 5 AT GAIN 0 AND STORE SAMPLE
IN wADval */
       if ((nErr = K_ADRead (hDev1600, 5, 0, &wADval)) != 0) {
        putch(7); printf ("Error %X in K_ADRead operation.", nErr);
        exit(1);
       } /* STRIP LEAST-SIGNIFICANT 4 BITS AND DISPLAY wADval */
       if(j%(15*mperiod) == 0) {
        val5=(((wADval >> 4) & 0xfff))/4.104;
       }/* Theoritical is 4.096 for 1000/4096 */

       /* SAMPLE AND READ CHANNEL 6 AT GAIN 1 AND STORE SAMPLE
IN wADval */
       if ((nErr = K_ADRead (hDev1600, 6, 1, &wADval)) != 0) {
        putch(7); printf ("Error %X in K_ADRead operation.", nErr);
        exit(1);
       } /* STRIP LEAST-SIGNIFICANT 4 BITS AND DISPLAY wADval */
       if(j%(15*mperiod) == 0) {
        val6=(((wADval >> 4) & 0xfff))/4.084;
       }/* Theoritical is 4.096 for 1000/4096 */
       if(j%(15*mperiod) == 0) {
       gettime(ct_ptr);
        printf("%d  %.2f %.2f %.2f %.2f  %8.2f %8.2f %d:%d:%d\n",
          run,val1,val2,val3,val4,val5,val6,*hr_ptr,*min_ptr,*sec_ptr);
        fprintf(file_1,"%d  %11f %11f %9f %10f %10f %10f %d:%d:%d\n",
          run,val1,val2,val3,val4,val5,val6,*hr_ptr,*min_ptr,*sec_ptr);
       }
       chan1[run]=val1;
       chan2[run]=val2;
       chan3[run]=val3;
       chan4[run]=val4;
       chan5[run]=val5;
                  chan6[run]=val6;
     }while(run < datapoints);

     for(i=1;i<=6;i++) {
      avg[i]=0;
      sum[i]=0.0;
     }
     for(i=1;i<=run;i++) {
      sum[1]=sum[1]+chan1[i];
      sum[2]=sum[2]+chan2[i];
      sum[3]=sum[3]+chan3[i];
      sum[4]=sum[4]+chan4[i];
      sum[5]=sum[5]+chan5[i];
                  sum[6]=sum[6]+chan6[i];
     }
     for(i=1;i<=6;i++) {
      avg[i]=sum[i]/run;
     }
     /*now calculate the standard deviation */
     /* initialize the array */
     for(i=1;i<=6;i++) {
      sumsq[i]=0;
     }
     /* calculate sum of squares */
     for(j=1;j<=run;j++) {
      sumsq[1]=sumsq[1]+chan1[j]*chan1[j];
```

```
        sumsq[2]=sumsq[2]+chan2[j]*chan2[j];
        sumsq[3]=sumsq[3]+chan3[j]*chan3[j];
        sumsq[4]=sumsq[4]+chan4[j]*chan4[j];
        sumsq[5]=sumsq[5]+chan5[j]*chan5[j];
                    sumsq[6]=sumsq[6]+chan6[j]*chan6[j];
      }
      for(i=1;i<=6;i++) {
       sdev[i]=sqrt((max(0.0,run*sumsq[i]-sum[i]*sum[i])/run/(run-1)));
      }
      gettime(ct_ptr);
      fprintf(file_2,"%3d %.2f %.2f %.2f %.2f %.2f %.2f %.2f %.2f %.2f %.2f
%.2f",
pos,avg[1],sdev[1],avg[2],sdev[2],avg[3],sdev[3],avg[4],sdev[4],avg[5],sdev[5],avg[6]
,sdev[6]);
      fprintf(file_2," %d:%d:%d\n", *hr_ptr, *min_ptr, *sec_ptr);
      printf("Chan.  Average     St. Dev.\n");
      for(i=1;i<=1;i++){
       printf("%d    %10.3f %10.3f   %.1f %.1f   %.1f\n",
       i, avg[i], sdev[i], avg[i]/2.0, sdev[i]/2.0,
       (avg[i]*0.49757650-1.22301437));
      } /*Po cal02s calibration PP*/
      for(i=2;i<=2;i++){
       printf("%d    %10.3f %10.3f   %.1f %.1f   %.1f\n",
       i, avg[i], sdev[i], avg[i], sdev[i], avg[i]);
      } /* Instrument Calibration Februrary 2002*/
      for(i=3;i<=6;i++){
       printf("%d    %10.3f %10.3f\n", i, avg[i], sdev[i]);
      }

      printf("□");
      printf("Pressure ratio = %8.3f for position: %d\n",(avg[2]/(avg[1]*0.49757650-
1.22301437-0.0),pos));
                  /* pressure calibration prange cal2002s */
                  /* 0.0 torr is for the pressure loss between the plenum (where
pressure is measured) and the entrance of the nozzle block. !NEEDS TO BE
MEASURED!  */
      P= (avg[2]);
      Po2= ((avg[1]/2-0.1002)/0.9969); /* numbers not updated */
      /* position calibration ptest 1603903s */
      /* PPo2= (2.0-P)/Po2; */ /*Takes into account nonisentropic pressure drop */
      printf("Pressure ratio = %f for position: %d hundredth-mm\n",(PPo2 =
P/Po2),pos);

      if(0.2 < PPo2 < 0.8){
       PPo2fit= 72.841/pow(((double)pos/1.009),0.6401); /* 1803901s fit */
       Pfit= Po2*PPo2fit;
       delP =P-Pfit;
       T= (avg[3]+273.15)*pow(PPo2,((gamma-1)/gamma));
       Tfit= (avg[3]+273.15)*pow(PPo2fit,((gamma-1)/gamma));
       delT=T-Tfit;
       printf("delP= %.2fTorr, delT = %.2fK\n",delP,delT);
      }

      run=0;
      printf ("(q)uit, or any other key to continue\n");
      testchar=getch();
     } while (testchar != 'q' && testchar !='s'
       && testchar != 'p');
   } while (testchar != 'q');

 /* THIS IS THE LAST STEP IN THE PROGRAM */
 /* CLOSE THE DRIVER AND RELEASE ALL RESOURCES */
 K_CloseDriver(hDrv1600) ;
 /* CLOSE THE FILE */
 fclose(file_1);
 return 0;
} /* end of main */
```

```
void DisplayError(char *szFuncName, short nErr)
{
 K_GetErrMsg(hDev1600, nErr, &szErrMsg);
 putch (7);
 printf("Error %X during %s operation: %Fs\n", nErr, szFuncName, szErrMsg);
}
```

C.3 PRESSURE DATA ANALYSIS CODE

The following is the source code of the program used for pressure trace analysis. With respect of previous works [12, 40], here the new calibration factors for the temperature

reading and the pressure reading have been implemented (see Appendix D), and the scaling factor for the pressure probe movement controlling system (see Appendix B) has been introduced.

```
c this program version includes the ability to update the latent heat as a
c   function of temperature for h2o and d2o based on clausius-clapeyron
c   approximations to liquid-vapor equations.
                    !chhfeb2001
c       nu4bg77.f previous version
c note : this is the pc version of the code! read statements have been modified.
c       should be completely transferable to the vax though if necessary.
c       bew: 11-20-92
c
c program nozltemp4.for-to calculate mass of condensate vs.position in a nozzle
c expansion of a condensable gas in excess carrier gas by solving gas
c dynamics equations for diabatic flow

c this version of the program calculates a "wet" isentrope based on the
c measured dry isentrope and corrected for the differences in gamma. it
c also starts the wet condensing flow integration on the desired data
c point rather than on the wet isentrope to avoid any extraneous extra
c shifts.

c smoothes all of the good density data first, then integrates from an
c initial value using finer integration grid (up to 5x)

c modified to take in pressure data instead of density data ....jul97, jlc
c cleaned up and fixed  integrator.  now reduces multiple data sets,
c finds the onset conditions, and prints out the t-tisw values for all
c data sets in one file..... mar99, bew
c note: stein used to smooth the integrated values as well... may consider
c doing this for rough data... not yet implemented but easy to do....  bew
c this version has been modified for Nozzle H on train B with Velmex (PP)
c RTD probe is calibrated and temperature calibration factor is included
c Now nu.dat has "tempcal" and this program reads in the value and does
c temperature calibration as "to(i)=to(i)+tempcal".....jun02, PP

      implicit real*8(a-h,o-z)
      real*8 msq,msqw,mssq,machno
      real*8 p0dummy,t0dummy, pc0, rg, pi, avog
      real*8 dotm,dotncal,pc10,pc20,pocal,poloss,tocal,zc10
      real*8 p0, t0, tempcal
      real*8 xstart, xthroat
      real*8 tt0(500),fc(500),g(500),u(500),
     *rr0(500),pp0(500),pp0i(500),pp0d(500)
      real*8 aratio(500),wg(500),wmug(500),t(500),tisw(500),
     *       tisd(500),rm(11)
      real*8 xd(500),xw(500),x(500)
      real*8 dry(500),dryf(500),sdry(500)
      real*8 wet(500),swet(500),wetf(500),sweti(500)
      real*8 po(200),p(200),deltapo(200),deltap(200),to(200)
      real*8 deltadry(500),deltadryf(500)
      real*8 deltawet(500),deltawetf(500),dtemp(500,20)
      character*30 dryfil,wetfil,rlsfil,a
      character*8 specie(2)
      character*4 title(3,2)
      common /xval/ xs(500)

*-------------------------------------------------------nomenclature
c dhc,fdhc(zc10,t(i))                  latent heat of condensible vapor
c pc10,pc20     condensible vapor pressure (read in 2*Torr, works in dyne/cm^2)
c t(i)                                 Temperature of inert in Kelvin
c zc10                                 Initial molar fraction of condensible vapor1
(zc10+zc20=1)
*-------------------------------------------------------nomenclature
      open(5,file='nu.dat',status='old')
      open(3,file='nu.out',status='unknown')
      open(9,file='nua.out',status='unknown')
      open(10,file='4pp.out',status='unknown')
      open(11,file='wilson.out',status='unknown')
      open(12,file='legend1.bat',status='unknown')
      open(13,file='dtemp.out',status='unknown')
      open(14,file='legend3.bat',status='unknown')
      open(15,file='legend4.bat',status='unknown')

      call echo

      pi=3.14159d0
      rg=8.3144d7
      avog=6.022d23

c read two condensible species
      read(5,41,end=50)specie
c     print 1006, specie
 1006 format (2a8)
   41 format(2a8)
c read stagnation conditions-temp, pressure, partial pressure of
c condensible--pressures are in mm of hg--note t0 and p0 are calculated from data
files later.
      read(5,*)t0dummy,p0dummy,poloss,tempcal                    !PP02    !RTD probe
calibration added
      write(*,*)"poloss = ",poloss,"    tempcal = ",tempcal
c convert pressures to dyn/cm**2
      pconv = 760.d0/1.01325d6
c read molecular weights of carrier (1) and condensible (2,3)
      read(5,*)wm1,wm2,wm3
c read specific heats
      read(5,*)cp1,cp2,cp3
c read latent heat, and specific heat of condensate
      read(5,*)dhc2,dhc3,cpc2,cpc3
c read starting value and the number of points in the output
                  read(5,*) xstart, ilast
c read the integration end points (may be different than ifrst, ilast)
c the number of integrations attempts, and the number of integration
c sub-intervals
      read(5,*)istart, ifin ,ni, nint
c read name of dry pressure data file
      read(5,1)dryfil
    1 format(a30)
c read smoothing parameters: m-order, n-number of points
      read(5,*)md,nd



c read x values and all of the dry data p0, p(x), and the associated standard deviations.
c correct the pressures i.e. baratron calibrations and pressure loss due to mesh.
      open(unit=4,file=dryfil,status='old')
c read total number of values in dry pressure data file
      read(4,1)a
      read(4,*)idend

      do i=1,idend
       read(4,*)xd(i),po(i),deltapo(i),p(i),deltap(i)      !p's in 2*torr
c       p(i)=p(i)*0.50581328+0.08075611                    !p(i) from black baratron (ppaci)
       po(i)=(po(i)*0.49757650-1.22301437)-poloss          !ppaci cal02s
       dry(i)=p(i)/po(i)
       deltadry(i)=dry(i)
     *   *((deltap(i)/p(i))**2.0+(deltapo(i)/po(i))**2.0)**0.5
c      write(*,*) i, xd(i), dry(i), deltadry(i)           !debug
      enddo
      close(unit=4)

c read the number of wet data sets
                  read(5,*)ndata, dotncal, pocal, tocal              !chh99

                  write(11,1302)dryfil


                  do kd = 1,ndata
```

```
      read(5,*)ntype,entry1,entry2                    !chh99
      if(ntype.eq.0)then          !pressure input (torr)
       pc10=entry1
       pc20=entry2
      else if(ntype.eq.1)then     !massflow and weight fraction input
       dotm=entry1
       wfc10=entry2
       wfc20=1.0d0-wfc10
c        dummy condition condensible pressures         !chh99
       pc10=dotm*wfc10/wm2/dotncal*p0dummy*(tocal/t0dummy)**.5 !pocal in torr
       write(*,*)"dummy pc10= ",pc10," torr"
       pc20=dotm*wfc20/wm3/dotncal*p0dummy*(tocal/t0dummy)**0.5 !chh01
       write(*,*)"dummy pc20= ",pc20," torr"
      else
       write(*,*)"need to specify pressure (0)"
       write(*,*)"or mass flow with first weight fraction input(1)"
       stop
      end if

c read name of wet pressure data file
      read(5,1)wetfil
      open(unit=4,file=wetfil,status='old')
c read total number of values in wet pressure data file
      read(4,1)a
      read(4,*)idenw

c read x values and all of the wet data p0, p(x), and the associated standard deviations.
c correct the pressures i.e. baratron calibrations and pressure loss due to mesh.
      do i=1,idenw
       read(4,*)xw(i),po(i),deltapo(i),p(i),deltap(i),to(i)  !p's in 2*torr
c       p(i)=p(i)*0.50581328+0.08075611                    !ppaci p(i) from black baratron
       po(i)=(po(i)*0.49757650-1.22301437)-poloss          !ppaci cal02s
       wet(i)=p(i)/po(i)
       deltawet(i)=wet(i)
     *     *((deltap(i)/p(i))**2.0+(deltapo(i)/po(i))**2.0)**0.5
       to(i)=to(i)+tempcal                          !ppaci02!    RTD probe calibration
c      write(*,*) xw(i), wet(i), deltawet(i)             !debug
      enddo
      close(unit=4)

c figure out the average stagnant pressure and temperature

      p0=0.0
      t0=0.0
      do i=1,idenw
       p0=p0+po(i)

       t0=t0+to(i)
      enddo
      p0=p0/idenw
      t0=t0/idenw+273.15
      devp0=0.0
      do i=1,idenw
       devp0=devp0+(po(i)-p0)**2.0
      enddo
      devp0=(devp0/(idenw-1))**0.5
      write(*,*) "average p0 is   ", p0,"torr"
      write(*,*) "p0 std dev is   ", devp0,"torr"
      write(*,*) "average t0 is   ",t0,"k"
c                                  !chh99
c now figure out pcondensible from calibration and average properties
      if(ntype.eq.1)then                !now calculate pcondensible
       pc10=dotm*wfc10/wm2/dotncal*p0*(tocal/t0)**0.5 !chh01 !pocal in torr
       write(*,*)"pc10= ",pc10," torr"
       pc20=dotm*wfc20/wm3/dotncal*p0*(tocal/t0)**0.5 !chh01
       write(*,*)"pc20= ",pc20," torr"
      endif

c                                  !chh22.02.01
      if((pc10+pc20).lt.1.d-18)then
       write(*,*)"Insufficient condensible vapor!"
       stop
      endif
c convert pressures to dyn/cm**2
      p0=p0/pconv
      pct0=pc10+pc20
      pc10=pc10/pconv
      pc20=pc20/pconv
      zc10=pc10/(pc10+pc20)              !chh22.02.01
c calculate stagnation gas mass density and condensible monomer mass
c density (g/cm**3)
c w2,w3 are mass fraction of condensible vapor in gas
      wmav=(wm1*(p0-pc10-pc20)+wm2*pc10+wm3*pc20)/p0
      w20=wm2*pc10/p0/wmav
      w30=wm3*pc20/p0/wmav
      wi=1.d0-w20-w30

c gw17-2-00 assuming vapor condenses at constant composition let's define
c a fictitious mean condensible vapor molecular weight wmc
      wmc=(wm2*pc10+wm3*pc20)/(pc10+pc20)

c also let's save the inital average molecular weight
      wmav0=wmav

      cp0=wi*cp1+w20*cp2+w30*cp3

c we also need a fictitious mean condensible specific heat
      cpv=(w20*cp2+w30*cp3)/(w20+w30)
c we also need a fictitious mean condensible specific heat of the condensed liquid
      cpc=(w20*cpc2+w30*cpc3)/(w20+w30)

      dhc=(dhc2*w20+dhc3*w30)/(w20+w30)              !only when not using fdhc
      write(*,*) ' wmav, wi =',wmav, wi
      write(*,*) "dhc=", dhc                         !debug
      gamma=cp1/(cp1-rg*1.d-7/wm1)                   !n2 gamma
      gamma0=cp0/(cp0-rg*1.d-7/wmav)                 !initial mixture gamma
      rhog0=p0/rg/t0*wmav
      write(*,*)"wmav"," w20"," w30"," wi"," cp0"," gamma0" !chh061098
      write(*,*)wmav, w20,w30,wi,cp0,gamma0
c calculate various exponents and constants involving gamma
      eai    = 2.d0*(gamma-1.d0)/(gamma+1.d0)
      eai0   = 2.d0*(gamma0-1.d0)/(gamma0+1.d0)
      ep     = -gamma/(gamma-1.d0)
      ep0    = -gamma0/(gamma0-1.d0)
      erho   = -1.d0/(gamma0-1.d0)
      emrho  = gamma-1.d0
      emrho0 = gamma0-1.d0
      eam2   = (gamma+1.d0)/(gamma-1.d0)
      eam20  = (gamma0+1.d0)/(gamma0-1.d0)
      c1     = 2.d0/(gamma-1.d0)
      c10    = 2.d0/(gamma0-1.d0)
      c2     = (gamma0+1.d0)/2.d0
      c0     = (gamma0-1.d0)/gamma0
      c3     = (gamma-1.d0)/gamma

c figure out where the throat is for the dry data
c first figure out the value of pstar/p0=pstp0

                    pstp0 = (1.d0+ 1.0d0/c1)**ep
                    write(*,*)'pstp0 ',pstp0


      do i=1,idend
c      write(*,*) i, xd(i), dry(i)                   !debug
       if((dry(i).gt.pstp0).and.(dry(i+1).le.pstp0))then
c       write(*,*) "true"                            !debug
        xthroat=(pstp0-dry(i))/(dry(i+1)-dry(i))*(xd(i+1)-xd(i))+xd(i)
        go to 5001
       endif
      enddo
5001              continue
      write(*,*) "dry throat of ",dryfil," is at  ",xthroat
c now shift all the x and scale so that x(i) is in units of cm.
c find number of unused points before xstart          !chh110698
      ixstart=0                                      !chh110698
      do i=1,idend
       x(i)=(xd(i)-xthroat)/10.0  ! in units of cm  !ppaci for Velmex on Train B
       if(x(i) .le. xstart)ixstart=i                 !chh110698
      enddo
      write(*,*) "ixstart= ",ixstart                 !chh110698

      do i=1,idend                                   !debug
      write(9,1201) x(i), dry(i)                     !debug
      enddo                                          !debug

c now do linear interpolation to get fixed x intervals

c     save steps in inner loop by beginning interp. where left off
      lasti=ixstart                                  !chh110698
      do j=1,ilast
       xs(j)=xstart+(j-1)*0.1     !in intervals of 1 mm

       do i=lasti,idend                              !chh110698
        if((x(i).le.xs(j)).and.(x(i+1).gt.xs(j)))then
         dryf(j)=dry(i)+(xs(j)-x(i))*(dry(i+1)-dry(i))/(x(i+1)-x(i))
         deltadryf(j)=deltadry(i)
         lasti=i                                     !chh110698
         goto 5
        endif
       enddo

       write(*,*) "can't interpolate for point", j
```

```
 5    enddo



c we now have an array dryf(j) at fixed xs(j) intervals.  now put
c through smoothing routine.

c
c smooth dry density values
c first do points at ends of good data range
      do j=1,(nd-1)/2
      k0=1
      i=j
      call smooth(md,nd,i,k0,sval,dryf)
      sdry(i)=sval
      k0=ilast-nd+1
      i=ilast+1-j
      call smooth(md,nd,i,k0,sval,dryf)
      sdry(i)=sval
      enddo
c next do points in good data range
      do i=3,(ilast-2)
      k0=i-(nd-1)/2
      call smooth(md,nd,i,k0,sval,dryf)
      sdry(i)=sval
      enddo


 1201  format(f10.4,f10.4,g14.4,f10.4,f10.4,g14.4)



c figure out where the throat is for the wet data
c first figure out the value of pstarw/p0=pstp0w

                        pstp0w= (1.d0+ 1.0d0/c10)**ep0
                        write(*,*)'pstp0w ',pstp0w


      do i=1,idenw
c     write(*,*) i, xw(i), wet(i)                       !debug
       if((wet(i).gt.pstp0w).and.(wet(i+1).le.pstp0w))then
c                       write(*,*) "true"                           !debug
        xthroat=(pstp0w-wet(i))/(wet(i+1)-wet(i))*(xw(i+1)-xw(i))+xw(i)
        go to 5002
       endif
      enddo
5002                  continue
      write(*,*) "wet throat of ",wetfil," is at  ",xthroat

c now shift all the x and scale so that x(i) is in units of cm.
c find the number of unused points before xstart.          !chh110698
      ixstart=0                                    !chh110698
      do i=1,idenw
       x(i)=(xw(i)-xthroat)/10.0  ! in units of cm   !ppaci  reading on Velmex on train B
       if(x(i).le.xstart)ixstart=i                       !chh110698
      enddo
      write(*,*) "ixstart= ",ixstart                     !chh110698
      write(*,*) "throat shifted"                        !debug

c now do linear interpolation to get fixed x intervals
      lasti=ixstart                                !chh110698
      do j=1,ilast
c xs values have already been assigned in dry data analysis
c     write(*,*) xs(j)                             !debug
       do i=lasti,idenw                             !chh110698
        if((x(i).le.xs(j)).and.(x(i+1).gt.xs(j)))then
         wetf(j)=wet(i)+(xs(j)-x(i))*(wet(i+1)-wet(i))/(x(i+1)-x(i))
         deltawetf(j)=deltawet(i)
         lasti=i                                 !chh110698
         goto 6
        endif
       enddo

       write(*,*) "can't interpolate for point", j
 6    enddo


c we now have an array wetf(j) at fixed xs(j) intervals.  now put
c through smoothing routine.
      write(*,*) "put through smoothing"
c
c smooth wet pressure values
c first do points at ends of good data range
      do j=1,(nd-1)/2
      k0=1
      i=j
      call smooth(md,nd,i,k0,sval,wetf)
      swet(i)=sval
      k0=ilast-nd+1
      i=ilast+1-j
      call smooth(md,nd,i,k0,sval,wetf)
      swet(i)=sval
      enddo
c next do points in good data range
      do i=3,(ilast-2)
      k0=i-(nd-1)/2
      call smooth(md,nd,i,k0,sval,wetf)
      swet(i)=sval
      enddo
      write(*,*) "finished interpolating points"

c msq is mach number squared
c calculate the "wet" isentrope
                        write(*,*) "calculate the wet isentrope"
      do k = 1, ilast
       msq=c1*((1.d0/sdry(k))**c3-1.d0)
       aratio(k)=dsqrt(((c1/eam2*(1.d0+msq/c1))**eam2)/msq)
       machno = dsqrt(msq)
 100   rm(1)=dsqrt(c10*(c2*(machno*aratio(k))**eai0-1.d0))
      do im=1,10
                        rm(im+1)=dsqrt(c10*(c2*(rm(im)*aratio(k))**eai0-1.d0))
      enddo
      machno=rm(11)
      if(dabs(machno-rm(10)).gt.1.d-12)goto 100
      sweti(k)=(1.d0+(1.d0/c10)*machno**2.d0)**ep0
c      write(*,*) "k= ", k                               !debug
c      write(*,*) "sweti= ", sweti(k)                    !debug
c      write(*,*) "aratio=", aratio(k)                   !debug
      write(9,1203)xs(k),sdry(k),sweti(k),swet(k),dsqrt(msq),
     & machno,aratio(k)
      enddo
 1203 format(4(f9.5),2(f5.2),f6.3)



c use finer integration step size than measured point spacing
c generate interior points by linear interpolation
c nint is the number of subintervals between each pair of original x values
      write(*,*) "nint=  ", nint

c calculated the finer grid, interpolating on the wet condensing and
c wet isentrope data
      write(*,*) "calculate the finer grid"

      npts=ifin-istart+1
      nnpts=(npts-1)*nint+1
      jinit=nnpts+2*nint+istart-1
      do i=ifin+1,istart,-1
      delx=xs(i)-xs(i-1)
      delprd  = sdry(i)-sdry(i-1)
      delprwi = sweti(i)-sweti(i-1)
      delprw  = swet(i)-swet(i-1)
      jinit=jinit-nint
      jp=0
      do j=jinit,jinit-nint+1,-1
      fint=1.d0*dfloat(jp)/(1.d0*nint)
      xs(j)=xs(i)-delx*fint
      pp0d(j) = sdry(i)-delprd*fint
      pp0i(j) = sweti(i)-delprwi*fint
      pp0(j) = swet(i)-delprw *fint
      jp=jp+1
      enddo
      enddo
      ifin1=istart+nnpts-1

c calculate flow properties at nozzle throat
                        write(*,*) "calculate flow properties at nozzle throat"
      tstar=t0/c2
      rhogst=rhog0*c2**erho
      ustar=dsqrt(gamma0*rg*tstar/wmav)
      rhoust=rhogst*ustar

      do k = 1,ni

c need to calculate at istart-1 so adjust if istart=1
c since there is no good data avaiable before 1
       write(*,*) "start"
       write(*,5000) istart
5000                  format(3(I3,2x))
      if(istart.eq.1)istart=istart+1

      rosro0=rhogst/rhog0
```

```
      tst0=tstar/t0
      msq  = c10*((1.d0/pp0i(istart-1))**c0-1.d0)
      aratio(istart-1)=dsqrt(((c10/eam20*(1.d0+msq/c10))**eam20)/msq)

c note! start the wet condensing flow integration on the desired data
c point (i.e. on the wet curve data) rather than on the wet isentrope
c to avoid any extraneous extra shifts/offsets in t etc.

      msqw = c10*((1.d0/pp0(istart-1))**c0-1.d0)
      tt0(istart-1)=1.d0/(1.d0+msqw/c10)
      rr0(istart-1)=(1.d0+msqw/c10)**erho

      msq  = c10*((1.d0/pp0i(istart))**c0-1.d0)
      msqw = c10*((1.d0/pp0( istart))**c0-1.d0)
      tt0(istart)=1.d0/(1.d0+msqw/c10)
      rr0(istart)=(1.d0+msqw/c10)**erho

      g(istart)=0.d0
      g(istart-1)=0.d0
      fc(istart)=0.0d0                        !fraction condensed
      u(istart-1)=rhoust/rhog0/aratio(istart-1)/rr0(istart-1)


      write(9,*)ifin1-istart+1
      write(9,1200)t0,pc10*pconv,pc20*pconv
 1200 format(f7.0, f7.2)

      write(9,1009)
 1009 format('  xs(i)cm    u(i)cm/s   t(i)k  g(i)gc/gnc   tis ',
     &'t(i)-tis k pp0i(i)  pp0(i) g(i)*wi/(w20+w30)*100')   !chh100698
      write(10,1010)                          !4pp plots
 1010 format('@with g1')                      !4pp plots
      write(10,1011)p0*pconv,devp0,t0-273.15   !4pp plots
 1011 format('@title "',f6.2,'+/-',f4.2,'torr ',f6.2,'celsius"')   !4pp plots
      write(10,1012)pc10*pconv,specie(1),pc20*pconv,
     +specie(2)                               !4pp plots
 1012 format('@subtitle "',2(f7.4,'torr ',a),'")      !4pp plots
      write(10,1013)                          !4pp plots
 1013 format('@with g3')                      !4pp plots
      write(10,1014)wetfil,dryfil             !4pp plots
 1014 format('@subtitle \"',a13,'with dry trace ',a13,'\"')  !4pp plots
      write(10,1015)                          !4pp plots
 1015 format('#@string def \"xscm um/s t k g*wi/wco%   tis k',
     &'   pp0i    pp0\" ')                    !4pp plots
      write(12,1016)kd,pc10*pconv,specie(1),pc20*pconv,
     +specie(2)                               !4pp plots
 1016 format('legend string ',i2,' \"',2(f7.4,'torr ',a),'\"')       !4pp plots
      write(14,1017)kd, wetfil                !4pp plots
 1017 format('legend string ',i2,' \"',a13,'\"')       !4pp plots
      write(15,1018)kd-1,p0*pconv,devp0,t0-273.15   !4pp plots
 1018 format('legend string ',i2,' \"',f6.2,'+/-',f4.2,'torr ',
     & f6.2,'celsius"')   !4pp plots


      write(*,*) "start integration"
      write(*,5000)istart,ifin1
      do i=istart,ifin1

c calculate local value of effective area ratio, aratio
c msq is local mach number squared, mssq = (u/u*)^2

      msq    = c10*((1.d0/pp0i(i))**c0-1.d0)
      tisw(i) = 1.d0/(1.d0+msq/c10)*t0                    !wet isentrope t
      tisd(i) = pp0d(i)**c0*t0
                                          !dry isentrope t
      risr0 = (1.d0+msq/c10)**erho                !wet isentrope density
      pisp0 = (1.d0+msq/c10)**ep0                  !wet isentrope pressure
      aratio(i)= dsqrt(((c10/eam20*(1.d0+msq/c10))**eam20)/msq)

      msq   = c10*((1.d0/pp0i(i+1))**c0-1.d0)
      aratio(i+1) = dsqrt(((c10/eam20*(1.d0+msq/c10))**eam20)/msq)
      u(i)=ustar*rosro0/rr0(i)/aratio(i)
      mssq=(u(i)/ustar)**2

      dar=dlog(aratio(i+1)/aratio(i-1))/2.d0
      dp=(pp0(i+1)-pp0(i-1))/2.d0

c gw2-17-00 update specific heat
      cp=wi*cp1+(w20+w30-g(i))*cpv+g(i)*cpc
      cpr=cp/cp0

c gw2-17-00 update "mu/(1-g)" = wmu, and related factors
      wmu=wm1*wmc/(wi*wmc+(w20+w30-g(i))*wm1)
      wmuu0=wmu/wmav0
      wg(i)=wmu/(wmc)
```

```
c gw 17-2-00 the following factor is almost one
      approx1=wmuu0*gamma0-(gamma0-1.d0)/cpr
      t(i)=tt0(i)*t0
c gw17-2-00 next eq. is slightly in error.  it's from wegener and
c should not be used.
c       dtt0=(1.d0-t(i)/tstar/gamma0/mssq)/rr0(i)*dp+tt0(i)*dar

c gw17-2-00 the next equation is ok.
      dr=dp/tst0/gamma0/mssq-rr0(i)*dar

c gw17-2-00 the next equation from wegener is wrong. don't use it
c       dgp=(1.d0-t(i)/tstar/mssq)/gamma0/rr0(i)*dp+tt0(i)*dar
c gw 17-2-00 this is the correct eq.
      dgp=(approx1-t(i)/tstar/mssq)/gamma0/rr0(i)*dp+tt0(i)*dar

c gw2-17-00 this eq. is from wegener. it is wrong. don't use it.
c       dg=dgp*cp0*t0/dhc
c gw2-17-00 need wg(i) term to get dg correctly
c gw2-17-00       dg=dgp*cp0*t0/(dhc-cp*t(i)*wg(i))
c       dg=dgp*cp0*t0/(dhc-cp*t(i)*wg(i))
      dg=dgp*cp0*t0/(fdhc(zc10,t(i))-cp*t(i)*wg(i))                    !chh21.02.01

c gw2-17-00 update dtt0
      dtt0=(wmuu0-t(i)/tstar/gamma0/mssq)/rr0(i)*dp+
     &   tt0(i)*(dar+wg(i)*dg)

c still need to fix this correction for the binary system for the pressure method
c if we think it matters!
c calculate dt with alt. eq. and dgp from more general results due to mod. eos
c gw2-17-00 note: cp2 should be cpv in the following eq. it's ok above.
c     cp=wi*cp1+(w20+w30-g(i))*cp2+g(i)*cpc
c     cpr=cp/cp0
c     c0fctr=cpr*wmug(i)/wmav/c0-1.d0
c     wgfctr=1.d0-wg(i)*cp*t(i)/dhc
c     dgp=(c0fctr*c0*dp/sdrwet(i)
c    & -tt0(i)*cpr*dlog(sdrwet(i+1)/sdrwet(i-1))/2.)/wgfctr
c     dg=dgp*cp0*t0/dhc

      tt0(i+1)=tt0(i-1)+2.0d0*dtt0
      rr0(i+1)=rr0(i-1)+2.0d0*dr
      g(i+1)=g(i-1)+2.0d0*dg

      if((w20+w30).gt.0.0)then
       fc(i+1)=g(i+1)*wi/(w20+w30)
      else
       fc(i+1)=0.0
      end if
      write(9,1000)xs(i),u(i),t(i),g(i),tisw(i),t(i)-tisw(i),
     &pp0i(i),pp0(i),fc(i)
      write(10,1020)xs(i),u(i)/100,t(i),fc(i)*100,tisw(i),   !4pp plots
     +pp0i(i),pp0(i),pisp0,tisd(i)                           !4pp plots
 1020 format(f8.3,f10.2,f8.2,e12.3,f8.2,3f8.4,f8.2)          !4pp plots
      write(3,1100) i, xs(i),rr0(i),risr0,rr0(i)/risr0,t(i)/tisw(i),
     *pp0(i)/pp0i(i)
      write(26,1110) xs(i),aratio(i)
 1000 format(e12.3,e12.3,f8.2,e12.3,f8.2,f7.3,2e12.4,e12.4)
 1100 format(i5,e12.3,5e12.4)
 1110 format(e12.3,5e12.4)
     enddo

                write(*,*)'start search'
c now search for the onset conditions using both t(i)-tisw(i) and t(i)-tisd

                do i = istart,ifin1-1
      dtemp(i,kd) = t(i)-tisw(i)
      dt1 = t(i) - tisw(i)
      dt2 = t(i+1) - tisw(i+1)
      if(dt1.le.0.5d0.and.dt2.gt.0.5d0)then
                 xon = xs(i)+(0.5-dt1)/(dt2-dt1)*(xs(i+1)-xs(i))
                 pp0on = pp0(i)+(0.5-dt1)/(dt2-dt1)*(pp0(i+1)-pp0(i))
                 pp0ion = pp0i(i)+(0.5-dt1)/(dt2-dt1)*(pp0i(i+1)-pp0(i))
                 ton = t(i)+(0.5-dt1)/(dt2-dt1)*(t(i+1)-t(i))
                 tiswon = tisw(i)+(0.5-dt1)/(dt2-dt1)*(tisw(i+1)-tisw(i))
                else
                endif
      enddo
      write(*,*)'using the t-tisw = 0.5 k'
                 write(*,1300)xon,pp0on*pct0,ton,
     &           pp0ion*pct0,tiswon
 1300 format('onset occurs at x =',f8.4,f8.4,f7.2,f8.4,f7.2)
                 write(11,1301)t0,p0*pconv,pct0,ton,pp0on*pct0,

     &     pp0on*pc10*pconv,pp0on*pc20*pconv,wetfil,xon
 1301 format(f8.2,f8.2,f8.4,f8.2,f8.4,f8.4,f8.4,2x,a13,f7.1)
 1302 format('@\"t0    p0    pct    ton    pon   p1on   p2on',
     &  6x,a13,'\"')
```

```
                    do i = istart,ifin1-1
       dt1 = t(i) - tisd(i)
       dt2 = t(i+1) - tisd(i+1)
       if(dt1.le.0.5d0.and.dt2.gt.0.5d0)then
                    xon = xs(i)+(0.5-dt1)/(dt2-dt1)*(xs(i+1)-xs(i))
                    pp0on = pp0(i)+(0.5-dt1)/(dt2-dt1)*(pp0(i+1)-pp0(i))
                    pp0ion = pp0i(i)+(0.5-dt1)/(dt2-dt1)*(pp0i(i+1)-pp0(i))
                    ton = t(i)+(0.5-dt1)/(dt2-dt1)*(t(i+1)-t(i))
                    tisdon = tisd(i)+(0.5-dt1)/(dt2-dt1)*(tisd(i+1)-tisd(i))
                   else
                   endif
      enddo
       write(*,*)'using the criterion t-tisd = 0.5 k'
                    write(*,1300)xon,pp0on*(pc10+pc20)*pconv,ton,
     &             pp0ion*(pc10+pc20)*pconv,tiswon

c                   if(istart-1.eq.1)then
c      istart=istart+nint-1
c     else
c      istart=istart+nint
c     endif
      write(*,*) "finished integration"
     enddo
                    enddo
c now write out the dtemp files to dtemp.out

                    do i = istart,ifin1
                    write(13,1313)xs(i),(dtemp(i,j),j=1,ndata)
                    enddo
1313                format(f8.4,20(f8.2))


   50 stop
     end
c
     subroutine smooth(m,n,k,k0,sval,y)
c this subroutine produces smoothed values of a tabulated function y
c based on technique described in ralston, "a first course in num. anal."
c y values do not have to be equally spaced, but x values must be supplied
c regardless of the spacing
c
c m - order of the highest polynomial used in smoothing
c n - number of y points in interval over which smoothing is performed
c k - point whose smoothed value is desired
c k0 - first point in set of n
c sval - smoothed value returned to calling program
c
     real*8 p(-2:5,1:200),b(0:5),omega(0:5),gamma(0:5),beta(-1:5)
     *,alpha(0:5),y(200),sval,x
     common /xval/ x(500)
     beta(-1)=0.
     beta(0)=0.
     gamma(0)=n
     omega(0)=0.
     alpha(1)=0.
     do i=k0,(n+k0-1)
     omega(0)=omega(0)+y(i)
     alpha(1)=alpha(1)+x(i)
     p(-2,i)=0.
     p(-1,i)=0.
     p(0,i)=1.
     enddo
     b(0)=omega(0)/gamma(0)
     alpha(1)=alpha(1)/gamma(0)
     sval=b(0)
     do j=1,m
      gamma(j)=0.
      omega(j)=0.
      alpha(j+1)=0.
      do i=k0,(n+k0-1)
       p(j,i)=(x(i)-alpha(j))*p(j-1,i) - beta(j-1)*p(j-2,i)
       gamma(j)=gamma(j)+p(j,i)*p(j,i)
       alpha(j+1)=alpha(j+1)+x(i)*p(j,i)*p(j,i)
       omega(j)=omega(j)+y(i)*p(j,i)
      enddo
      alpha(j+1)=alpha(j+1)/gamma(j)
      beta(j)=gamma(j)/gamma(j-1)
      b(j)=omega(j)/gamma(j)
      sval=sval+b(j)*p(j,k)
     enddo
     return
     end


     subroutine echo
     character*100 a
     write(9,3)
   15 read(5,1,end=99)a
     write(3,1)a
     write(9,2)a
     goto 15
   99 continue
     rewind 5
     return
    1 format(0x,a100)
    2 format(1x,a100)
    3 format(1h1,20x,'input file',//)
     end
*-------------------------------------------------------------------------------chh22.02.01---*
*
c     real function fdhc(dhc)
c      fdhc = dhc
c      return
*
     real function fdhc(zc10,tk)
     double precision zc10,tk,rg
*-------------------------------------------------------general nomenclature-*
c     rg              universal gas constant in units of
c     tk              temperature of vapor condensing in kelvin
c     zc10            molar fraction of condensible 1 in vapor (zc10+zc20=1.0)
*-------------------------------------------------condensible nomenclature-*
c     a2h2o - a4h2o h2o vapor pressure constants, wagner correlation
c     a1d2o - a6d2o d2o vapor pressure constants,
c     mwd2o         d2o molecular weight
c     z                                   d2o intermediate variable
*-----------------------------------------------------------------------*
     double precision a2h2o,a3h2o,a4h2o,mwh2o              !h2o pve constants
     double precision a1d2o,a2d2o,a3d2o,a4d2o,a5d2o,a6d2o,z,mwd2o  !d2o pve
constants

     rg=8.3144d0

*-----------------------------------------------------------------------*
*-d2o clausius-clapeyron relation applied to equilibrium vapor pressure
*-d2o valid for temperature range of ?-? K
*-d2o hill, mcmillan, and lee, j. phys chem ref data, vol 11, no.1, p1-14 (1982)
     a1d2o= -7.81583d0
     a2d2o= 17.6012d0
     a3d2o=-18.1747d0
     a4d2o= -3.92488d0
     a5d2o=  4.19174d0
     a6d2o=643.89d0
     mwd2o=20.03d0

     z=1-tk/a6d2o
     d2oa=a1d2o*z+a2d2o*z**1.9+a3d2o*z**2+a4d2o*z**5.5+a5d2o*z**10.
     d2ob=a1d2o+1.9d0*a2d2o*z**0.9+2.d0*a3d2o*z+5.5d0*a4d2o*z**4.5
    &+10.d0*a5d2o*z**9.
     dhcd2o=-rg*(a6d2o*d2oa+tk*d2ob)/mwd2o

*-----------------------------------------------------------------------*
*-h2o clausius-clapeyron relation applied to equilibrium vapor pressure
*-h2o valid for temperature range of ?-? K
*-h2o wagner thesis as reported in
     a2h2o=7235.42d0
     a3h2o=  -8.2d0
     a4h2o=   0.0057113d0
     mwh2o=18.02d0

     dhch2o=rg*(a2h2o+a3h2o*tk+a4h2o*tk**2)/mwh2o

*-----------------------------------------------------------------------*
     fdhc = zc10*dhch2o+(1.d0-zc10)*dhcd2o

    write(28,*)"dhc debug: fdhc= ",fdhc," zc10= ",zc10," tk= ",tk," K"  !debug dhc
    return

     end
*-------------------------------------------------------------------------------------*
```

APPENDIX D

INSTRUMENTS CALIBRATION

In this section the calibrations that have been performed are described. We calibrated the RTDs, the pressure transducers, the TDL system (for each set of runs), and the peristaltic pump according to the procedure discussed in the following sections.

D.1 TEMPERATURE CALIBRATION

Each RTD probe (Omega Engineering, fine diameter - 1/16" - platinum RTD) coupled with one of the available display meters (Omega engineering, DP41-RTD high performance temperature indicator) has been calibrated against a high accuracy NIST certified ASTM - 37C - CC mercury reference thermometer following the procedure described in the next 5 steps:

(1) The reference thermometer and RTD probes have been placed into a water bath (VWR Scientific, model No. 1157) and the temperature has been raised slowly to the desired level by setting the water bath temperature control.

(2) An adequate amount of time (usually about 5 minutes) has been allotted in order to ensure stabilization of the temperature.

(3) The temperature shown by the thermometer has been recorded as well as the temperature measured from the RTD probe and displayed by the indicator.

(4) The water bath set temperature has been raised to a different level and the steps from (1) to (3) have been repeated. This has been done for three temperatures in the normal working range of our experiments.

(5) Calibration tables and a plot of the temperature measured versus the real temperature (given by the high accuracy thermometer) have been built.

ACTUAL TEMPERATURE: 25.00 °C							ACTUAL TEMPERATURE: 45.00 °C						
Bath set: 24.40 °C		dysplay meter/channel					Bath set: 44.30 °C		dysplay meter/channel				
		A1	A5	A10	B4	B8			A1	A5	A10	B4	B8
RTD probe	A1	24.09	-	-	-	24.19	RTD probe	A1	43.38	-	-	-	43.57
	A5	-	24.02	-	23.96	-		A5	-	43.21	-	43.65	-
	A10	-	-	//	-	-		A10	-	-	//	-	-
	B4	-	-	-	-	-		B4	-	-	-	-	-
	B8	24.14	-	-	-	24.09		B8	43.40	-	-	-	43.58
ACTUAL TEMPERATURE: 35.00 °C							Notes: 1) Actual Temperature measured with a certified, high accuracy ASTM-37C-CC thermometer; 2) Probe named A10 has been verified not working properly and therefore has been discarded; 3) The calibration has been performed on June 2002						
Bath set: 34.30 °C		dysplay meter/channel											
		A1	A5	A10	B4	B8							
RTD probe	A1	33.75	-	-	-	33.80							
	A5	-	33.59	-	33.66	-							
	A10	-	-	//	-	-							
	B4	-	-	-	-	-							
	B8	33.71	-	-	-	33.79							

Figure D1 - 2002 Temperature calibration tables

The display indicators have been named A and B, according to the nozzle train to which they are dedicated, and each of their input channels is numerated progressively. Several different probe/indicator/channel combinations have been tested, in order to

ensure a certain immediate flexibility and backup possibility. Figures D1 and D2 summarize the results for the 2002 Temperature calibration.

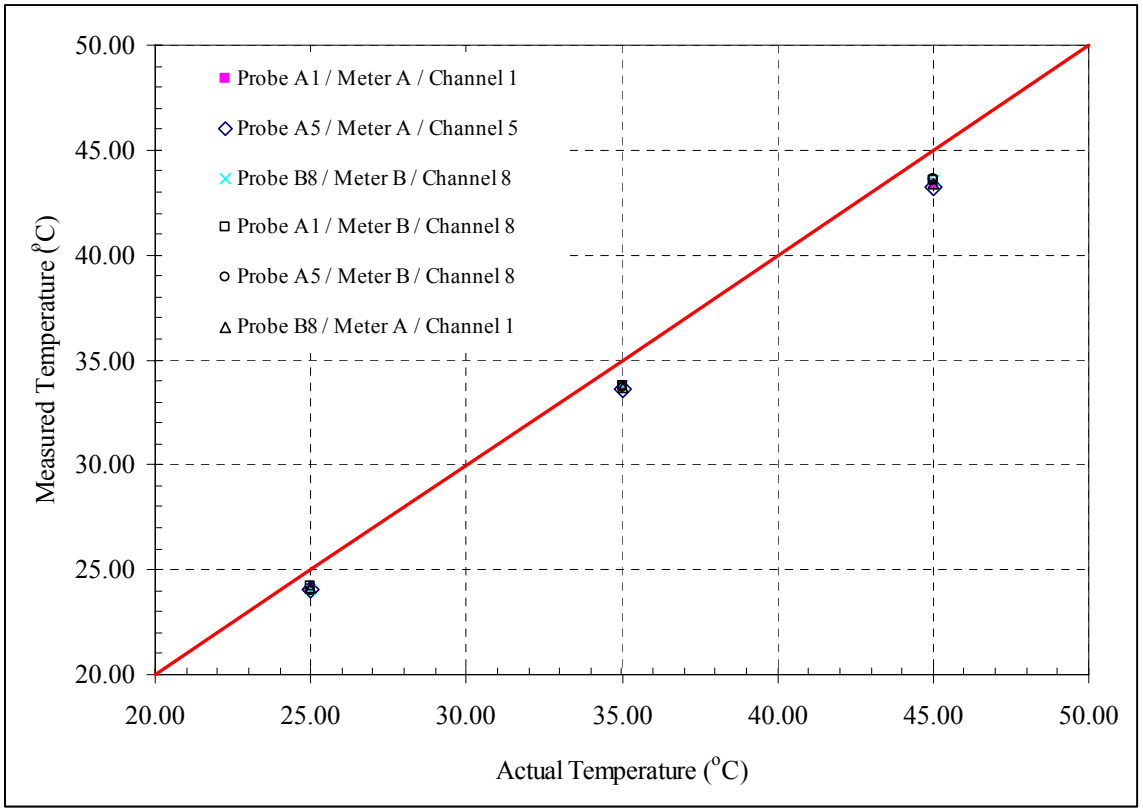

Figure D2 - 2002 Temperature calibration graph

D.2 PRESSURE TRANSDUCERS CALIBRATION

The pressure transducer used for measuring the static pressure (MKS 690A Baratron absolute pressure sensor) has been calibrated against a high precision laboratory tested transducer (MKS 120AA Baratron absolute capacitance manometer), successively used

in our train to measure the static pressure via movable probe along the nozzle during the pressure traces experiments.

The procedure followed to perform the calibration is the same developed earlier in our laboratory [12] and can be summarized in the following steps:

(1) The reference transducer and the transducer(s) to be calibrated are connected together and to a vacuum pump. A connection to a high pressure liquid dewar is also provided in order to raise the pressure above 1 atm during the process;

(2) Vacuum conditions are reached and then the pressure is slowly raised. At predefined interval steps the pressure is recorded from the instruments. After reaching atmospheric conditions, the pressure is raised above 1 atm introducing nitrogen in the system, up to near the limit of the working range of the instruments.

(3) A calibration curve - measured pressure versus real pressure - is then built fitting the data.

The results from the data fitting for the 690A transducer used in nozzle system B for measuring the static pressure in the nozzle are shown in Figure D3. As it is possible to see in the figure, the value of the calibrated instrument is given in a (2×Torr) units because of the display meter used, which works on a 10,000 range scale, while the 690A Baratron returns a signal in a 0-5,000 mV range scale.

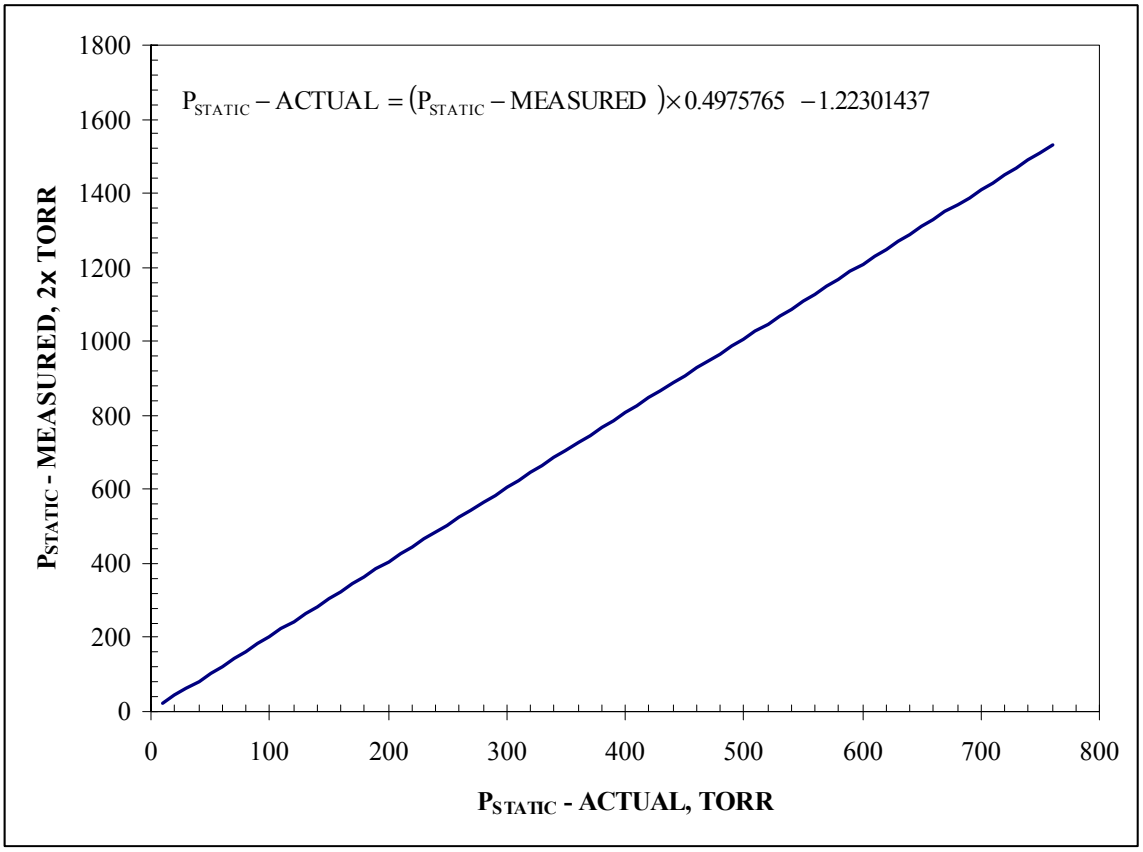

Figure D3 - 2002 Pressure transducers calibration graph

In this work, all the experiments have been performed at a static pressure measured in a pressure tap located in the flat part of the nozzle of 60 ± 0.07 kPa (450 ± 0.5 Torr, displayed and recorded as 907 ± 1 "double" Torr in the calibrated display meter), corresponding to a stagnation pressure at the inlet of the nozzle equal to 60.4 ± 0.07 kPa (453.3 ± 0.5 Torr).

The relation occurring between the static and the stagnation pressure is shown in the following equation [45]:

$$P_{STAGN} = P_{STATIC} + \frac{1}{2} \cdot \rho \cdot vel^2 \qquad \text{(E-1)}$$

Where:

P_{STAGN} = Stagnation pressure;
P_{STATIC} = Static pressure;
vel = velocity of flow;
ρ = gas density;

In the previous equation the velocity of the flow is easily obtainable knowing the flowrate (from the mass balance) and the flowing section.

D.3 TDL SYSTEM CALIBRATIONS

The first calibration performed on the TDL system is relevant to the lead screw mounted on the side of the plenum that provides the translational movement and is rotated manually. The arrangement is attached to an optical counter, has a working range of about 20 cm and provides a way to resolve the position of the laser beam with respect to the nozzle better than 0.02 mm. The optical counter calibration is shown in the following Table D1. The zero position has been set in between the small and the big CaF_2 windows, and the entire length of both windows has been made available for the measurement.

Table D1 - Nozzle translational movement device - optical counter calibration

OPTICAL COUNTER STEPS(1)	cm	cm from the throat	NOTES
-300	-0.60	-4.86	Center of the small window
0	**0.00**	-4.26	Conventional zero position
1660	3.30	-0.96	Beginning of the main window
2144	4.26	**0.00**	Position of the nozzle throat
5510	10.95	6.69	Last spectroscopically useful main window position
5560	11.05	6.79	End of the main window

(1) Each step corresponds to about 2 hundredths of millimeter

To know exactly the position of the throat is essential for comparing results from the pressure trace experiments to results from the TDL experiments.

The most important (and basically the only one) spectroscopic calibration performed on the TDL system is relevant to the mixing ratios values returned from the instrument and depends mainly on the optical arrangement used. Theoretically, one of the characteristics that makes the Tunable Diode Laser Spectroscopy so interesting in our specific application is that absolute species mixing ratios are returned directly from the nonlinear least squares fits and therefore calibration should not be required [13, 26].

However, TDLAS instruments are complex, the diode lasers themselves can be unreliable and each laser is unique, leading to the need to recharacterize the instrument whenever a new laser is installed. In our system, in addition to the previous issues, depending on the optical arrangement used, and given the fact that more than 99% of the beam's pathlength is in the open atmosphere, some backscattering and alteration of the

signal is to be expected, and a certain error is expected to come from the available D_2O spectroscopic data [33], as discussed earlier in Table 2.2. As a consequence, a calibration of the mixing ratios measured by the TDL instrument against a known value had to be performed.

The calibration has been developed according to the following steps:

(1) Spectroscopic measures have been taken at several known stagnation conditions and condensible flowrates, as well as at the corresponding background conditions;

(2) Background subtraction has been performed and the mixing ratios have been derived by fitting the spectra for several different positions along the nozzle before the onset of condensation. This has been done for all the different stagnation conditions analyzed;

(3) The spectroscopically derived mixing ratios have been calibrated against mixing ratios predictions from the mass balance, known exactly for each position where condensation didn't occur yet;

(4) The constant calibration factors obtained have been then applied to the remainder of the spectroscopically measured mixing ratios varying the intensity of the absorption line examined and performing again the fitting procedure.

STEP 1
Spectroscopic measures are taken at several known stagnation conditions and condensible flowrates, as well as at the corresponding background conditions.

STEP 2
Background subtraction is performed and the mixing ratios are derived.

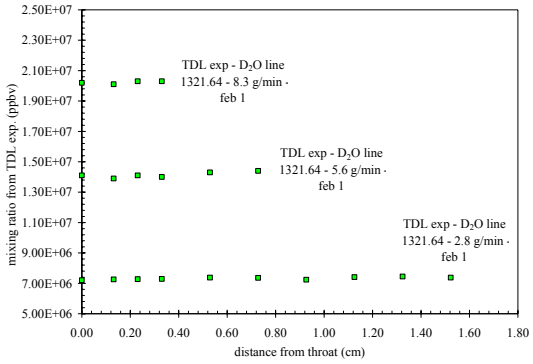

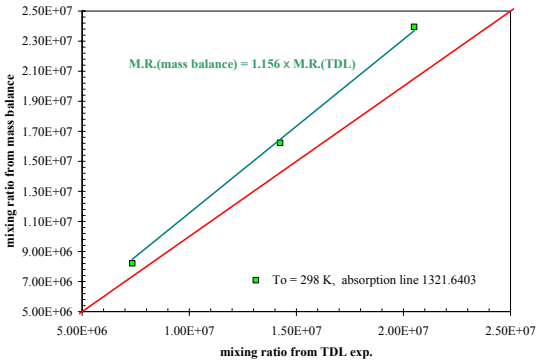

STEP 3
The spectroscopically derived mixing ratios are calibrated against mixing ratios predictions from the mass balance.

STEP 4
The constant calibration factor obtained is applied, for each experiment, to the remainder of the spectroscopically measured mixing ratios varying the intensity of the absorption line examined and performing again the fitting procedure.

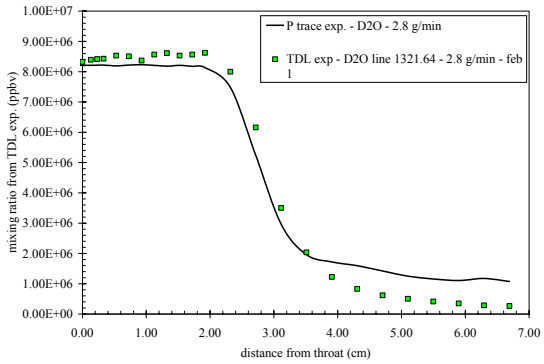

Figure D4 - TDL calibration procedure

The returned mixing ratio is directly proportional to the line intensity, given all the other parameters, therefore, in practice, previous step (4) is done changing the value for the line intensity at 296 K in the Hitran parameter (*.hit) file when performing the fit through the TDLWintel Software. This can be done without violating any fundamental

principle [34] and is in theory a justified procedure since up to a ± 21% error is originally to be expected in this parameter, according to the source [33].

Table D2 - Calibration factors for the TDL system as a function of absorption lines and operating conditions

TDL experiment	Cal. factor(1)	runs id.
TDL exp - D_2O line 1321.64 $T_0 = 25^oC$ - feb 1	1.156	020103_2ml 020103_4ml 020103_6ml
TDL exp - D_2O line 1321.64 $T_0 = 35^oC$ - feb 11	1.163	021103_2ml 021103_4ml 021103_6ml
TDL exp - D_2O lines 1321.294/1321.292 $T_0 = 25^oC$ - feb 1	0.9596	020103_2ml 020103_4ml 020103_6ml
TDL exp - D_2O lines 1321.294/1321.292 $T_0 = 35^oC$ - feb 11	0.9763	021103_2ml 021103_4ml 021103_6ml

(1) expressed as average M.R.(p. trace)/average M.R.(TDL exp.)

The process described above is schematically illustrated in Figure D4 for one stagnation condition and three different flowrates and the calibration factors and curves are reported, for the D_2O lines used in this work, respectively in Table D2 and Figure D5.

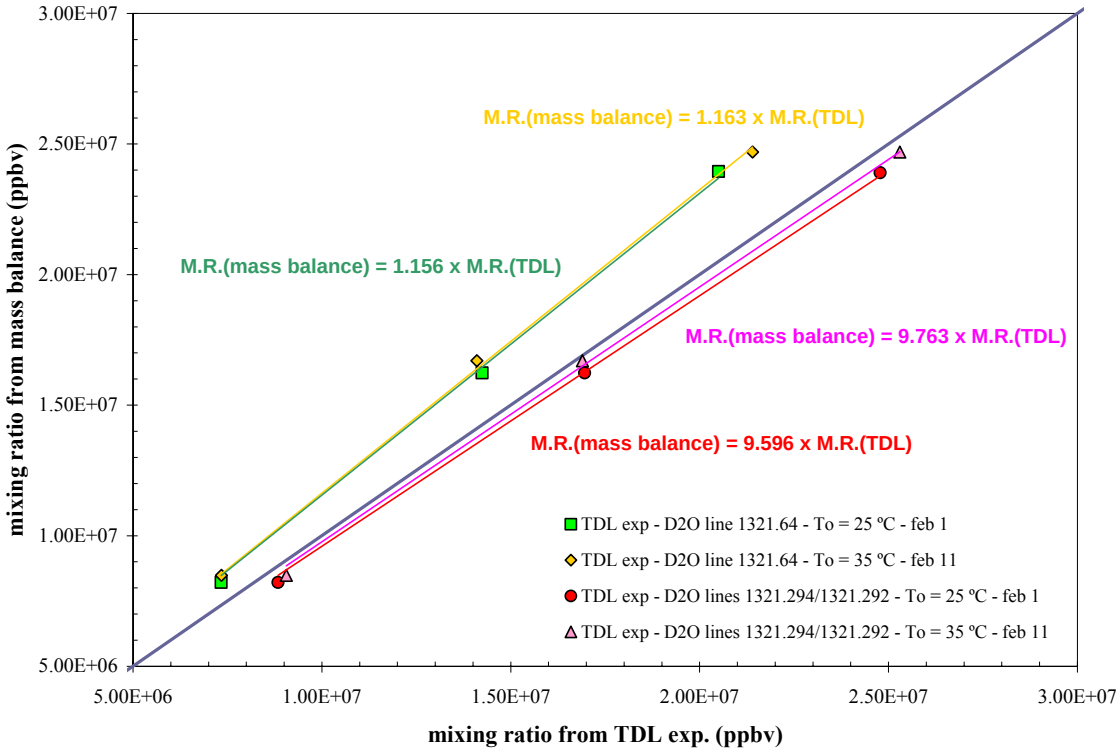

Figure D5 - Calibration curves for the TDL system

D.4 PERISTALTIC PUMP CALIBRATION

In our vapor generation system, condensible material is pumped as liquid into the vaporizer using a peristaltic pump (Masterflex Pump Model 7523-20), and the mass flow rate of the condensible material is measured by weighing the liquid dispensed during the course of an experiment using a balance.

Peristaltic pumps operate on a simple principle. The alternating pattern of squeezing and releasing the tubing moves the fluid through the pump.

As a roller passes over the tubing, it is first occluded (squeezed), then released. The progression of this squeezed area forces fluid to move in front of the roller. The tubing behind the rollers recovers its shape, creates a vacuum, and draws fluid in behind it. The distance between the rollers creates a "pillow" of fluid. Volumetric flow rate is determined by multiplying pump head speed by the size of the pillow by the number of pillows per revolution.

Because each fluid is different, the actual mass flowrate has to be determined experimentally, creating a "calibration curve" typical of the substance which has to be used in planning the work and ensure experimental reproducibility.

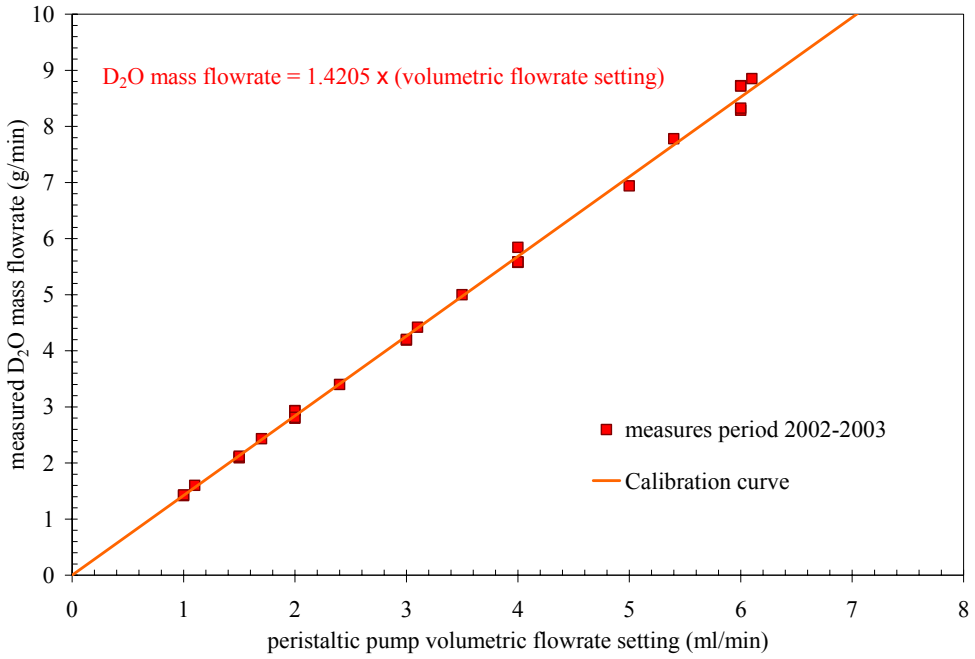

Figure D6 - Calibration curve for the peristaltic pump - D_2O

We perform a mass balance during each of our pressure trace experiments, obtaining the calibration curve typical of each substance, and then we determine the correct volumetric flowrate to use for the TDL experiments by means of this curve.

Figures D6 and D7 illustrate the calibration curves for D_2O and H_2O, respectively, obtained in the period 2002-2003 in our laboratory on both Nozzle systems A and B, where the same pump has been used.

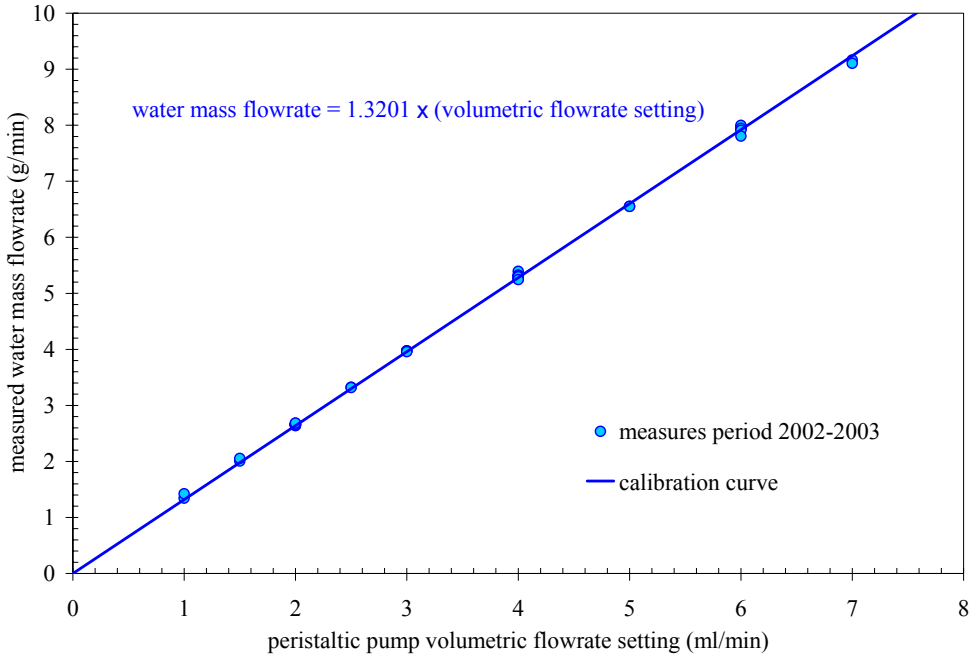

Figure D7 - Calibration curve for the peristaltic pump - Water

APPENDIX E

TABLES OF RESULTS

In this appendix, the tables reporting the TDL experiments results are shown. The same results have been shown earlier in a graphical fashion in Chapter 3.

Tables from E1 to E6 show the Mixing Ratio determination results for two different stagnation conditions and three different flowrates using the TDL system.

Table E1 - Mixing Ratio results - TDL exp. - D_2O line 1321.64 - 2.8 g/min - 25°C

position		Results from P trace data inversion Pov = 0.501 kPa, To = 25.02 ºC			Results from TDL experiment TDL exp - D2O line 1321.64 - 2.8 g/min - feb 1	
STEPS(1)	cm from throat	p (kPa)	T (K)	mixing ratio (ppbv)	mixing ratio (ppbv)(2)	Saved spectrum
-300	-4.86	60.4	298	8.21E+06	8.88E+06	Saved spectrum as 030203_145126_1.spe
2144	0.00	31.7	246	8.21E+06	8.32E+06	Saved spectrum as 030204_063226_1.spe
2210	0.13	30.4	244	8.21E+06	8.39E+06	Saved spectrum as 030204_063333_1.spe
2260	0.23	29.2	242	8.22E+06	8.42E+06	Saved spectrum as 030204_063452_1.spe
2310	0.33	28.3	240	8.22E+06	8.43E+06	Saved spectrum as 030204_063554_1.spe
2410	0.53	26.7	236	8.19E+06	8.53E+06	Saved spectrum as 030204_063703_1.spe
2510	0.73	25.3	233	8.22E+06	8.51E+06	Saved spectrum as 030204_063850_1.spe
2610	0.93	24.0	229	8.23E+06	8.37E+06	Saved spectrum as 030204_064011_1.spe
2710	1.13	23.0	226	8.21E+06	8.57E+06	Saved spectrum as 030204_064207_1.spe
2810	1.32	22.1	224	8.18E+06	8.61E+06	Saved spectrum as 030204_064322_1.spe
2910	1.52	21.4	222	8.21E+06	8.53E+06	Saved spectrum as 030204_064548_1.spe
3010	1.72	20.7	220	8.18E+06	8.57E+06	Saved spectrum as 030204_065839_1.spe
3110	1.92	20.0	218	8.14E+06	8.62E+06	Saved spectrum as 030204_065949_1.spe
3310	2.32	19.0	216	7.48E+06	8.00E+06	Saved spectrum as 030204_070802_1.spe
3510	2.72	18.8	219	5.24E+06	6.16E+06	Saved spectrum as 030204_071116_1.spe
3710	3.11	18.6	222	2.96E+06	3.50E+06	Saved spectrum as 030204_071253_1.spe
3910	3.51	18.0	222	1.96E+06	2.03E+06	Saved spectrum as 030204_071925_1.spe
4110	3.91	17.2	219	1.72E+06	1.23E+06	Saved spectrum as 030204_072044_1.spe
4310	4.31	16.4	217	1.60E+06	8.31E+05	Saved spectrum as 030204_072229_1.spe
4510	4.70	15.7	214	1.42E+06	6.17E+05	Saved spectrum as 030204_072340_1.spe
4710	5.10	15.0	212	1.25E+06	5.03E+05	Saved spectrum as 030204_072558_1.spe
4910	5.50	14.4	210	1.16E+06	4.13E+05	Saved spectrum as 030204_072714_1.spe
5110	5.90	13.9	208	1.11E+06	3.49E+05	Saved spectrum as 030204_072854_1.spe
5310	6.29	13.4	205	1.17E+06	2.87E+05	Saved spectrum as 030204_073119_1.spe
5510	6.69	12.9	204	1.08E+06	2.62E+05	Saved spectrum as 030204_073441_1.spe

(1) From Plenum translational device optical counter
(2) After Calibration (see Appendix D)

Table E2 - Mixing Ratio results - TDL exp. - D_2O line 1321.64 - 5.6 g/min - 25°C

position		Results from P trace data inversion Pov = 0.997 kPa, To = 25.04 ºC			Results from TDL experiment TDL exp - D2O line 1321.64 - 5.6 g/min - feb 1	
STEPS(1)	cm from throat	p (kPa)	T (K)	mixing ratio (ppbv)	mixing ratio (ppbv)(2)	Saved spectrum
-300	-4.86	60.4	298	1.62E+07	1.72E+07	Saved spectrum as 030203_113627_1.spe
2144	0.00	31.7	246	1.62E+07	1.63E+07	Saved spectrum as 030203_113854_1.spe
2210	0.13	30.4	244	1.62E+07	1.61E+07	Saved spectrum as 030203_114453_1.spe
2260	0.23	29.0	242	1.62E+07	1.63E+07	Saved spectrum as 030203_114650_1.spe
2310	0.33	28.1	240	1.62E+07	1.62E+07	Saved spectrum as 030203_115417_1.spe
2410	0.53	26.6	237	1.62E+07	1.65E+07	Saved spectrum as 030204_062840_1.spe
2510	0.73	25.2	233	1.61E+07	1.66E+07	Saved spectrum as 030204_062951_1.spe
2610	0.93	23.9	230	1.60E+07	1.61E+07	Saved spectrum as 030207_125209_1.spe
2710	1.13	23.2	229	1.55E+07	1.65E+07	Saved spectrum as 030207_130430_1.spe
2810	1.32	23.3	232	1.38E+07	1.61E+07	Saved spectrum as 030203_115632_1.spe
2910	1.52	24.1	239	1.10E+07	1.41E+07	Saved spectrum as 030207_130849_1.spe
3010	1.72	24.5	244	8.66E+06	1.12E+07	Saved spectrum as 030207_133242_1.spe
3110	1.92	24.0	245	7.54E+06	9.02E+06	Saved spectrum as 030207_142228_1.spe
3310	2.32	22.7	244	5.96E+06	5.63E+06	Saved spectrum as 030207_142427_1.spe
3510	2.72	21.4	241	5.32E+06	4.00E+06	Saved spectrum as 030207_142705_1.spe
3710	3.11	20.2	238	4.89E+06	3.19E+06	Saved spectrum as 030207_143609_1.spe
3910	3.51	19.2	235	4.57E+06	2.61E+06	Saved spectrum as 030207_144219_1.spe
4110	3.91	18.2	232	4.34E+06	2.29E+06	Saved spectrum as 030207_192715_1.spe
4310	4.31	17.4	229	4.06E+06	1.88E+06	Saved spectrum as 030207_193006_1.spe
4510	4.70	16.6	227	3.85E+06	1.62E+06	Saved spectrum as 030207_193249_1.spe
4710	5.10	15.9	225	3.60E+06	1.35E+06	Saved spectrum as 030207_194024_1.spe
4910	5.50	15.2	222	3.54E+06	1.13E+06	Saved spectrum as 030207_202736_1.spe
5110	5.90	14.6	220	3.37E+06	1.05E+06	Saved spectrum as 030207_203156_1.spe
5310	6.29	14.2	218	3.26E+06	9.56E+05	Saved spectrum as 030207_203535_1.spe
5510	6.69	13.7	217	2.91E+06	8.45E+05	Saved spectrum as 030207_203938_1.spe

(1) From Plenum translational device optical counter
(2) After Calibration (see Appendix D)

Table E3 - Mixing Ratio results - TDL exp. - D_2O line 1321.64 - 8.3 g/min - 25°C

position		Results from P trace data inversion Pov = 1.482 kPa, To = 25.00 ºC			Results from TDL experiment TDL exp - D2O line 1321.64 - 8.3 g/min - feb 1	
STEPS(1)	cm from throat	p (kPa)	T (K)	mixing ratio (ppbv)	mixing ratio (ppbv)(2)	Saved spectrum
-300	-4.86	60.4	298	2.39E+07	2.50E+07	Saved spectrum as 030203_145343_1.spe
2144	0.00	31.7	246	2.39E+07	2.34E+07	Saved spectrum as 030204_050102_1.spe
2210	0.13	30.4	244	2.39E+07	2.32E+07	Saved spectrum as 030204_050459_1.spe
2260	0.23	29.0	243	2.39E+07	2.35E+07	Saved spectrum as 030204_050745_1.spe
2310	0.33	28.2	241	2.39E+07	2.35E+07	Saved spectrum as 030204_054844_1.spe
2410	0.53	26.9	238	2.36E+07	2.42E+07	Saved spectrum as 030204_055121_1.spe
2510	0.73	26.4	239	2.24E+07	2.43E+07	Saved spectrum as 030204_055340_1.spe
2610	0.93	27.2	246	1.97E+07	2.30E+07	Saved spectrum as 030204_055512_1.spe
2710	1.13	27.9	251	1.74E+07	2.12E+07	Saved spectrum as 030204_055720_1.spe
2810	1.32	27.8	254	1.56E+07	1.80E+07	Saved spectrum as 030204_055915_1.spe
2910	1.52	27.2	255	1.43E+07	1.50E+07	Saved spectrum as 030204_060043_1.spe
3010	1.72	26.3	254	1.33E+07	1.27E+07	Saved spectrum as 030204_060213_1.spe
3110	1.92	25.4	253	1.24E+07	1.13E+07	Saved spectrum as 030204_060359_1.spe
3310	2.32	23.7	251	1.09E+07	9.33E+06	Saved spectrum as 030204_060511_1.spe
3510	2.72	22.3	248	1.01E+07	7.51E+06	Saved spectrum as 030204_060927_1.spe
3710	3.11	21.1	246	9.36E+06	6.42E+06	Saved spectrum as 030204_061055_1.spe
3910	3.51	20.1	244	8.73E+06	5.39E+06	Saved spectrum as 030204_061418_1.spe
4110	3.91	19.1	241	8.25E+06	4.90E+06	Saved spectrum as 030204_061558_1.spe
4310	4.31	18.2	239	7.89E+06	4.42E+06	Saved spectrum as 030204_061916_1.spe
4510	4.70	17.4	236	7.45E+06	3.93E+06	Saved spectrum as 030204_061844_1.spe
4710	5.10	16.6	234	7.09E+06	3.18E+06	Saved spectrum as 030204_062034_1.spe
4910	5.50	16.0	232	6.82E+06	2.75E+06	Saved spectrum as 030204_062147_1.spe
5110	5.90	15.4	230	6.56E+06	1.55E+06	Saved spectrum as 030204_062303_1.spe
5310	6.29	14.8	228	6.51E+06	2.42E+06	Saved spectrum as 030204_062413_1.spe
5510	6.69	14.3	226	6.22E+06	2.14E+06	Saved spectrum as 030204_062520_1.spe

(1) From Plenum translational device optical counter
(2) After Calibration (see Appendix D)

Table E4 - Mixing Ratio results - TDL exp. - D_2O line 1321.64 - 2.8 g/min - 35°C

position		Results from P trace data inversion Pov = 0.517 kPa, To = 35.04 ºC			Results from TDL experiment TDL exp - D2O line 1321.64 - 2.8 g/min - feb 11	
STEPS(1)	cm from throat	p (kPa)	T (K)	mixing ratio (ppbv)	mixing ratio (ppbv)(2)	Saved spectrum
-300	-4.86	60.4	308	8.48E+06	9.04E+06	Saved spectrum as 030212_023633_1.spe
2144	0.00	32.0	258	8.48E+06	8.49E+06	Saved spectrum as 030212_030914_1.spe
2210	0.13	30.4	254	8.48E+06	8.44E+06	Saved spectrum as 030212_031109_1.spe
2260	0.23	29.2	250	8.49E+06	8.34E+06	Saved spectrum as 030212_031219_1.spe
2310	0.33	28.3	248	8.48E+06	8.47E+06	Saved spectrum as 030212_031339_1.spe
2410	0.53	26.8	244	8.48E+06	8.43E+06	Saved spectrum as 030212_031557_1.spe
2510	0.73	25.4	241	8.49E+06	8.43E+06	Saved spectrum as 030212_031700_1.spe
2610	0.93	24.0	237	8.52E+06	8.42E+06	Saved spectrum as 030212_031924_1.spe
2710	1.13	23.0	234	8.51E+06	8.64E+06	Saved spectrum as 030212_032306_1.spe
2810	1.32	22.1	231	8.51E+06	8.61E+06	Saved spectrum as 030212_032450_1.spe
2910	1.52	21.4	229	8.52E+06	8.44E+06	Saved spectrum as 030212_032613_1.spe
3010	1.72	20.7	227	8.50E+06	8.65E+06	Saved spectrum as 030212_032736_1.spe
3110	1.92	20.0	225	8.50E+06	8.75E+06	Saved spectrum as 030212_032928_1.spe
3310	2.32	18.8	221	8.50E+06	8.39E+06	Saved spectrum as 030212_033042_1.spe
3510	2.72	17.8	217	8.49E+06	8.85E+06	Saved spectrum as 030212_145439_1.spe
3710	3.11	17.0	215	8.32E+06	8.54E+06	Saved spectrum as 030212_145626_1.spe
3910	3.51	16.5	215	7.26E+06	7.47E+06	Saved spectrum as 030212_145750_1.spe
4110	3.91	16.3	218	5.19E+06	5.76E+06	Saved spectrum as 030212_145916_1.spe
4310	4.31	16.1	220	3.39E+06	3.72E+06	Saved spectrum as 030212_165906_1.spe
4510	4.70	15.6	220	2.43E+06	2.55E+06	Saved spectrum as 030212_170100_1.spe
4710	5.10	15.0	218	2.00E+06	1.51E+06	Saved spectrum as 030212_170434_1.spe
4910	5.50	14.4	216	1.87E+06	1.03E+06	Saved spectrum as 030212_170745_1.spe
5110	5.90	13.9	214	1.74E+06	8.86E+05	Saved spectrum as 030212_170933_1.spe
5310	6.29	13.4	212	1.66E+06	7.52E+05	Saved spectrum as 030212_171117_1.spe
5510	6.69	13.0	211	1.39E+06	6.97E+05	Saved spectrum as 030212_171307_1.spe

(1) From Plenum translational device optical counter
(2) After Calibration (see Appendix D)

Table E5 - Mixing Ratio results - TDL exp. - D_2O line 1321.64 - 5.6 g/min - 35°C

position		Results from P trace data inversion Pov = 1.026 kPa, To = 35.04 ºC			Results from TDL experiment TDL exp - D2O line 1321.64 - 5.6 g/min - feb 11	
STEPS(1)	cm from throat	p (kPa)	T (K)	mixing ratio (ppbv)	mixing ratio (ppbv)(2)	Saved spectrum
-300	-4.86	60.4	308	1.67E+07	1.63E+07	Saved spectrum as 030212_035727_1.spe
2144	0.00	32.0	258	1.67E+07	1.65E+07	Saved spectrum as 030212_104642_1.spe
2210	0.13	30.4	254	1.67E+07	1.64E+07	Saved spectrum as 030212_104757_1.spe
2260	0.23	29.0	251	1.67E+07	1.65E+07	Saved spectrum as 030212_105005_1.spe
2310	0.33	28.1	248	1.67E+07	1.63E+07	Saved spectrum as 030212_105123_1.spe
2410	0.53	26.6	245	1.67E+07	1.64E+07	Saved spectrum as 030212_105232_1.spe
2510	0.73	25.2	241	1.67E+07	1.63E+07	Saved spectrum as 030212_105532_1.spe
2610	0.93	23.9	237	1.67E+07	1.64E+07	Saved spectrum as 030212_105652_1.spe
2710	1.13	22.8	234	1.67E+07	1.65E+07	Saved spectrum as 030212_105819_1.spe
2810	1.32	22.0	232	1.67E+07	1.64E+07	Saved spectrum as 030212_171552_1.spe
2910	1.52	21.3	230	1.66E+07	1.64E+07	Saved spectrum as 030212_171725_1.spe
3010	1.72	20.7	228	1.65E+07	1.64E+07	Saved spectrum as 030212_171854_1.spe
3110	1.92	20.1	227	1.61E+07	1.63E+07	Saved spectrum as 030212_172020_1.spe
3310	2.32	20.2	234	1.25E+07	1.37E+07	Saved spectrum as 030212_172131_1.spe
3510	2.72	20.6	242	8.34E+06	9.27E+06	Saved spectrum as 030212_173207_1.spe
3710	3.11	20.1	243	6.61E+06	6.07E+06	Saved spectrum as 030212_174242_1.spe
3910	3.51	19.1	241	6.03E+06	4.64E+06	Saved spectrum as 030212_174646_1.spe
4110	3.91	18.2	238	5.68E+06	3.79E+06	Saved spectrum as 030212_175221_1.spe
4310	4.31	17.4	235	5.42E+06	3.34E+06	Saved spectrum as 030212_180135_1.spe
4510	4.70	16.6	233	4.99E+06	2.63E+06	Saved spectrum as 030212_183900_1.spe
4710	5.10	15.9	231	4.67E+06	2.24E+06	Saved spectrum as 030212_184042_1.spe
4910	5.50	15.3	229	4.46E+06	2.09E+06	Saved spectrum as 030212_184155_1.spe
5110	5.90	14.7	227	4.38E+06	2.21E+06	Saved spectrum as 030212_184623_1.spe
5310	6.29	14.2	225	4.26E+06	1.65E+06	Saved spectrum as 030212_184855_1.spe
5510	6.69	13.7	223	3.98E+06	1.49E+06	Saved spectrum as 030212_185334_1.spe

(1) From Plenum translational device optical counter
(2) After Calibration (see Appendix D)

Table E6 - Mixing Ratio results - TDL exp. - D_2O line 1321.64 - 8.3 g/min - 35°C

position		Results from P trace data inversion Pov = 1.530 kPa, To = 35.03 ºC			Results from TDL experiment TDL exp - D2O line 1321.64 - 8.3 g/min - feb 11	
STEPS(1)	cm from throat	p (kPa)	T (K)	mixing ratio (ppbv)	mixing ratio (ppbv)(2)	Saved spectrum
-300	-4.86	60.4	308	2.47E+07	2.63E+07	Saved spectrum as 030212_110809_1.spe
2144	0.00	32.0	258	2.47E+07	2.48E+07	Saved spectrum as 030212_111347_1.spe
2210	0.13	30.4	254	2.47E+07	2.47E+07	Saved spectrum as 030212_111528_1.spe
2260	0.23	29.0	251	2.47E+07	2.44E+07	Saved spectrum as 030212_111641_1.spe
2310	0.33	28.1	249	2.47E+07	2.44E+07	Saved spectrum as 030212_111748_1.spe
2410	0.53	26.7	245	2.47E+07	2.49E+07	Saved spectrum as 030212_111915_1.spe
2510	0.73	25.2	241	2.47E+07	2.48E+07	Saved spectrum as 030212_112140_1.spe
2610	0.93	23.9	238	2.46E+07	2.45E+07	Saved spectrum as 030212_201021_1.spe
2710	1.13	23.0	235	2.44E+07	2.54E+07	Saved spectrum as 030212_201427_1.spe
2810	1.32	22.6	236	2.35E+07	2.52E+07	Saved spectrum as 030212_202231_1.spe
2910	1.52	23.2	242	2.09E+07	2.37E+07	Saved spectrum as 030212_202800_1.spe
3010	1.72	24.1	250	1.78E+07	2.22E+07	Saved spectrum as 030212_203022_1.spe
3110	1.92	24.2	254	1.56E+07	1.93E+07	Saved spectrum as 030212_203144_1.spe
3310	2.32	23.2	255	1.33E+07	1.31E+07	Saved spectrum as 030212_203443_1.spe
3510	2.72	22.0	253	1.22E+07	1.16E+07	Saved spectrum as 030212_203718_1.spe
3710	3.11	20.9	251	1.14E+07	9.62E+06	Saved spectrum as 030212_204111_1.spe
3910	3.51	19.9	249	1.08E+07	8.64E+06	Saved spectrum as 030212_204242_1.spe
4110	3.91	19.0	246	1.02E+07	8.28E+06	Saved spectrum as 030212_210325_1.spe
4310	4.31	18.1	244	9.70E+06	7.91E+06	Saved spectrum as 030212_210635_1.spe
4510	4.70	17.3	242	9.23E+06	6.34E+06	Saved spectrum as 030212_210815_1.spe
4710	5.10	16.6	240	8.78E+06	5.49E+06	Saved spectrum as 030212_210933_1.spe
4910	5.50	15.9	238	8.44E+06	5.12E+06	Saved spectrum as 030212_211105_1.spe
5110	5.90	15.4	236	8.16E+06	4.77E+06	Saved spectrum as 030212_211254_1.spe
5310	6.29	14.8	234	7.96E+06	4.07E+06	Saved spectrum as 030212_211537_1.spe
5510	6.69	14.3	233	7.59E+06	4.04E+06	Saved spectrum as 030212_211728_1.spe

(1) From Plenum translational device optical counter
(2) After Calibration (see Appendix D)

Tables from E7 to E12 report the Temperature determination for the same conditions shown above using two different absorption lines (1321.29 and 1321.64 cm^{-1} intensity lines), by following the procedure described in Chapter 2. The mixing ratio has been then recalculated performing a new fit imposing the new temperature. As remarked earlier in Chapter 3 of the present work, the newly obtained mixing ratio values are relatively close to the previous ones, even when the change in the temperature is large, since they are dominated by the absorption line with the biggest linestrenght (1321.64 cm^{-1} intensity line) but, unfortunately, with lowest energy of the lower level of the transition (see Table 2.2 for further details).

Table E7 - TDL exp. - Temperature determination from ratio of D_2O line 1321.64 to line(s) 1321.29 - 2.8 g/min - 25°C

position		Results from P trace data inversion Pov = 0.501 kPa, To = 25.02 ºC			Results from TDL experiment Ratio of D2O line 1321.64 to line(s) 1321.29 - 2.8 g/min - feb 1		
STEPS[1]	cm from throat	p (kPa)	T (K)	M.R. (ppbv)	Saved spectrum	derived T (K)[2]	derived M.R. (ppbv)[2][3]
-300	-4.86	60.4	298	8.21E+06	Saved spectrum as 030422_053128_1.spe	291.5	8.79E+06
2144	0.00	31.7	246	8.21E+06	Saved spectrum as 030422_054408_1.spe	245.0	8.28E+06
2210	0.13	30.4	244	8.21E+06	Saved spectrum as 030422_054847_1.spe	243.6	8.29E+06
2260	0.23	29.2	242	8.22E+06	Saved spectrum as 030422_055218_1.spe	242.0	8.45E+06
2310	0.33	28.3	240	8.22E+06	Saved spectrum as 030422_055414_1.spe	239.7	8.37E+06
2410	0.53	26.7	236	8.19E+06	Saved spectrum as 030224_154044_1.spe	234.3	8.48E+06
2510	0.73	25.3	233	8.22E+06	Saved spectrum as 030224_154656_1.spe	231.7	8.53E+06
2610	0.93	24.0	229	8.23E+06	Saved spectrum as 030224_155204_1.spe	225.2	8.32E+06
2710	1.13	23.0	226	8.21E+06	Saved spectrum as 030224_155751_1.spe	225.8	8.59E+06
2810	1.32	22.1	224	8.18E+06	Saved spectrum as 030224_160007_1.spe	224.0	8.58E+06
2910	1.52	21.4	222	8.21E+06	Saved spectrum as 030224_160548_1.spe	224.1	8.67E+06
3010	1.72	20.7	220	8.18E+06	Saved spectrum as 030422_060525_1.spe	236.3	8.70E+06
3110	1.92	20.0	218	8.14E+06	Saved spectrum as 030224_162645_1.spe	217.4	8.63E+06
3310	2.32	19.0	216	7.48E+06	Saved spectrum as 030224_163135_1.spe	215.2	7.97E+06
3510	2.72	18.8	219	5.24E+06	Saved spectrum as 030224_163441_1.spe	219.0	6.17E+06
3710	3.11	18.6	222	2.96E+06	Saved spectrum as 030224_164411_1.spe	230.4	3.60E+06
3910	3.51	18.0	222	1.96E+06	Saved spectrum as 030422_061228_1.spe	235.4	2.05E+06
4110	3.91	17.2	219	1.72E+06	Saved spectrum as 030224_182656_1.spe	236.0	1.24E+06
4310	4.31	16.4	217	1.60E+06	Saved spectrum as 030224_185105_1.spe	230.2	8.42E+05
4510	4.70	15.7	214	1.42E+06	Saved spectrum as 030422_061728_1.spe	239.0	6.33E+05
4710	5.10	15.0	212	1.25E+06	Saved spectrum as 030224_173926_1.spe	221.8	5.33E+05
4910	5.50	14.4	210	1.16E+06	Saved spectrum as 030422_062614_1.spe	232.5	4.80E+05
5110	5.90	13.9	208	1.11E+06	Saved spectrum as 030422_064812_1.spe	224.0	3.91E+05
5310	6.29	13.4	205	1.17E+06	Saved spectrum as 030422_065527_1.spe	219.0	3.15E+05
5510	6.69	12.9	204	1.08E+06	Saved spectrum as 030422_070346_1.spe	225.0	3.32E+05

(1) From Plenum translational device optical counter
(2) After Calibration (see Appendix D)
(3) Obtained performing a new fit on line 1321.64, imposing the newly derived temperature as input

Table E8 - TDL exp. - Temperature determination from ratio of D_2O line 1321.64 to line(s) 1321.29 - 5.6 g/min - 25°C

position		Results from P trace data inversion Pov = 0.997 kPa, To = 25.04 ºC			Results from TDL experiment Ratio of D2O line 1321.64 to line(s) 1321.29 - 5.6 g/min - feb 1		
STEPS[1]	cm from throat	p (kPa)	T (K)	M.R. (ppbv)	Saved spectrum	derived T (K)[2]	derived M.R. (ppbv)[2][3]
-300	-4.86	60.4	298	1.62E+07	Saved spectrum as 030214_042617_1.spe	292.0	1.70E+07
2144	0.00	31.7	246	1.62E+07	Saved spectrum as 030214_042912_1.spe	248.3	1.63E+07
2210	0.13	30.4	244	1.62E+07	Saved spectrum as 030214_043220_1.spe	243.8	1.60E+07
2260	0.23	29.0	242	1.62E+07	Saved spectrum as 030214_043309_1.spe	241.0	1.61E+07
2310	0.33	28.1	240	1.62E+07	Saved spectrum as 030214_043433_1.spe	240.0	1.62E+07
2410	0.53	26.6	237	1.62E+07	Saved spectrum as 030214_043515_1.spe	236.5	1.65E+07
2510	0.73	25.2	233	1.61E+07	Saved spectrum as 030214_043721_1.spe	233.5	1.67E+07
2610	0.93	23.9	230	1.60E+07	Saved spectrum as 030214_043818_1.spe	231.0	1.60E+07
2710	1.13	23.2	229	1.55E+07	Saved spectrum as 030214_043856_1.spe	229.2	1.64E+07
2810	1.32	23.3	232	1.38E+07	Saved spectrum as 030214_043949_1.spe	229.4	1.59E+07
2910	1.52	24.1	239	1.10E+07	Saved spectrum as 030214_044157_1.spe	234.8	1.39E+07
3010	1.72	24.5	244	8.66E+06	Saved spectrum as 030214_044327_1.spe	242.6	1.12E+07
3110	1.92	24.0	245	7.54E+06	Saved spectrum as 030214_044539_1.spe	247.6	9.01E+06
3310	2.32	22.7	244	5.96E+06	Saved spectrum as 030214_044657_1.spe	247.7	5.64E+06
3510	2.72	21.4	241	5.32E+06	Saved spectrum as 030214_044905_1.spe	245.3	4.10E+06
3710	3.11	20.2	238	4.89E+06	Saved spectrum as 030214_044948_1.spe	246.5	3.23E+06
3910	3.51	19.2	235	4.57E+06	Saved spectrum as 030226_082857_1.spe	241.5	2.64E+06
4110	3.91	18.2	232	4.34E+06	Saved spectrum as 030226_083720_1.spe	236.7	2.40E+06
4310	4.31	17.4	229	4.06E+06	Saved spectrum as 030226_084919_1.spe	234.5	1.95E+06
4510	4.70	16.6	227	3.85E+06	Saved spectrum as 030226_080321_1.spe	244.6	1.67E+06
4710	5.10	15.9	225	3.60E+06	Saved spectrum as 030226_082032_1.spe	239.7	1.46E+06
4910	5.50	15.2	222	3.54E+06	Saved spectrum as 030226_085449_1.spe	246.8	1.21E+06
5110	5.90	14.6	220	3.37E+06	Saved spectrum as 030214_050129_1.spe	238.2	1.09E+06
5310	6.29	14.2	218	3.26E+06	Saved spectrum as 030214_050240_1.spe	234.1	9.77E+05
5510	6.69	13.7	217	2.91E+06	Saved spectrum as 030214_050338_1.spe	234.4	8.69E+05

(1) From Plenum translational device optical counter
(2) After Calibration (see Appendix D)
(3) Obtained performing a new fit on line 1321.64, imposing the newly derived temperature as input

Table E9 - TDL exp. - Temperature determination from ratio of D_2O line 1321.64 to line(s) 1321.29 - 8.3 g/min - 25°C

position		Results from P trace data inversion Pov = 1.482 kPa, To = 25.00 ºC			Results from TDL experiment Ratio of D2O line 1321.64 to line(s) 1321.29 - 8.3 g/min - feb 1		
STEPS(1)	cm from throat	p (kPa)	T (K)	M.R. (ppbv)	Saved spectrum	derived T (K)(2)	derived M.R. (ppbv)(2)(3)
-300	-4.86	60.4	298	2.39E+07	Saved spectrum as 030422_081307_1.spe	292.5	2.51E+07
2144	0.00	31.7	246	2.39E+07	Saved spectrum as 030422_081509_1.spe	248.2	2.37E+07
2210	0.13	30.4	244	2.39E+07	Saved spectrum as 030422_081645_1.spe	244.5	2.34E+07
2260	0.23	29.0	243	2.39E+07	Saved spectrum as 030422_081804_1.spe	242.4	2.34E+07
2310	0.33	28.2	241	2.39E+07	Saved spectrum as 030422_081912_1.spe	239.9	2.35E+07
2410	0.53	26.9	238	2.36E+07	Saved spectrum as 030422_082015_1.spe	234.1	2.40E+07
2510	0.73	26.4	239	2.24E+07	Saved spectrum as 030225_182943_1.spe	235.4	2.40E+07
2610	0.93	27.2	246	1.97E+07	Saved spectrum as 030422_082304_1.spe	241.5	2.24E+07
2710	1.13	27.9	251	1.74E+07	Saved spectrum as 030422_082459_1.spe	247.0	2.05E+07
2810	1.32	27.8	254	1.56E+07	Saved spectrum as 030422_082649_1.spe	249.8	1.76E+07
2910	1.52	27.2	255	1.43E+07	Saved spectrum as 030422_082850_1.spe	254.5	1.48E+07
3010	1.72	26.3	254	1.33E+07	Saved spectrum as 030422_083034_1.spe	255.0	1.27E+07
3110	1.92	25.4	253	1.24E+07	Saved spectrum as 030422_083424_1.spe	255.0	1.13E+07
3310	2.32	23.7	251	1.09E+07	Saved spectrum as 030422_083536_1.spe	254.0	9.38E+06
3510	2.72	22.3	248	1.01E+07	Saved spectrum as 030422_083725_1.spe	254.5	7.62E+06
3710	3.11	21.1	246	9.36E+06	Saved spectrum as 030422_083933_1.spe	257.7	6.64E+06
3910	3.51	20.1	244	8.73E+06	Saved spectrum as 030422_084257_1.spe	247.2	5.57E+06
4110	3.91	19.1	241	8.25E+06	Saved spectrum as 030422_085115_1.spe	251.0	5.12E+06
4310	4.31	18.2	239	7.89E+06	Saved spectrum as 030422_085338_1.spe	248.5	4.44E+06
4510	4.70	17.4	236	7.45E+06	Saved spectrum as 030422_085624_1.spe	251.0	3.96E+06
4710	5.10	16.6	234	7.09E+06	Saved spectrum as 030422_085822_1.spe	247.8	3.52E+06
4910	5.50	16.0	232	6.82E+06	Saved spectrum as 030422_090816_1.spe	252.7	3.12E+06
5110	5.90	15.4	230	6.56E+06	Saved spectrum as 030422_091216_1.spe	249.7	2.82E+06
5310	6.29	14.8	228	6.51E+06	Saved spectrum as 030422_092131_1.spe	246.0	2.57E+06
5510	6.69	14.3	226	6.22E+06	Saved spectrum as 030422_092535_1.spe	241.5	2.34E+06

(1) From Plenum translational device optical counter
(2) After Calibration (see Appendix D)
(3) Obtained performing a new fit on line 1321.64, imposing the newly derived temperature as input

Table E10 - TDL exp. - Temperature determination from ratio of D_2O line 1321.64 to line(s) 1321.29 - 2.8 g/min - 35°C

position		Results from P trace data inversion Pov = 0.517 kPa, To = 35.04 ºC			Results from TDL experiment Ratio of D2O line 1321.64 to line(s) 1321.29 - 2.8 g/min - feb 11		
STEPS(1)	cm from throat	p (kPa)	T (K)	M.R. (ppbv)	Saved spectrum	derived T (K)(2)	derived M.R. (ppbv)(2)(3)
-300	-4.86	60.4	308	8.48E+06	Saved spectrum as 030317_063715_1.spe	303.8	8.94E+06
2144	0.00	32.0	258	8.48E+06	Saved spectrum as 030317_064037_1.spe	255.5	8.49E+06
2210	0.13	30.4	254	8.48E+06	Saved spectrum as 030317_064305_1.spe	254.7	8.53E+06
2260	0.23	29.2	250	8.49E+06	Saved spectrum as 030317_064543_1.spe	253.2	8.46E+06
2310	0.33	28.3	248	8.48E+06	Saved spectrum as 030317_064726_1.spe	250.0	8.57E+06
2410	0.53	26.8	244	8.48E+06	Saved spectrum as 030317_065814_1.spe	245.6	8.52E+06
2510	0.73	25.4	241	8.49E+06	Saved spectrum as 030317_065950_1.spe	242.4	8.43E+06
2610	0.93	24.0	237	8.52E+06	Saved spectrum as 030317_070859_1.spe	240.0	8.51E+06
2710	1.13	23.0	234	8.51E+06	Saved spectrum as 030317_081808_1.spe	238.5	8.79E+06
2810	1.32	22.1	231	8.51E+06	Saved spectrum as 030317_082133_1.spe	232.6	8.63E+06
2910	1.52	21.4	229	8.52E+06	Saved spectrum as 030317_082512_1.spe	233.8	8.55E+06
3010	1.72	20.7	227	8.50E+06	Saved spectrum as 030317_082642_1.spe	228.7	8.68E+06
3110	1.92	20.0	225	8.50E+06	Saved spectrum as 030317_082900_1.spe	228.1	8.79E+06
3310	2.32	18.8	221	8.50E+06	Saved spectrum as 030317_083026_1.spe	221.0	8.44E+06
3510	2.72	17.8	217	8.49E+06	Saved spectrum as 030317_083915_1.spe	216.7	8.87E+06
3710	3.11	17.0	215	8.32E+06	Saved spectrum as 030317_084233_1.spe	220.2	8.65E+06
3910	3.51	16.5	215	7.26E+06	Saved spectrum as 030317_084624_1.spe	222.3	7.61E+06
4110	3.91	16.3	218	5.19E+06	Saved spectrum as 030317_085010_1.spe	226.5	5.88E+06
4310	4.31	16.1	220	3.39E+06	Saved spectrum as 030317_092358_1.spe	227.1	3.79E+06
4510	4.70	15.6	220	2.43E+06	Saved spectrum as 030317_103940_1.spe	238.0	2.60E+06
4710	5.10	15.0	218	2.00E+06	Saved spectrum as 030317_104600_1.spe	232.7	1.56E+06
4910	5.50	14.4	216	1.87E+06	Saved spectrum as 030317_104939_1.spe	242.0	1.12E+06
5110	5.90	13.9	214	1.74E+06	Saved spectrum as 030317_105919_1.spe	231.1	9.26E+05
5310	6.29	13.4	212	1.66E+06	Saved spectrum as 030317_110356_1.spe	230.5	7.65E+05
5510	6.69	13.0	211	1.39E+06	Saved spectrum as 030317_111608_1.spe	225.8	7.08E+05

(1) From Plenum translational device optical counter
(2) After Calibration (see Appendix D)
(3) Obtained performing a new fit on line 1321.64, imposing the newly derived temperature as input

Table E11 - TDL exp. - Temperature determination from ratio of D_2O line 1321.64 to line(s) 1321.29 - 5.6 g/min - 35°C

position		Results from P trace data inversion Pov = 1.026 kPa, To = 35.04 ºC			Results from TDL experiment Ratio of D2O line 1321.64 to line(s) 1321.29 - 5.6 g/min - feb 11		
STEPS[1]	cm from throat	p (kPa)	T (K)	M.R. (ppbv)	Saved spectrum	derived T (K)[2]	derived M.R. (ppbv)[2][3]
-300	-4.86	60.4	308	1.67E+07	Saved spectrum as 030319_205246_1.spe	301.0	1.60E+07
2144	0.00	32.0	258	1.67E+07	Saved spectrum as 030319_212533_1.spe	255.5	1.64E+07
2210	0.13	30.4	254	1.67E+07	Saved spectrum as 030319_213015_1.spe	251.5	1.64E+07
2260	0.23	29.0	251	1.67E+07	Saved spectrum as 030319_213058_1.spe	250.4	1.64E+07
2310	0.33	28.1	248	1.67E+07	Saved spectrum as 030319_213203_1.spe	247.5	1.63E+07
2410	0.53	26.6	245	1.67E+07	Saved spectrum as 030319_213534_1.spe	244.5	1.64E+07
2510	0.73	25.2	241	1.67E+07	Saved spectrum as 030319_213624_1.spe	241.0	1.63E+07
2610	0.93	23.9	237	1.67E+07	Saved spectrum as 030319_213802_1.spe	240.5	1.63E+07
2710	1.13	22.8	234	1.67E+07	Saved spectrum as 030319_214304_1.spe	235.5	1.66E+07
2810	1.32	22.0	232	1.67E+07	Saved spectrum as 030319_214418_1.spe	234.0	1.67E+07
2910	1.52	21.3	230	1.66E+07	Saved spectrum as 030319_214516_1.spe	232.3	1.65E+07
3010	1.72	20.7	228	1.65E+07	Saved spectrum as 030319_214954_1.spe	228.4	1.64E+07
3110	1.92	20.1	227	1.61E+07	Saved spectrum as 030319_215116_1.spe	230.7	1.64E+07
3310	2.32	20.2	234	1.25E+07	Saved spectrum as 030319_215148_1.spe	234.0	1.37E+07
3510	2.72	20.6	242	8.34E+06	Saved spectrum as 030319_215603_1.spe	247.2	9.39E+06
3710	3.11	20.1	243	6.61E+06	Saved spectrum as 030319_215717_1.spe	244.0	6.11E+06
3910	3.51	19.1	241	6.03E+06	Saved spectrum as 030319_215926_1.spe	246.3	4.71E+06
4110	3.91	18.2	238	5.68E+06	Saved spectrum as 030322_101226_1.spe	250.0	3.89E+06
4310	4.31	17.4	235	5.42E+06	Saved spectrum as 030322_101810_1.spe	232.4	3.32E+06
4510	4.70	16.6	233	4.99E+06	Saved spectrum as 030322_102132_1.spe	242.0	2.62E+06
4710	5.10	15.9	231	4.67E+06	Saved spectrum as 030322_105520_1.spe	237.5	2.34E+06
4910	5.50	15.3	229	4.46E+06	Saved spectrum as 030322_105806_1.spe	251.0	2.11E+06
5110	5.90	14.7	227	4.38E+06	Saved spectrum as 030322_111133_1.spe	260.0	2.38E+06
5310	6.29	14.2	225	4.26E+06	Saved spectrum as 030322_111831_1.spe	227.0	1.61E+06
5510	6.69	13.7	223	3.98E+06	Saved spectrum as 030322_112324_1.spe	210.0	1.53E+06

(1) From Plenum translational device optical counter
(2) After Calibration (see Appendix D)
(3) Obtained performing a new fit on line 1321.64, imposing the newly derived temperature as input

Table E12 - TDL exp. - Temperature determination from ratio of D_2O line 1321.64 to line(s) 1321.29 - 8.3 g/min - 35°C

position		Results from P trace data inversion Pov = 1.530 kPa, To = 35.03 ºC			Results from TDL experiment Ratio of D2O line 1321.64 to line(s) 1321.29 - 8.3 g/min - feb 11		
STEPS[1]	cm from throat	p (kPa)	T (K)	M.R. (ppbv)	Saved spectrum	derived T (K)[2]	derived M.R. (ppbv)[2][3]
-300	-4.86	60.4	308	2.47E+07	Saved spectrum as 030322_120053_1.spe	303.0	2.54E+07
2144	0.00	32.0	258	2.47E+07	Saved spectrum as 030322_120148_1.spe	258.0	2.48E+07
2210	0.13	30.4	254	2.47E+07	Saved spectrum as 030322_120236_1.spe	254.0	2.46E+07
2260	0.23	29.0	251	2.47E+07	Saved spectrum as 030322_120443_1.spe	251.0	2.44E+07
2310	0.33	28.1	249	2.47E+07	Saved spectrum as 030322_120600_1.spe	249.1	2.44E+07
2410	0.53	26.7	245	2.47E+07	Saved spectrum as 030322_120905_1.spe	246.5	2.50E+07
2510	0.73	25.2	241	2.47E+07	Saved spectrum as 030322_121157_1.spe	241.5	2.46E+07
2610	0.93	23.9	238	2.46E+07	Saved spectrum as 030322_121459_1.spe	240.6	2.44E+07
2710	1.13	23.0	235	2.44E+07	Saved spectrum as 030322_121621_1.spe	237.8	2.55E+07
2810	1.32	22.6	236	2.35E+07	Saved spectrum as 030322_121909_1.spe	235.5	2.53E+07
2910	1.52	23.2	242	2.09E+07	Saved spectrum as 030322_122111_1.spe	240.0	2.37E+07
3010	1.72	24.1	250	1.78E+07	Saved spectrum as 030322_122303_1.spe	248.8	2.21E+07
3110	1.92	24.2	254	1.56E+07	Saved spectrum as 030322_122551_1.spe	254.2	1.93E+07
3310	2.32	23.2	255	1.33E+07	Saved spectrum as 030322_122817_1.spe	258.5	1.33E+07
3510	2.72	22.0	253	1.22E+07	Saved spectrum as 030322_122907_1.spe	258.0	1.18E+07
3710	3.11	20.9	251	1.14E+07	Saved spectrum as 030322_123351_1.spe	260.0	9.68E+06
3910	3.51	19.9	249	1.08E+07	Saved spectrum as 030322_123529_1.spe	256.0	8.80E+06
4110	3.91	19.0	246	1.02E+07	Saved spectrum as 030322_123724_1.spe	261.8	8.59E+06
4310	4.31	18.1	244	9.70E+06	Saved spectrum as 030322_124133_1.spe	254.3	7.53E+06
4510	4.70	17.3	242	9.23E+06	Saved spectrum as 030322_124341_1.spe	254.3	6.53E+06
4710	5.10	16.6	240	8.78E+06	Saved spectrum as 030322_124515_1.spe	245.2	5.67E+06
4910	5.50	15.9	238	8.44E+06	Saved spectrum as 030322_124856_1.spe	248.9	5.38E+06
5110	5.90	15.4	236	8.16E+06	Saved spectrum as 030322_125037_1.spe	249.3	4.97E+06
5310	6.29	14.8	234	7.96E+06	Saved spectrum as 030322_125302_1.spe	256.5	4.24E+06
5510	6.69	14.3	233	7.59E+06	Saved spectrum as 030322_125503_1.spe	250.0	4.12E+06

(1) From Plenum translational device optical counter
(2) After Calibration (see Appendix D)
(3) Obtained performing a new fit on line 1321.64, imposing the newly derived temperature as input

APPENDIX F

ADDENDUM

One of the very last improvements tested on the system has been the attempt to compensate for the change in pressure and temperature inside the nozzle when condensation occurs, trying to flow a "blank" substance whose fluidodynamic behavior is similar to the substance under investigation but the spectroscopic characteristic totally different, so that the TDL experiment can remain unaltered. This has been tried in order to reduce the size of the fringes that occurs as a result of a not perfect subtraction of the background signal.

In fact one of the reasons for which the subtraction is not perfect is surely due to a natural drift of the instrument, circumstance that limits the time for a full set of measures (sample + background) at any given point to less than 1 minute. On the other hand, fringes are apparently sensitive to even minor changes in the fluidodynamic conditions. This last characteristic is a problem in our system, since the change in pressure and temperature is a direct consequence of condensation and leads to a certain difference in between the sample measure and the background measure that translate directly into a magnifying effect of the fringes amplitude. This amplification is particularly important in the very downstream part of the nozzle, where the state variable difference is greatest, and where the absorption signal is lowest, leading to a situation where very difficulty can be obtained results from a TDL experiment.

To compensate for the changes in pressure and temperature and therefore we tested the possibility to take the background "blank" measure flowing not the only carrier gas (as have been done in the remainder of this work) but a mixture of carrier gas and another condensible substance that would adjust pressure and temperature without affecting the spectroscopic measures. Being D_2O the condensible substance for the TDL experiment, we checked the possibility to use Water as "blank" substance.

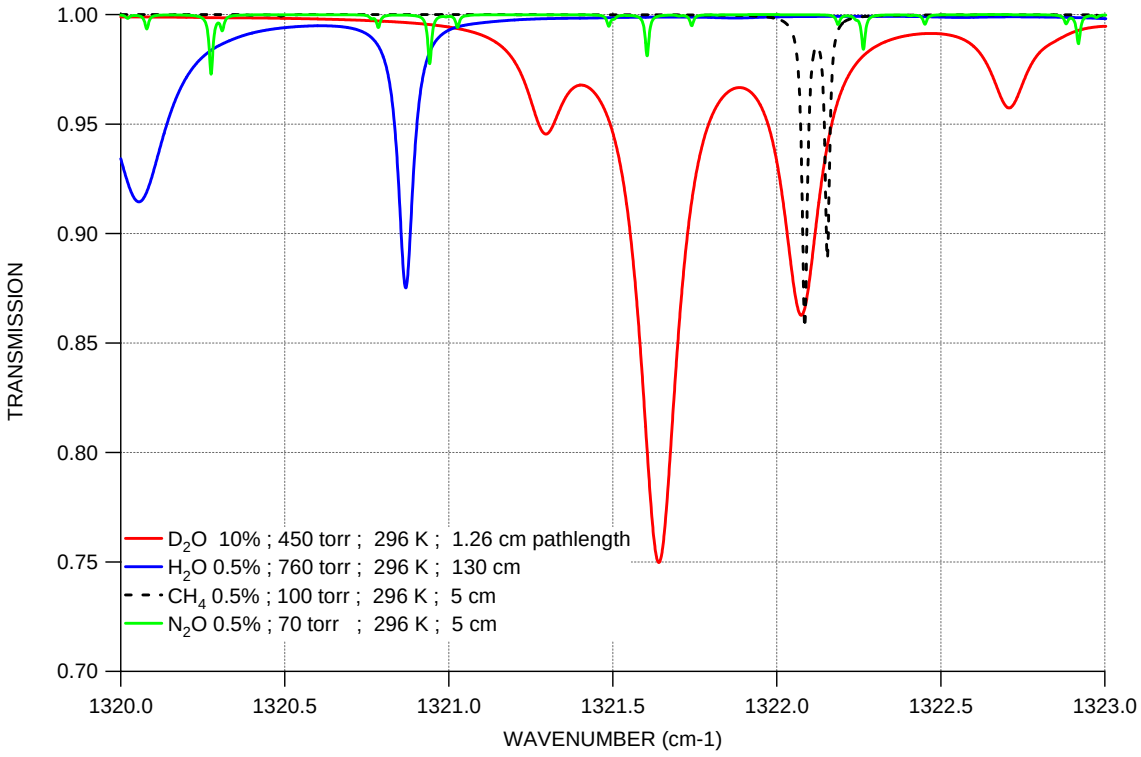

Figure F1 - Simulation of light absorption for selected substances from literature spectroscopic data [27-30, 33].

First we checked that no interference from the water would have occurred in the working region of our laser. As it is possible to infer from Figure F1, no water absorption is expected in between 1321 and 1322 wavenumbers [27-30, 33].

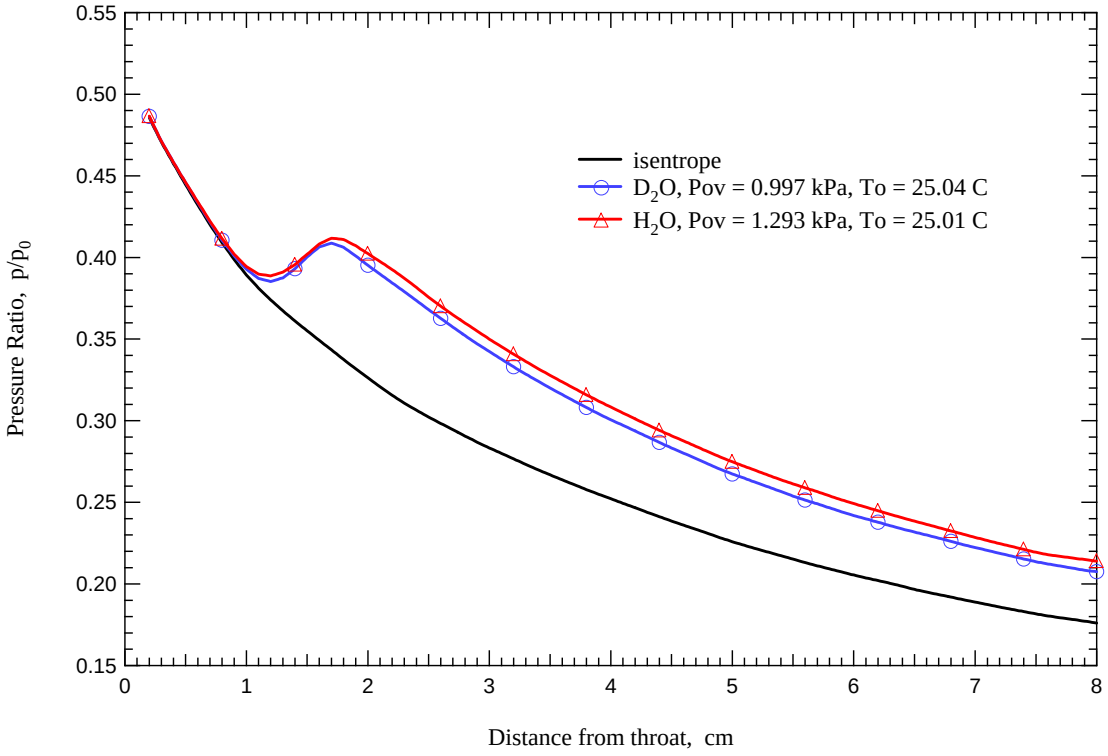

Figure F2 - D_2O and H_2O pressure traces best matching the trend along the nozzle for the P_{0V} = 60.4 kPa, T_0 = 298 K stagnation condition.

Then we verified what operating conditions should have been used for the water in order to best match the experimental D_2O conditions. Looking at the pressure trace experiments results, we selected two D_2O and water flowrates, among the traces we had immediately available, for the same stagnation conditions that represented the best

compromise between onset position closeness, pressure and temperature trend along the nozzle. The two curves are shown in Figure F2.

NORMAL CASE: ONLY CARRIER GAS IN THE BACKGROUND	**IMPROVED VERSION: WATER FLOW IN THE BACKGROUND**
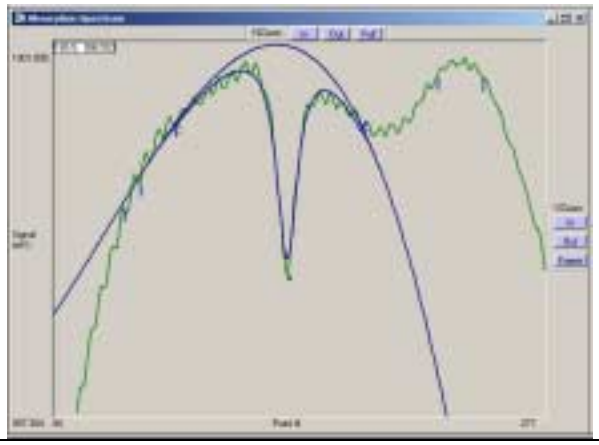	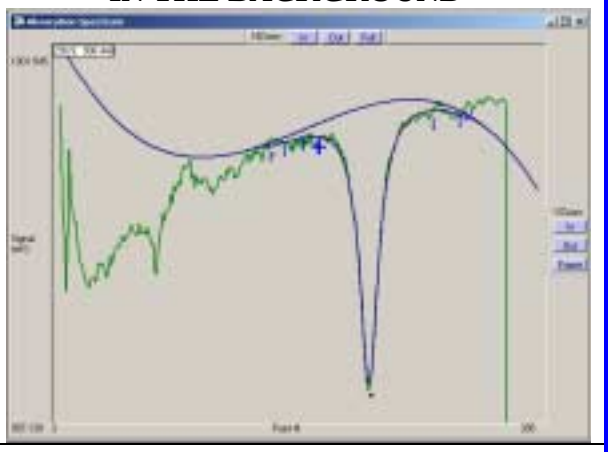

The left part shows a spectrum look after background subtraction when only carrier gas is flown in the background measure. Pressure and temperature are different between sample and background measure and subtraction is not perfect: a large sinusoidal pattern imputable to the occurrence of fringes arise.

The right figure shows a net spectrum (after background subtraction) where the background measure is taken flowing water along with the carrier gas. A conveniently selected water flowrate makes pressure and temperature after condensation very close to those in the sample measure. The final result is a much more "flat" baseline, where is easier to perform a fit.

NOTE: Both spectra have been taken at position 5510, corresponding to 6.69 cm downstream of the throat.

Figure F3 - Comparison between normal and improved background subtraction method.

To practically being able to switch between D_2O and H_2O inside the nozzle, we added a second vapor generation section (vaporizer, peristaltic pump, flow meters and heating tape), in series with the existing one. By electrically switching from one pump to the other we have been able to replace the D_2O vapor with the H_2O vapor inside the nozzle in

the tight time interval (less than 60 seconds) allotted for a complete TDL measure in each position.

Table F1 - Mixing Ratio result - TDL exp. - D_2O line 1321.64 - 5.6 g/min - 25°C - 6.6 g/min water flow in the background measure

position		Results from P trace data inversion Pov = 0.997 kPa, To = 25.04 ºC			Results from TDL experiment D2O line 1321.64 - 5.6 g/min -- 6.6 g/min water flow in the background	
STEPS(1)	cm from throat	p (kPa)	T (K)	mixing ratio (ppbv)	mixing ratio (ppbv)(2)	Saved spectrum
-300	-4.86	60.4	298	1.62E+07	1.75E+07	Saved spectrum as 030425_131444_1.spe
2144	0.00	31.7	246	1.62E+07	1.65E+07	Saved spectrum as 030425_131343_1.spe
2210	0.13	30.4	244	1.62E+07	1.64E+07	Saved spectrum as 030425_131255_1.spe
2260	0.23	29.0	242	1.62E+07	1.63E+07	Saved spectrum as 030425_131209_1.spe
2310	0.33	28.1	240	1.62E+07	1.44E+07	Saved spectrum as 030425_131125_1.spe
2410	0.53	26.6	237	1.62E+07	1.51E+07	Saved spectrum as 030425_131033_1.spe
2510	0.73	25.2	233	1.61E+07	1.68E+07	Saved spectrum as 030425_153514_1.spe
2610	0.93	23.9	230	1.60E+07	1.66E+07	Saved spectrum as 030425_153720_1.spe
2710	1.13	23.2	229	1.55E+07	1.67E+07	Saved spectrum as 030425_153908_1.spe
2810	1.32	23.3	232	1.38E+07	1.66E+07	Saved spectrum as 030425_154053_1.spe
2910	1.52	24.1	239	1.10E+07	1.27E+07	Saved spectrum as 030425_154223_1.spe
3010	1.72	24.5	244	8.66E+06	1.10E+07	Saved spectrum as 030425_154809_1.spe
3110	1.92	24.0	245	7.54E+06	6.51E+06	Saved spectrum as 030425_155012_1.spe
3310	2.32	22.7	244	5.96E+06	4.63E+06	Saved spectrum as 030425_155743_1.spe
3510	2.72	21.4	241	5.32E+06	4.33E+06	Saved spectrum as 030425_160357_1.spe
3710	3.11	20.2	238	4.89E+06	3.35E+06	Saved spectrum as 030425_160310_1.spe
3910	3.51	19.2	235	4.57E+06	2.76E+06	Saved spectrum as 030425_160622_1.spe
4110	3.91	18.2	232	4.34E+06	2.31E+06	Saved spectrum as 030425_160958_1.spe
4310	4.31	17.4	229	4.06E+06	2.16E+06	Saved spectrum as 030425_161139_1.spe
4510	4.70	16.6	227	3.85E+06	1.86E+06	Saved spectrum as 030425_161345_1.spe
4710	5.10	15.9	225	3.60E+06	1.65E+06	Saved spectrum as 030425_161604_1.spe
4910	5.50	15.2	222	3.54E+06	1.36E+06	Saved spectrum as 030425_161834_1.spe
5110	5.90	14.6	220	3.37E+06	9.80E+05	Saved spectrum as 030425_162415_1.spe
5310	6.29	14.2	218	3.26E+06	1.10E+06	Saved spectrum as 030425_162322_1.spe
5510	6.69	13.7	217	2.91E+06	1.01E+06	Saved spectrum as 030425_162755_1.spe

(1) From Plenum translational device optical counter
(2) After Calibration (see Appendix D)

After performing background subtraction it is possible to see that the net spectra presents a much more flat baseline shape. The sinusoidal pattern typical of the fringes-dominated spectra, usually common at any point after the onset of condensation has been replaced with a much more flat baseline where results much easier to perform a fit. The difference is clearly visible in Figure F3, where a snapshot of the TDLWintel software is

provided for the "normal" case (with only carrier gas in the background measure) and this improved version (flowing water in the background).

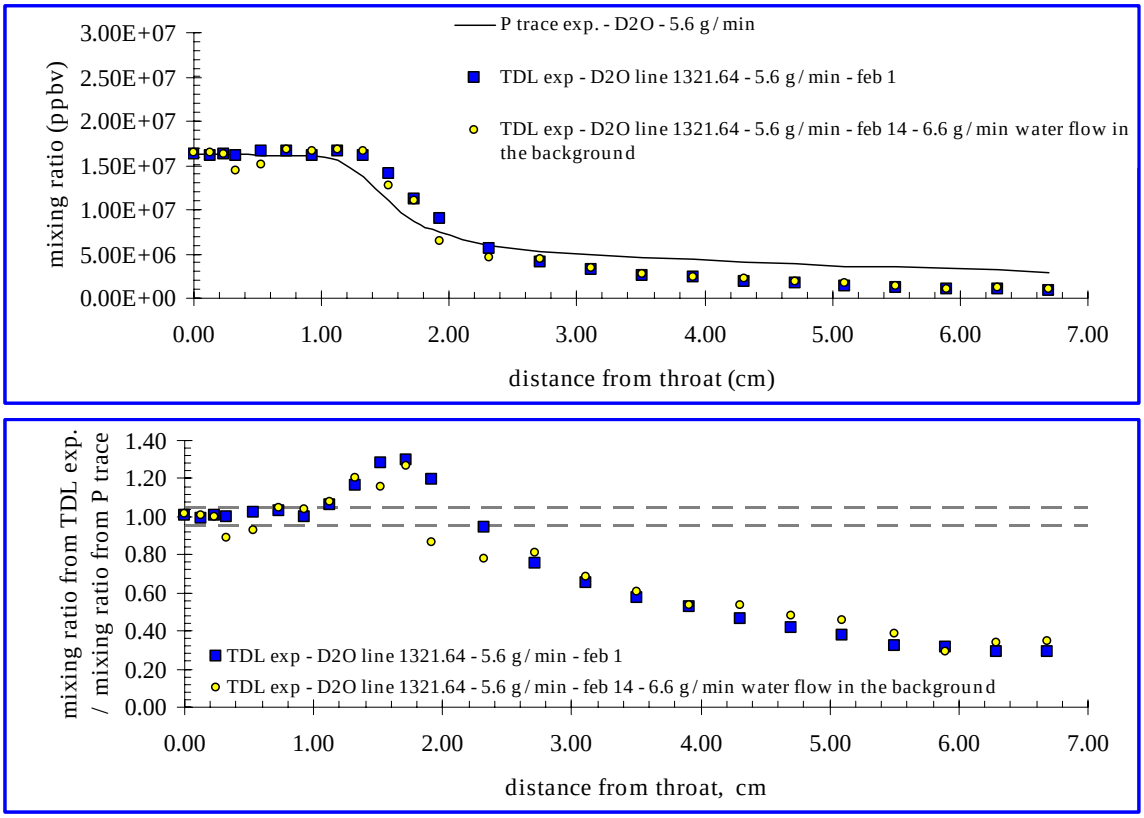

Figure F4 - D_2O mixing ratios derived from the TDL experiment flowing water in the background measure.

Results for the present attempt of compensating for pressure and temperature changes in the nozzle are shown in Table F1 and then are compared with the equivalent "normal" case in Figure F4.

As a matter of fact, a considerable improvement of the fitting procedure process comes from this new approach (the sinusoidal pattern almost disappears at any point), but results, so far, are clearly on the same precision level of the previous ones. Moreover the data collection procedure is complicated with respect to the normal case by the presence of the vapor generation system for the second condensible substance.

However the procedure works, fringes are clearly reduced by even one order of magnitude and therefore this new approach to the data collection appears very promising.